Investigating Novel Beta-Catenin Interactions in Wnt Target Gene Regulation in Human and Drosophila Cells

by

Richard Stewart

A dissertation submitted in partial fulfillment
of the requirements for the degree of
Doctor of Philosophy
(Molecular, Cellular, and Developmental Biology)
in the University of Michigan
2024

Doctoral Committee:

Professor Kenneth M. Cadigan, Chair
Professor Györgyi Csankovszki
Associate Professor Jayakrishnan Nandakumar
Assistant Professor Kaushik Ragunathan

Richard Stewart
stewra@umich.edu
ORCID iD: 0000-0003-4756-3022

Acknowledgements

I would like to thank my mentor, Ken Cadigan, and the members of the Cadigan lab that I have worked with over the years for their feedback and support. It's hard to overstate Ken's dedication to his students, for which I am grateful. I'll fondly remember our impromptu weekend science discussions in the fly room. I am also grateful for the feedback and guidance provided by my thesis committee throughout this process. I would also like to thank John Moran and Anthony Antonellis for their work organizing the Michigan Predoctoral Training Program in Genetics.

I would like to thank Savita Khanna, Cameron Rink, Sashwati Roy, Chandan Sen, Subhadip Ghatak, Mithun Sinha, Piya Das Ghatak, William Lawrence, and everyone else that I worked with at Ohio State for really helping me get started in research and encouraging me to get a PhD in the first place.

I would also like to thank my family for their continuous support and encouragement: mom, dad, my brothers- Ryan and Steven, my wife- Sangeetha.

Table of Contents

List of Tables

List of Figures

Abstract

Activation of Wnt target genes requires the nuclear localization of β-catenin, a transcriptional co-regulator, to Wnt-regulated enhancers (WREs). β-catenin is recruited to WREs through direct binding to TCF-family transcription factors and mediates transcriptional activation by binding additional transcriptional co-activators. This process has traditionally been conceptualized through traditional mechanisms of protein-protein interaction. A recent study suggests that human β-catenin can form biomolecular condensates, which implies an alternative mechanism of protein-protein interaction and suggests that these condensates may be important for β-catenin's function as a transcriptional co-regulator. The primary focus of this thesis is to further examine the requirement of β-catenin condensate formation in regulating Wnt target genes by utilizing a variety of experimental readouts in *Drosophila* and human tissue.

I characterized the transcriptional activity of a panel of β-catenin mutants which are defective in the ability to form biomolecular condensates. These mutants had different combinations of aromatic amino acid residues within β-catenin's terminal, intrinsically disordered regions (IDRs) mutated to alanine. The results of the experiments with these mutants support a model in which the ability of β-catenin to form biomolecular condensates is tightly linked to its ability to regulate Wnt target genes.

A significant portion of my thesis work also focused on changes in the histone modification profile of Wnt target genes in response to Wnt activity. It has been previously observed that in response to Wnt signaling, Wnt target gene loci exhibit widespread histone acetylation. This is different from the general histone acetylation profile of active genes, which exhibit histone acetylation at cis-regulatory elements, such as enhancers and promoters. I sought to determine whether the widespread histone acetylation pattern emanated from a single WRE. To that end, I generated and characterized a *Drosophila* strain that had a WRE that regulates *notum*, a Wnt target gene, deleted with CRISPR/Cas9. These flies still expressed *notum*, suggesting that

there are additional WREs that regulate *notum's* expression. Additionally, we observed that histone acetylation is sufficient for transcription of the Wnt target gene, *naked cuticle*. Our results illustrate a complicated relationship between histone acetylation, WRE activity, and Wnt target gene transcription.

In total, my dissertation research characterizes the role of β-catenin-containing biomolecular condensates and histone acetylation in Wnt target gene regulation. My work provides a strong functional characterization of biomolecular condensates in Wnt target gene regulation and foundational studies for the sufficiency of histone acetylation in Wnt target gene expression. Future studies aimed at elucidating a direct link between biomolecular condensates and Wnt target gene transcription, in addition to characterizing a biomolecular condensate 'grammar' with β-catenin and additional transcriptional co-regulators, will be important next steps for this work.

Chapter 1 Introduction to the Wnt Signaling Pathway

Cell Signaling affects cellular behavior by altering gene expression patterns

Metazoan development requires proper cell fate specification, concurrent with precise coordination of cellular functions, such as migration and division. Failure or misregulation of these processes can result in a variety of developmental defects (Godard and Heisenberg, 2019; Scarpa and Mayor, 2016). To safeguard against this, metazoa have evolved robust cell-cell communication mechanisms to regulate cell activity. Cells use a wide variety of signals to communicate, from inorganic ions to metabolites and proteins. Cell signaling through proteins can broadly be categorized as occurring through ligand-receptor, receptor-receptor, and extracellular matrix-receptor interactions (Armingol et al., 2021). The emphasis here will be on ligand-receptor signaling.

Ligand-receptor signaling between cells involves one cell synthesizing a ligand molecule and either secreting it into extracellular space or presenting the signal on its plasma membrane. These cells that synthesize ligands are classically referred to as ‘inducers.’ Cells that receive the signal and react are classically referred to as ‘responders’ (Perrimon et al., 2012). Responders typically express receptors that can recognize and bind to the ligand protein. When that binding event occurs, an intracellular signal transduction cascade of protein interactions is triggered, which ultimately ends in altering gene expression programs in the responder cell (Heldin et al., 2016). Altering gene expression occurs through modulating the activity of proteins that bind to DNA, which are known as transcription factors (TFs), proteins that bind to TFs, which are known as transcriptional co-regulators, or sometimes both TFs and co-regulators.

Eleven major developmental cell signaling pathways have evolved in metazoa and they can be broadly categorized as ligand-receptor signaling pathways. They are: cytokine (non-receptor tyrosine kinase JAK-STAT), EGF, FGF, Hedgehog, Hippo, Jun Kinase (JNK), NF-κB, Notch, retinoic acid receptor (RAR), transforming growth factor β (TGF-β)/BMPs, and Wnt/Wingless. These pathways, except for RAR signaling, all work through cell membrane-associated receptors (Perrimon et al., 2012). Retinoic acid is able to passively diffuse through the cell membrane to activate the RAR (which is a TF), negating the need for a cell surface receptor (Perrimon et al., 2012; Petkovich and Chambon, 2022). It is surprising that nature has selected so few pathways to regulate the vast number of events that need to occur during development. Since these pathways are utilized in many different and often unrelated contexts, the output of these pathways must be highly cell-type specific and variable.

One brief example of these signaling pathways in action is the development of skeletal muscle in the embryo, which requires active Notch signaling (Siebel and Lendahl, 2017). Early, somite-derived, skeletal muscle precursor cells express the transcription factor Pax3 and have the potential to differentiate into either skeletal muscle cells or endothelial cells (Mayeuf-Louchart et al., 2014). This decision is partially regulated by Notch signaling activity, with high levels of Notch promoting an endothelial cell fate and low levels of Notch promoting a skeletal muscle cell fate (Siebel and Lendahl, 2017). A partial mechanistic explanation for this is Notch signaling activity upregulates the expression of the *Hes1* gene, which functions as a transcriptional repressor of the *MyoD* gene, which produces the MyoD protein, a TF that has critical activity for skeletal muscle development (Berkes and Tapscott, 2005; Kuroda et al., 1999). Without *MyoD* expression, the somite-derived precursor cells will fail to differentiate into skeletal muscle cells, and instead favor adopting an endothelial cell fate (Siebel and Lendahl, 2017). This simplified gene regulatory network (i.e. Notch activates *Hes1*, *Hes1* represses *MyoD*, repressed *MyoD* fails to promote skeletal muscle development) highlights the role that signaling pathways have in regulating cellular behavior through gene expression. In this example, *Hes1* is one of many genes that are regulated by Notch signaling to control skeletal muscle/endothelial differentiation. Additionally, Notch signaling is active in nearly every other tissue types at

multiple points throughout development, activating different sets of genes within each context (Siebel and Lendahl, 2017). This general notion is applicable for all signaling pathways. Thus, an integral part of understanding how signaling pathways function is understanding how they regulate their target gene expression.

Regulation of gene expression

A gene is a DNA sequence that stores information for the creation of one or more RNA/protein molecules (Portin and Wilkins, 2017). Gene expression is the act of accessing and processing this genetic information into an RNA molecule (a process termed transcription), with the end goal of translating this RNA into a protein (Buccitelli and Selbach, 2020), although sometimes the RNA molecule is the functional end product. As proteins perform most of the work of living cells, proper cellular function requires that the correct proteins be present in the correct amounts. There are approximately 20,000 protein-coding genes in the human genome and many of these genes code for proteins which have antagonistic functions or can inappropriately drive cell death (Gates et al., 2021). As a result, gene expression needs to be coordinated such that the proper protein content of a cell is produced, which is a complex task.

Cis-regulatory elements (CREs) are relatively short DNA sequences that control gene expression through TF binding. Two well-studied classes of CREs are enhancers and promoters (Wittkopp and Kalay, 2012). Promoters are present directly upstream of the transcription start site of a gene, and are important for regulating the precise location of the transcription start site and the direction of transcription (Andersson and Sandelin, 2020). Enhancer elements are bound by tissue-specific transcription factors and regulate the spatial and temporal expression of genes by acting with their cognate promoters. Traditionally, enhancer function is said to not be constrained by orientation or distance, allowing them to regulate promoters/genes in distant genomic locations (Panigrahi and O'Malley, 2021). More recent work has shown that enhancers tend to act on promoters that are present within the same topologically associated domain (TAD). TADs can inhibit enhancer activity on a promoter within a different TAD, therefore TAD architecture can add some distance constraint to enhancer function (Cavalheiro et al., 2021). Fully understanding promoter and enhancer function requires a nuanced view of

these elements. There are many examples of promoters with enhancer function, some enhancers are transcribed by RNA pol II, and the chromatin signature between these two elements are generally similar (Andersson and Sandelin, 2020). These facts highlight the complex nature of gene regulation and the difficulty of trying to define discreet genomic elements or events. However, for a general overview, it is sufficient to treat enhancers and promoters as distinct genomic elements.

Assembly of the transcriptional pre-initiation complex (PIC) on promoters is a critical step in the activation of transcription (Malik and Roeder, 2023). It is during this step that RNA pol II, the enzyme that synthesizes RNA from a DNA template, gets recruited to promoters. For many promoters that regulate protein-coding genes, PIC assembly is initiated by TATA binding protein (TBP) binding to the core promoter (Malik and Roeder, 2023). This triggers the recruitment of the general transcription factors (TFII A, B, D, E, F, and H) which in turn recruit RNA pol II to the promoter (Orphanides et al., 1996). Once fully assembled on the promoter, the PIC can then be activated by cell type-specific and gene-specific regulatory inputs, allowing for productive RNA synthesis (Malik and Roeder, 2023).

Enhancers are relatively small (typically 50 to several hundred base-pairs) elements that are comprised of clusters of TF binding sites (Spitz and Furlong, 2012). Enhancer activity is regulated by tissue specific TF binding. Activating enhancers typically requires a combinatorial input from different types of TFs, which partially explains how enhancers are able to control the spatiotemporal expression of genes (Spitz and Furlong, 2012). The flexible billboard model is a common model to explain the coordinated effects of TF binding on enhancer activity and it is supported by a considerable amount of experimental evidence. This model emphasizes that it is the ability of an enhancer to recruit the correct TFs to chromatin that is paramount to its function, and the orientation or spacing between TFs on the chromatin is not functionally relevant. This includes TFs binding directly to DNA and TFs recruited through protein-protein interactions with DNA-bound TFs (Vockley et al., 2017).

Once bound to an enhancer, TFs are bound by additional co-regulators to regulate target gene expression. Transcriptional co-regulators have a variety of functions, including modifying the accessibility of DNA to serving as linkers between

proteins that are bound to enhancers and promoters. DNA is packaged in the nucleus by histone proteins to form a structure that is called a nucleosome. In a nucleosome, DNA is wrapped around the histone octamer, rendering it inaccessible to most protein binding, yet transcription requires that DNA is accessible. Swi/Snf complexes are referred to as chromatin remodelers because they bind to a broad array of transcription factors and function to slide or evict histone proteins from DNA. This increases the underlying DNAs accessibility to protein binding (Wilson and Roberts, 2011). Importantly, chromatin remodelers do not evict all histone proteins from enhancer and promoter elements. The remaining histones are post-translationally modified on the histone 'tail' by additional co-regulators that are also recruited to TFs. These modifications mark actively expressed or repressed regulatory elements or genes. Histone acetylation is catalyzed by histone acetyltransferases, such as CBP/p300, and this mark is highly correlated with active regulatory elements and genes (Bose et al., 2017; Martin et al., 2021; Ogryzko et al., 1996; Zhang et al., 2015). Histone methylation is catalyzed by histone methyltransferases, such as the EZH2 subunit of the Polycomb repressive complex, and methyl marks are present at both active and inactive genetic elements (Simon and Lange, 2008). For example, the H3K27me3 is present at repressed elements, and H3K4me3 is present at sites of active transcription (Cai et al., 2021; Greer and Shi, 2012; Wang et al., 2023). Additionally, the Mediator complex is a transcriptional co-regulator that serves as a scaffold between transcription factors bound at enhancer elements and the PIC at the promoter (Soutourina, 2018). As there can be large genomic distances between enhancers and the genes they regulate, ensuring that enhancers come in close physical proximity to their cognate promoters is a complex task (Schoenfelder and Fraser, 2019). The mediator complex is part of the mechanism of that process and, as a result, is generally required for transcription (Soutourina, 2018). These examples illustrate some, but not all, of the transcriptional co-regulators that are involved in gene expression.

There are many proteins involved in regulating gene expression. The general transcription factors and TBP are important for positioning RNA pol II at the promoter. Enhancer-bound, tissue-specific transcription factors, which are also bound by many transcriptional co-regulators are brought into proximity to the promoter by proteins such

as the mediator complex. Ultimately, it is the interaction between proteins bound at the enhancer and proteins bound at the promoter that allows for RNA pol II to be released into the gene body for productive transcription. Each protein interaction in the gene expression process involves a degree of regulation, so overall, there is an extensive degree of regulation involved in this process.

The Wnt/β-catenin signaling pathway

From sponges to humans, Wnt signaling is highly conserved in metazoa. Perhaps reflected in its deep evolutionary conservation, proper function of this pathway is necessary for animal life, as Wnt signaling is required for development and maintenance of adult tissues. Misregulation of Wnt signaling during development can be lethal at the embryonic level and, at the adult stage, misregulation is implicated in cancer etiology of many types of cancers (Grigoryan et al., 2008; Zhan et al., 2017). Wnt signaling can be categorized into several different pathways, such as Wnt/Ca^{2+}, which utilizes calcium as a second messenger, and Wnt/Planar cell polarity (PCP), which signals through the proteins Van Gogh and Van Gogh-like. These pathways are just two examples of what is commonly referred to as 'noncanonical' Wnt signaling (De, 2011; Yang and Mlodzik, 2015). The focus here will be on the Wnt/β-catenin pathway, the so-called 'canonical' Wnt signaling pathway (Fig 1.1). This pathway is responsible for regulating essential cellular processes such as cell fate decisions, mitosis, and gene expression (Rim et al., 2022). Given its broad role in metazoan life, the Wnt/β-catenin pathway is an excellent context to study basic biological principles such as signal transduction and transcriptional regulation.

Wnts are secreted proteins that act on cell surface receptors to activate an intracellular signal transduction cascade (Rim et al., 2022). Wnt/β-catenin signaling is said to be 'off' when there is not a binding event between Wnt proteins and the Frizzled (Fzd) and LDL related receptor protein 5/6 (LRP5/6). The relevant cytoplasmic event that occurs when the pathway is 'off' is the constant synthesis and degradation of β-catenin. β-catenin is synthesized, and then phosphorylated by a multi-subunit complex that is termed the 'destruction complex.' Important constituent proteins of the destruction complex are Adenomatous polyposis coli (APC), which binds to β-catenin; Axin, a

scaffold protein; and the kinases Casein Kinase 1 (CK1) and Glycogen Synthase Kinase 3 (GSK3). β-catenin is phosphorylated by a dual-kinase mechanism which begins with CK1 phosphorylating the serine 45 (S45) residue, followed by GSK3 phosphorylating threonine 41 (T41), S37 and S33. Following phosphorylation, β-catenin is polyubiquitinated and subsequently degraded by the proteasome (Jung and Park, 2020). The net effect is that β-catenin levels in the cytosol are kept low.

When Wnt proteins bind to the co-receptors Frizzled (Fzd) and Low-density Lipoprotein Related Receptor protein 5/6 (LRP 5/6), the pathway is said to be 'on' (Rim et al., 2022). When the pathway is activated, the major cytoplasmic event that occurs is the inhibition of the destruction complex. The mechanism by which this occurs is not fully understood, but a leading model proposes that the Disheveled (Dvl) protein binds to the intracellular domains of Fzd/LRP5/6 when they are bound by Wnt protein. This allows for recruitment of the destruction complex to the cell membrane, which inactivates it (Rim et al., 2022). Once the destruction complex is inhibited, β-catenin concentration increases in the cytoplasm, and subsequently translocates to the nucleus where it functions as a transcriptional co-regulator.

Wnts are traditionally thought to be morphogens, which are secreted proteins that establish a gradient in tissue, and cells within the tissue respond to the morphogen signal in a concentration-dependent manner (Simsek and Özbudak, 2022). This idea is supported by immunostainings showing gradients of Wg/Wnt protein emanating from Wg/Wnt-producing cells in embryos and larval imaginal discs (Cadigan et al., 1998; Strigini and Cohen, 2000; van den Heuvel et al., 1989). However, when the hypothesis that Wnts were a morphogen was directly tested by creating a fly that expressed a plasma membrane-tethered Wnt mutant (NRT-Wg), it was realized that perhaps secretion of Wnts may be dispensable, as the flies were mostly normal, which was a controversial find (Alexandre et al., 2014). The *Drosophila* do exhibit some phenotypes, as the adults are sterile and there is a minor developmental delay (Stewart et al., 2019). More recently, additional evidence shows that specific tissues within the fly show more severe defects, such as the midgut-hindgut boundary of the fly intestines (Tian et al., 2019). Part of the controversy over Wnt's function as a morphogen stems from the fact that studying Wnt diffusion through tissue is historically difficult. There is a lack of visual

evidence and tagging Wnts with fluorescent proteins affects their biological activity. Perhaps the tissues that are affected the most require long-range Wnt signaling and tissues that are minimally affected require short-range signaling, which is less likely to be disrupted by NRT-Wg (Stewart et al., 2019).

TCF/LEF's role in the transcriptional Regulation of Wnt/β-catenin target genes

The primary output of Wnt/β-catenin signaling is the differential regulation of the pathway's target genes. TCF/LEF-family TFs and β-catenin function as the primary regulators of target gene expression (Anthony et al., 2020). Gene regulation by Wnt/β-catenin signaling is typically presented as a transcriptional 'switch.' When Wnt signaling is off, DNA-bound TCF/LEFs bind to transcriptional co-repressors, such as Transducin-Like Enhancer of split (TLE) proteins, to keep basal gene expression repressed. When Wnt signaling is activated, β-catenin localizes to the nucleus, binds to TCF/LEFs, and activates gene expression (Ramakrishnan et al., 2018). Invertebrates typically have one TCF/LEF, which therefore functions as both a transcriptional repressor and activator, dependent on context. Mammals, on the other hand, have four TCF/LEFs, which allows for some degree of functional specialization. For example, TCF3 primarily functions as a transcriptional repressor and LEF1 primarily functions as a transcriptional activator (Cadigan and Waterman, 2012).

The transcriptional switch isn't the only mechanism that can describe Wnt/β-catenin target gene regulation. In the *Drosophila* Kc167 cell line only ~37.5% of genes which are activated by Wnt/β-catenin signaling (termed Wingless, Wg, signaling in *Drosophila*) are de-repressed by the loss of Pangolin (Pan, the *Drosophila* ortholog of LEF1) (Franz et al., 2017). In human HEK293T cells with all four TCF/LEF proteins knocked out, dysregulation of Wnt/β-catenin target gene expression is observed, but the degree to which de-repression is occurring is currently unknown (Doumpas et al., 2019, 2021). The observations in *Drosophila* suggest that the transcriptional switch model, though broadly discussed, may only represent a minority of Wg target genes. Most Wg target genes in the Kc167 cell line likely follow a more 'traditional' model of transcriptional regulation in which the basal rate of gene expression is enhanced when the gene's enhancers are activated.

Of all the WREs that were identified by self-transcribing active regulatory region sequencing (STARR-seq) in the Kc167 cell line, approximately 80% did not respond to Wg signaling when Pan was knocked out. The remaining 20% exhibited significantly reduced activity (Franz et al., 2017). This observation is consistent with published Chromatin immunoprecipitation (ChIP) experiments showing that Wg signaling increases Pan localization to an intronic WRE that regulates the gene *naked cuticle* (*nkd*). When Wg signaling is off, this WRE exhibits weak levels of Pan binding (Fang et al., 2006; Parker et al., 2008). Interestingly, *nkd* is strongly de-repressed in Pan knockout Kc167 cells, suggesting that weak Pan localization to a WRE is sufficient to repress Wnt target gene basal transcription (Franz et al., 2017). The observation that Wg signaling increases Pan localization to WREs contradicts the popular 'switch' model, which suggests that Pan is always localized to WREs.

Most TCF/LEF proteins contain two DNA binding domains: the HMG domain, which binds to the HMG recognition site, and a C-clamp, which binds to 'helper' sites (Archbold et al., 2014). In *C. elegans*, select WREs require both HMG recognition sites and helper sites for maximum target gene expression, while the presence of helper sites is not required for repression (Bhambhani et al., 2014). Studies in *Drosophila* have also shown that the C-clamp was required for developmental readouts consistent with active Wg signaling, but was not required for repression (Bhambhani et al., 2014). Additionally, the C-clamp enhances TCF/LEF affinity for DNA (M. V. Chang et al., 2008; Ravindranath and Cadigan, 2014). These results suggest a model in which weak localization of TCF/LEF to WREs is sufficient for repression, but strong, Wnt/Wg-induced localization is required for transcriptional activation.

As previously mentioned, mammals have four TCF/LEF proteins: TCF1, LEF1, TCF3, and TCF4 (Hrckulak et al., 2016). LEF1 primarily functions as an activator, TCF3 primarily functions as a repressor, and TCF1 and TCF4 exhibit both functions, depending on the context and isoform being studied (Mao and Byers, 2011). The expression of multiple TCF/LEF family members adds another layer of complexity to Wnt gene regulation. For example, during *Xenopus* gastrulation, Wnt signaling promotes the phosphorylation of the *Xenopus* ortholog of TCF3 (xTCF3), decreasing it's affinity for WREs and thereby de-repressing xTCF3 regulated genes (Hikasa et al.,

2010; Hikasa and Sokol, 2011). In this context, it was also observed that xTCF1 was required for maximizing target gene expression/de-repression (Yi et al., 2011), suggesting a mechanism in which Wnt signaling promotes the swapping of TCF3 with TCF1 to facilitate the switch from target gene repression to activation. It's likely that this mechanism for vertebrate Wnt target gene expression is not broadly generalizable, but it does illustrate an increasing complexity of TCF/LEF function.

Enhancers are clusters of TF binding sites that can confer some type of specificity, i.e., tissue or temporal, to the expression of their cognate promoters. Since the discovery of the SV40 enhancer more than 40 years ago, trying to understand the 'grammar' of TF binding that leads to enhancer activity has been a fundamental topic of gene regulation (Banerji et al., 1981; Jindal and Farley, 2021). Perhaps the most insightful model for TF binding site grammar is the 'flexible billboard' model. This model of enhancer activity emphasizes the importance of TF localization to enhancer chromatin. It proposes that TF binding site order and orientation is not important for activity, but rather, it is primarily the direct and indirect TF binding that promotes enhancer activation (Arnosti and Kulkarni, 2005; Spitz and Furlong, 2012; Swanson et al., 2010).

Consistent with the flexible billboard model, WREs that regulate Wnt target genes exhibit different TCF/LEF binding site patterns. In the *Drosophila* Kc167 cell line, two WREs that simultaneously regulate *nkd*, termed UpE and IntE, differ in both the number and relative positions of Pan sites (Archbold et al., 2014; J. L. Chang et al., 2008). There is also no consistency between WREs that regulate *nkd* and another Wg target gene, *notum* (Archbold et al., 2014). Presumably the TFs that regulate these WREs in addition to Pan exhibit no consistent pattern. This has also been observed in humans. At some WREs, TCF/LEFs work with Sox9 and CDX TFs and no specific pattern of TF binding site motifs is observed. The idea that the specificity that enhancer elements confer to gene expression is reflected in TF binding site patterns is an attractive one, but not supported by current evidence (Ramakrishnan et al., 2023, 2021).

β-catenin's role in the transcriptional Regulation of Wnt/β-catenin target genes

The most important step in converting TCF/LEFs into transcriptional activators is the binding of β-catenin. Once bound to TCF/LEFs at WRE chromatin, β-catenin's primary function is to recruit additional transcriptional co-regulators to affect Wnt target gene expression (Rim et al., 2022). β-catenin can be divided into 3 domains: The intrinsically disordered N-terminal domain, a structured, central armadillo repeat domain, and an intrinsically disordered C-terminal domain. Each domain has distinct functions that are important for β-catenin's activity in the nucleus (Fig 1.2).

β-catenin's central armadillo repeat region (amino acids 141-664 in human β-catenin) is comprised of 12 imperfect armadillo repeats (Mosimann et al., 2009). β-catenin binds to the N-terminus of TCF/LEFs through repeats 3-9, and the specific amino acids that mediate this interaction have been identified with X-ray crystallography (Graham et al., 2000; Poy et al., 2001; Valenta et al., 2012). These repeats are also important for binding to other β-catenin interactors, such as α-catenin and e-cadherin, but these binding partners do not have a role in transcription (Valenta et al., 2012). BCL9, a transcriptional co-activator that is required for Wnt target gene expression, binds to β-catenin at armadillo repeat 1 (De La Roche et al., 2008; Sampietro et al., 2006a). Repeat 12 is also important for binding to many transcriptional co-regulators that bind to the C-terminus of β-catenin (Valenta et al., 2012). Overall, the generally accepted function of this region is to facilitate protein-protein interactions.

The N-terminal domain of β-catenin (amino acids 1-141) is important for regulating the stability of the protein. As stated previously, when Wnt signaling is off, amino acid residues S45, T41, S37, and S33 are phosphorylated by kinases within the destruction complex to prime the protein for proteasomal degradation (Jung and Park, 2020). Exon 3 of the *CTNNB1* (β-catenin) gene codes for amino acids 5-75, and is a mutation/deletion hotspot for cancer associated alleles (Kim and Jeong, 2019). Mutating the serine and threonine residues that are phosphorylated has a stabilizing/activating effect, due to the inability of the destruction complex to post-translationally modify β-catenin. Inappropriate activation of β-catenin is associated with many cancers, partially

as a result of β-catenin's ability to drive cell proliferation and differentiation (Zhang and Wang, 2020).

According to current β-catenin dogma, the N-terminal domain is not important for transcriptional function. However, there is a small amount of evidence from the late 1990's that suggest that the N-terminal domain has a transcriptional role. It was observed that increasingly severe deletions affecting the N-terminus (Δ1-47, 1-89, 1-132), progressively inhibit the activation of TopFlash, a sensitive Wnt reporter, in a rat cell line (Kolligs et al., 1999). Although it appears that the N-terminal deletion mutants are less stable than full-length β-catenin, confounding experimental results. It was also observed that a C-terminal domain deletion (Δ696-781) was able to weakly activate TopFlash, suggesting that the N-terminus has weak transcriptional activity (Hsu et al., 1998). However, endogenous β-catenin may be affecting this result and limiting interpretation. The N-terminus of β-catenin was also shown to interact with TATA-binding protein (TBP), but TBP can also interact with domains within the armadillo repeat region and the C-terminus, making this site not necessarily required for function (Hecht et al., 1999). Due to significant confounding variables in these experiments, the idea that the N-terminus was involved in transcriptional regulation fell out of favor over the past two decades. Particularly when studies began to show that transcriptional co-activators preferentially bound to the C-terminal domain.

The C-terminus of β-catenin is primarily thought to be important for regulating transcription. This region primarily serves as a platform to recruit additional transcriptional co-regulators to WRE chromatin. Swi/Snf chromatin remodelers, the histone acetyltransferases CBP/p300, components of the RNA pol II pre-initiation complex, Mediator complex subunits, and more, all bind to the last armadillo repeat and the disordered C-terminal domain (Valenta et al., 2012). C-terminal domain deletion mutants fail to activate Wnt reporters and endogenous genes (Cong et al., 2003; Hecht et al., 1999). Unlike the N-terminus, mutations to the C-terminus would be predicted to inactivate β-catenin function, as they can potentially inhibit co-activator binding that is required for transcription.

The primary mode of β-catenin localization to WREs is traditionally thought to occur through direct binding to TCF/LEFs. Recent work has shown that β-catenin's terminal IDRs are sufficient for localization to WREs (Zamudio et al., 2019). A chimeric protein consisting of GFP flanked by β-catenin's N- and C-terminal IDRs was detected at super-enhancers and typical enhancers by ChIP-seq in mouse embryonic stem cells (Zamudio et al., 2019). This data cannot be explained by current, commonly accepted models of β-catenin function because the IDRs are not known to interact with TCF/LEFs. The authors of this study propose a new model in which biomolecular condensates formed by transcriptional co-regulators can interact with β-catenin's IDRs and recruit it to active enhancers.

Biomolecular condensates in transcriptional regulation

Biomolecular condensates (BMCs) are dynamic, membraneless cellular compartments that are comprised of proteins and nucleic acids in high local concentrations relative to the cytoplasm or nucleoplasm (Sabari et al., 2020). They are typically thought to be formed through a liquid-liquid phase separation (LLPS) mechanism and can exhibit a spectrum of material properties from liquid-like to gel-like and even solid amyloids (Woodruff et al., 2018). Low affinity, multivalent interactions between the IDRs of constituent molecules have been identified as drivers of LLPS/BMC formation (Alberti et al., 2019; Sabari et al., 2020). Interactions among IDRs that are thought to lead to BMC formation are primarily π-π, π-cation, and electrostatic (Sabari et al., 2020). Functionally, BMCs are thought to potentiate or inhibit biochemical reactions by concentrating and compartmentalizing proteins (Sabari et al., 2020). BMCs have generated an intense research interest over the last several years, perhaps because many proteins appear to be able to form BMCs and it is an intuitive model to explain complex biological processes such as transcription.

Transcription is an intensely regulated process involving hundreds of proteins and various nucleic acid species (Cramer, 2019; Sabari, 2020). Adding a BMC-centric model to transcriptional regulation is appealing because it can help explain how proteins become concentrated at cis-regulatory regions and interact with each other to preform necessary functions. Many proteins necessary for transcription have been shown to form BMCs *in vitro*, *in vivo*, or both. Including, but not limited to, RNA pol II (Lewis et al.,

2023; Palacio and Taatjes, 2022), p300 (Zhang et al., 2021), and mediator complex subunits (Cho et al., 2018).

Beyond just functioning to localize proteins to chromatin, BMCs are also thought to be involved in regulating dynamic transcriptional processes such as bursting (Palacio and Taatjes, 2022). Productive transcription is known to occur in series of discontinuous bursts that is linked to enhancer-promoter interactions (Fukaya et al., 2016). Previous work has shown that RNA pol II nuclear clusters are dynamic and short lived, but upon transcriptional stimulation, the lifetime of the clusters positively correlates with increased RNA pol II gene loading (Cho et al., 2016; Cisse et al., 2013). Eventually, the cluster is depleted, and RNA pol II loading onto the gene is halted.

Recent work suggests that RNA pol II clusters at promoters may be BMCs (Palacio and Taatjes, 2022). These clusters exhibit the usual properties of BMCs, as they are dynamic, and the disordered RNA pol II C-terminal domain has been shown to form condensates *in vitro* and is important for clustering *in vivo* (see Table 1.1 for common experimental approaches to identify BMCs) (Boehning et al., 2018; Cho et al., 2016). A putative model is that RNA pol II BMCs concentrate RNA pol II molecules at promoter regions. Upon receiving a transcription signal, RNA pol II molecules are rapidly released from the condensate into the gene body until the condensate is depleted and a refractory period is reached (Palacio and Taatjes, 2022). This exemplifies how BMCs can provide mechanistic insights into biological questions beyond ‘enhancer and promoter interactions.’

Mechanisms invoking BMC formation should be carefully analyzed as the difference between protein clusters formed by site-specific interactions and ones formed by phase separation are often difficult to experimentally delineate (Musacchio, 2022). For example, sites of active transcription are known to form distinct foci that are often called ‘transcription factories’ (Palacio and Taatjes, 2022). Transcription factories are known to have a high local concentration of RNA pol II and other factors that are required for transcription. Site-specific protein interactions, the traditional conception of protein-protein interactions, are sufficient to create functional, high-density protein clusters (Musacchio, 2022). Spherical clusters of RNA pol II have been shown to coalesce *in vivo*, along with other physical properties suggesting that RNA pol II clusters

in the nucleus have liquid-like properties consistent with BMCs (Cho et al., 2018; Flores-Solis et al., 2023; Sabari et al., 2018). Functionally, the strongest evidence that RNA pol II BMCs are involved in transcription is the observation that the presence of RNA pol II clusters/BMCs co-localize with sites of active transcription (Cho et al., 2016). Currently, there does not appear to be any published experiments directly testing whether the ability of RNA pol II to form clusters/BMCs is required for transcription, and furthermore, it is unknown whether the expression of all genes requires BMC formation (Palacio and Taatjes, 2022).

Biomolecular condensates in the Destruction Complex

In the cytoplasm, BMCs have been broadly evoked as part of positive and negative regulatory mechanisms for Wnt signaling and suggested to have a role in almost every level of the signal transduction cascade (Schaefer and Peifer, 2019). The focus here will be on Disheveled (Dvl) and Axin, which have long been known to form punctate structures in the cytoplasm when overexpressed (Cliffe et al., 2003; Schaefer and Peifer, 2019). The presence of these structures is correlated with activity, but considerations of the material properties of the puncta and its effect on Wnt signaling is a relatively recent phenomenon (Schaefer and Peifer, 2019).

Axin and Dvl are both known to undergo head-to-tail polymerization via their DIX domains (Schwarz-Romond et al., 2007). Polymerization is an important aspect of function for both proteins, as DIX domain mutations that disrupt polymerization also disrupt function (Fiedler et al., 2011; Schaefer and Peifer, 2019; Schwarz-Romond et al., 2007). Recent experimental efforts have focused on determining whether these Axin and Dvl polymers are BMCs. Axin1 and Dvl2 have been shown to form BMCs *in vitro* (Kang et al., 2022; Nong et al., 2021). In these experiments, the DIX domain was required for Dvl2 BMC formation, but was dispensable for Axin1, which suggests separate mechanisms for Axin1 polymerization and BMC formation. *In vivo,* primary evidence of BMC formation for both proteins is the presence of puncta (Kang et al., 2022; Nong et al., 2021), and Dvl2 puncta are shown to be regulated by Wnt signaling (Schubert et al., 2022). Both of these proteins can co-localize in the same puncta, which is consistent with their function in the destruction complex (Schubert et al., 2022).

Currently, it is difficult to discern the difference between spherical polymers of Axin and Dvl and BMCs. Additional future experiments will be needed to address this difference.

Puncta in the cytoplasm that are formed with the overexpression of an Axin1 IDR can be co-localized with APC, GSK3β, CK1α, and β-catenin (Nong et al., 2021). An increase β-catenin phosphorylation is correlated with the presence of puncta, suggesting a role in the functionality of the destruction complex. Overexpression of other domains of Axin1 which do not form puncta are not correlated with increases in β-catenin phosphorylation (Nong et al., 2021). Dvl2 forms puncta at near-physiological expression levels, which co-localize with Axin1 and APC and promote destruction complex function at the centrosomes (Schubert et al., 2022). Current limitations of these studies are a reliance on correlations between the presence of puncta and functional readouts. With current technology, it is extremely difficult to pinpoint BMCs as the site of the readout. For example, an Axin1 BMC as the site of β-catenin phosphorylation. Further studies will need to definitively show that BMCs are indeed potentiating protein function.

Biomolecular condensates in Wnt/β-catenin target gene regulation

LEF1 and β-catenin have both been shown to form BMCs, which are linked to transcriptional function (Zamudio et al., 2019; Zhao et al., 2023). BMC regulation of Wnt target gene expression is a fresh aspect of Wnt biology, as there are only two publications in this specific field (Zamudio et al., 2019; Zhao et al., 2023) and one additional publication describing the role of BMCs in regulating TCF1's role in T cell development (Goldman et al., 2023).

LEF1 forms BMCs *in vitro* and *in vivo*, which co-localize with β-catenin in both contexts, suggesting transcriptional relevancy (Zhao et al., 2023). Deletion mutants that affect LEF1's central IDR compromise its ability to form BMCs, which correlates with a failure to activate a Wnt reporter gene. Additionally, Lef1 overexpression in a colorectal cancer cell line (HCT116) promotes colony formation while the central IDR deletion mutant does not. This indicates compromised transcriptional function, presumably through a failure to form BMCs (Zhao et al., 2023). This work provides a strong

correlation between LEF1 BMCs but does not directly show that BMCs are required for LEF1 function.

Experiments that substitute a protein's endogenous IDR with a heterologous IDR and show function while maintaining the ability to form BMCs establish strong evidence for a role that involves BMCs. For TCF/LEFs, it was observed that the transcriptional defect caused by a small deletion in TCF1's central IDR, which is analogous to the LEF1 IDR, is rescued by substitution with a heterologous IDR from the protein Early B-cell Factor 1 (Goldman et al., 2023). The assumption here is that the heterologous IDR will be unable to perform the protein's usual functions and only promote BMC formation. In the TCF1 example, Goldman and colleagues used a heterologous IDR from EBF1, which is a TF. This is not ideal, as a heterologous IDR from another TF has a higher probability of having a transcriptional function in addition to the ability to promote BMC formation. A stronger candidate would be an IDR from a protein with no known nuclear function. In addition, Goldman and colleagues did not show that their heterologous IDR TCF1 mutant could form BMCs either *in vitro* or *in vivo*, and therefore the mechanism of rescue for this construct is still ambiguous.

The N- and C-termini of β-catenin are IDRs, flanking a highly structured armadillo repeat region. Both IDRs are necessary and sufficient for BMC formation by β-catenin, and more specifically, it is the aromatic amino acid residues within the IDRs that drive BMC formation (Zamudio et al., 2019). Zamudio and colleagues convincingly show that β-catenin forms BMCs *in vitro* and *in vivo*. The evidence suggests that in addition to LEF1, β-catenin condensates can co-localize with an IDR from the Med1 subunit of the Mediator complex, and that nuclear β-catenin foci also co-localize with *nanog* RNA, suggesting transcriptional relevancy.

A β-catenin construct with mutated aromatic residues within its IDRs is defective in forming BMCs *in vitro*, which correlates with reduced activity of a sensitive Wnt transcriptional reporter and endogenous Wnt target genes (Zamudio et al., 2019). Interestingly, Zamudio and colleagues report that β-catenin's IDRs are sufficient for localization to WREs, as a chimeric protein consisting of GFP flanked by β-catenin's N- and C-terminal IDRs can be identified at WREs via ChIP-seq. This data immediately suggests that the Wnt gene regulation dogma, which suggests that interactions between

TCF/LEF and β-catenin's armadillo repeat region is required for WRE localization, needs to be updated.

It's tempting to link the correlation of β-catenin BMCs and gene regulatory function, but there are still some key points that need to be addressed. β-catenin does not have a canonical NLS, and a specific mechanism of nuclear import is not known (Lu et al., 2021). Therefore, the aromatic mutations can potentially inhibit β-catenin nuclear localization, providing a strong alternative hypothesis to aromatic mutations inhibit β-catenin transcriptional activity through a BMC mechanism. Additionally, endogenous β-catenin may be recruiting the GFP-β-catenin IDR chimera to WREs. Clearly, additional experiments need to be performed to increase confidence in a BMC model for Wnt target gene regulation, but the field is new and exciting and can potentially uncover a novel mechanism for β-catenin function.

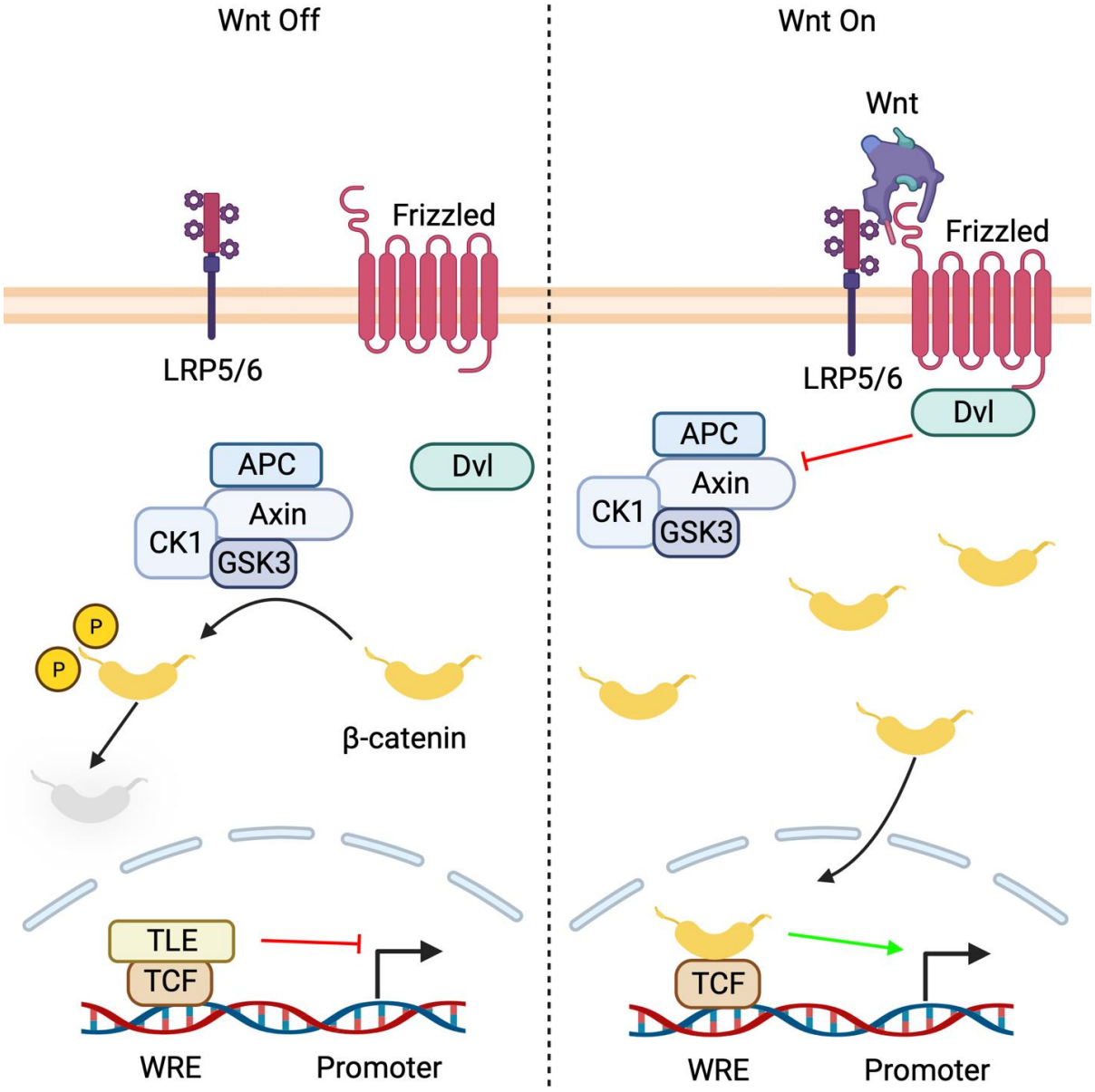

Fig 1.1. A simplified molecular overview of the Wnt/β-catenin signaling pathway. In the absence of a Wnt protein binding to the Frizzled and LRP5/6 receptors, Wnt signaling is 'off.' β-catenin is continually synthesized, phosphorylated by the destruction complex containing Axin, APC, CK1, and GSK3, and degraded by the proteasome. The net effect is that cytoplasmic β-catenin levels are kept low, and the expression of Wnt target genes is inhibited. When Wnt protein binds to the Frizzled and LRP5/6 receptors, the pathway is activated, the destruction complex is inhibited, cytoplasmic β-catenin levels increase, β-catenin translocates to the nucleus and activates Wnt target genes. Figure created with Biorender.com.

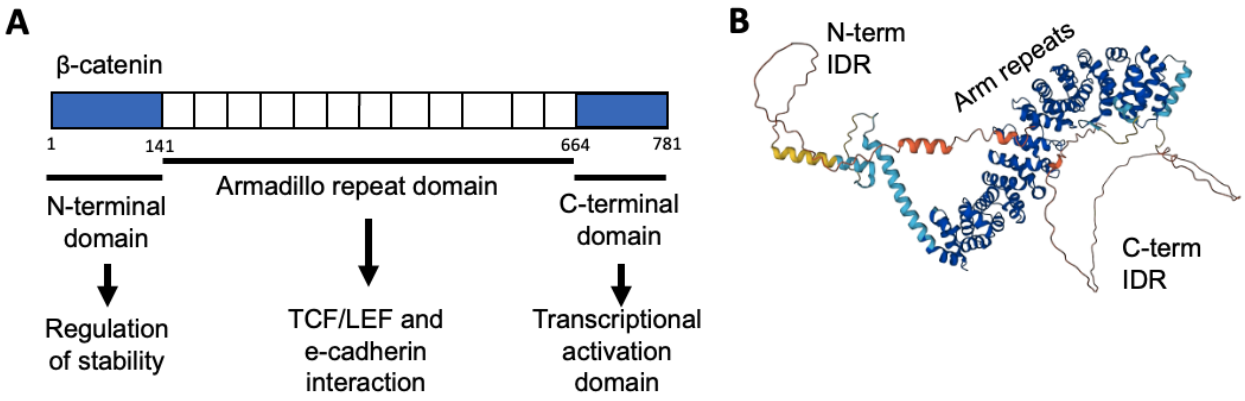

Fig 1.2. Structural representations of β-catenin. (**A**) A cartoon of β-catenin depicting it's 3 main domains and their generally accepted functions. (**B**) An AlphaFold predicted 3D structure of β-catenin, depicting the N-terminal IDR, the central, highly structured, Armadillo repeat region (Arm repeats), and the C-terminal IDR.

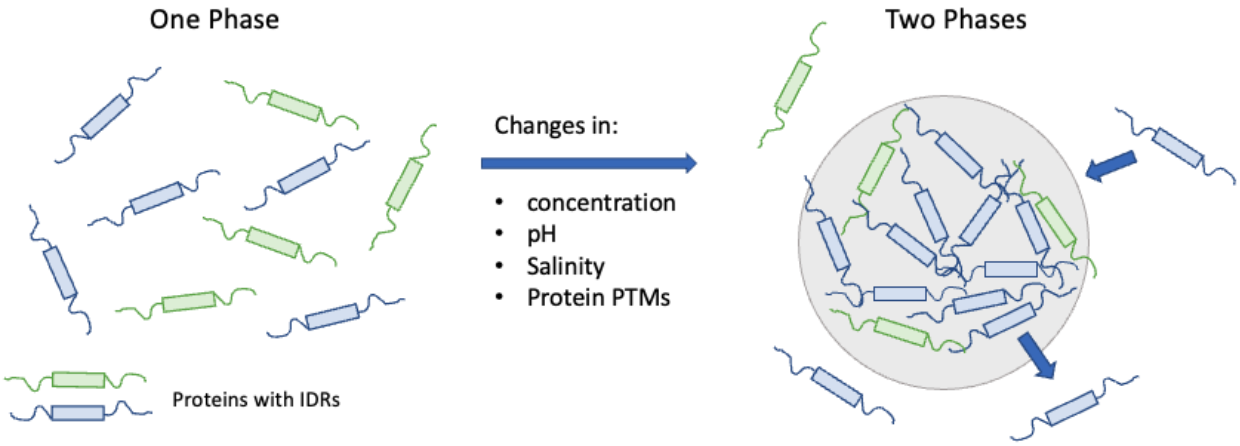

Fig 1.3. Liquid-liquid phase separation of proteins. Some proteins in solution or cells can form liquid-liquid phase separated (LLPS) biomolecular condensates. Changes in cellular or protein states, such as pH, salinity, protein post-translational modifications (PTMs), or concentration can trigger the clustering of proteins into two phases: a concentrated phase and a dilute phase. The concentrated phase is sometimes referred to as a biomolecular condensate. Biomolecular condensates are dynamic, meaning that proteins can enter and exit, and typically exhibits liquid-like properties, such as internal mixing. Protein interactions that lead to biomolecular condensate formation are thought to occur through IDRs.

Experimental Approach	Pros	Cons
In vitro droplet formation assay	• Biochemically establishes BMC formation. • Concentration-dependent testing of proteins. • Easy to generate and test mutants. • Can test single or defined combinations of proteins.	• Not physiologically relevant. • Frequently utilizes molecular crowding agents. • Purified proteins do not capture all interactions that would occur *in vivo*.
Fluorescence recovery after photobleaching	• Tests material properties of BMCs. • Can be performed *in vivo* or *in vitro*.	• Difficult to determine if recovery is due to internal mixing of BMC or protein exchange with dilute phase. • Factors that are unrelated to BMC material properties also affect recovery, such as size of photobleached area and size of photobleached droplet.
Sensitivity to 1,6-hexanediol	• Chemical disruptor of BMCs.	• Poorly characterized mechanism of action, thought to disrupt hydrophobic interactions that lead to BMC formation. • Limited use *in vivo*, toxic to cells.
Presence of puncta *in vivo*	• Establishes BMC formation *in vivo*. • More physiologically relevant than *in vitro* droplets.	• Unable to determine material properties of puncta if cells are fixed prior to imaging. • Unable to determine if puncta are functional. • Unclear if forces that drive BMC formation *in vivo* are the same as *in vitro*.
Coalescing puncta *in vivo*	• *In vivo* evidence for presence of liquid-like BMCs. • Shows surface tension and viscosity of droplets.	• BMCs that do not have liquid-like properties will not pass this assay.

Table 1.1. Common experimental approaches to assay BMCs and their pros and cons.

Chapter 2 β-catenin-mediated Activation of Wnt Target Genes Utilizes a Biomolecular Condensate-dependent Mechanism

This chapter is reprinted from Stewart, R. A., Goodman, L. B., Tran, J. J., Zientko, J. P., Sabu, M., Jeon, U. S., & Cadigan, K. M. (2023). Beta-catenin-mediated activation of Wnt target genes utilizes a biomolecular condensate-dependent mechanism. bioRxiv, 2023-10. https://doi.org/10.1101/2023.10.09.561634. At the time of writing, this article has not undergone a full peer review process.

Introduction

The Wnt/β-catenin signaling pathway is evolutionarily conserved across metazoans and is indispensable for organismal development and a variety of adult tissue functions (Archbold et al., 2012; Rim et al., 2022). The primary output of this pathway is the differential regulation of gene expression programs, which is accomplished through the nuclear accumulation of β-catenin, a transcriptional co-regulator. β-catenin regulates Wnt targets in conjunction with transcription factors, the most prominent of which are members of the T-cell factor/lymphoid enhancer binding factor (TCF/LEF) family. Nuclear β-catenin binds with TCF/LEFs on the chromatin at *cis*-regulatory Wnt-responsive enhancers (WREs) (Mosimann et al., 2009; Pagella et al., 2023). Many cancers are causally linked to the inappropriate elevation of nuclear β-catenin, which can occur through loss of function mutations in negative regulators of the pathway, such as Adenomatosis polyposis coli (APC), Axin, and Ring finger protein 43 (RNF43), or through oncogenic mutations in β-catenin that prevent its turnover (Nusse and Clevers, 2017).

β-catenin is conventionally understood to be comprised of three distinct domains: an intrinsically disordered N-terminal domain (N-IDR), a highly structured internal

domain consisting of twelve Armadillo (Arm) repeats, followed by an intrinsically disordered C-terminal domain (C-IDR) (Dar et al., 2017; Mosimann et al., 2009). β-catenin's N-IDR is necessary for regulating the stability of the protein and contains a region bound by α-catenin (Dar et al., 2017). Cytosolic β-catenin is bound by a "destruction complex", which contains APC, Axin, as well as two kinases, Casein Kinase I (CKI) and Glucagon Synthase Kinase-3 (GSK3), which serially phosphorylate four serine/threonine residues, priming the protein for proteasomal degradation (Kimelman and Xu, 2006). The Arm repeat region contains binding sites for TCF/LEF transcription factors and E-cadherin (repeats 3-8), as well as co-activators BCL9 and BCL9L (repeat 1) (Graham et al., 2000; Huber and Weis, 2001; Mosimann et al., 2009; Sampietro et al., 2006b). The last four Arm repeats and the C-IDR are bound by a variety of transcriptional regulators, including chromatin remodelers such as Brg-1 and the histone acetyltransferases CBP/p300 (Barker, 2001; Hecht, 2000; Mosimann et al., 2009; Takemaru and Moon, 2000). The current model suggests that factors are sequentially recruited to WRE chromatin (i.e. TCF/LEFs recruit β-catenin, β-catenin recruits additional co-regulators) and this is sometimes referred to as the "chain of adaptors" model (Städeli and Basler, 2005). While there is significant support for TCF/LEFs, β-catenin, and other co-regulators physically interacting with each other to promote transcription, the exact nature of these interactions remains to be determined.

Recent studies indicate a role for biomolecular condensates (BMCs) in transcriptional activation (Plys and Kingston, 2018; Sabari et al., 2020, 2018; Wagh et al., 2021). BMCs are dynamic, membraneless assemblies comprised of proteins and, frequently, nucleic acids. Weak, multivalent interactions between the IDRs of constituent proteins drive the formation of BMCs, which is usually thought to occur through a liquid-liquid phase separation mechanism. Functionally, BMCs are thought to affect biochemical reactions by concentrating molecules, which can have potentiating or inhibitory effects (Sabari et al., 2020). The evidence for BMCs having a role in transcriptional regulation is derived from live imaging studies demonstrating the existence of dynamic puncta at enhancer chromatin and the propensity for many transcriptional regulators to form BMCs *in vitro* (Palacio and Taatjes, 2022; Sabari et al.,

2020; Wagh et al., 2021). However, rigorous evidence for a physiological role for BMCs, e.g., provided by specific mutations in transcriptional regulators is still lacking.

A previous report by Zamudio and colleagues demonstrated that β-catenin protein can form homotypic and heterotypic BMCs *in vitro* (Zamudio et al., 2019). β-catenin's terminal IDRs were necessary and sufficient for BMC formation, and this behavior was dependent on aromatic amino acid residues within the IDRs. An endogenously GFP-tagged β-catenin was shown to form dynamic puncta in response to Wnt signaling in cultured cells, providing evidence that β-catenin-containing BMCs exist in living cells. Consistent with this, a mutant of β-catenin with IDRs lacking aromatic residues (19 total aromatic amino acid substitutions in the terminal IDRs) was defective in regulating Wnt target genes, recruitment to WRE chromatin, and puncta formation (Zamudio et al., 2019).

While the work of Zamudio and colleagues is consistent with a physiological role for β-catenin condensates, several key issues remain uncertain. For example, it was not clear in that report that condensate-deficient β-catenin accumulates in the nucleus at levels comparable to wild-type β-catenin. Additionally, the alteration of 19 aromatic residues in β-catenin's terminal IDRs may disrupt key protein-protein interactions that are essential for β-catenin function, regardless of a condensate mechanism. These factors are potential explanations for the defect in recruitment to chromatin and transcriptional activation of the β-catenin aromatic mutant in that report (Zamudio et al., 2019). Whether the ability of β-catenin to form BMCs is linked to its activity as a transcriptional co-activator requires further investigation.

In this report, we address the hypothesis that BMC formation is important for β-catenin-mediated regulation of Wnt target genes by generating and characterizing a panel of β-catenin mutants utilizing *in vitro* and *in vivo* experimental systems. The results support a model in which the aromatic amino acid residues in both the N- and C-IDRs contribute to BMC formation and transcriptional activity. Importantly, we found that the N-IDR of β-catenin has a previously underappreciated role in transcriptional regulation (Kolligs et al., 1999). Supporting these findings, β-catenin was found to efficiently form heterotypic condensates with LEF1 *in vitro*, which also depends on IDR

aromaticity. Transgenic *Drosophila* lines expressing analogous Armadillo (Arm, the fly ortholog of β-catenin) mutants demonstrated the importance of aromatic residues for Arm activity in the context of fly development. Interestingly, while the mutants displayed lower signaling activity, different Wnt targets (in both human cells and *Drosophila*) had different sensitivities to the loss aromatic residues. Finally, heterologous IDRs from proteins with no known role in transcriptional regulation were able to functionally replace the N-IDR of β-catenin, providing compelling evidence that the ability of β-catenin to form biomolecular condensates is inextricably linked to its role as a transcriptional activator of Wnt target genes.

Results

Aromatic amino acid residues within β-catenin's terminal IDRs contribute to homotypic and heterotypic condensate formation *in vitro*

For many proteins, BMC formation is thought to arise from weak, multivalent interactions between protein IDRs (Sabari et al., 2020). The N- and C-terminal regions of β-catenin are predicted to be disordered, illustrated by two independent methods of analysis, IUPred2A (Erdős and Dosztányi, 2020; Mészáros et al., 2018) and AlphaFold (Jumper et al., 2021; Varadi et al., 2022) (Fig S2.1 A and B). Both protein structure prediction programs use different algorithms to determine protein structure, and therefore there are differences between IUPRED and AlphaFold. For example, IUPRED's calculations suggest that the amino acids 20-25 might be structured, whereas AlphaFold does not. Previous work from Zamudio and colleagues demonstrated that β-catenin can form homotypic BMCs *in vitro*, and that the terminal IDRs are necessary and sufficient for condensate formation. Additionally, they showed that the aromatic amino acid residues within both IDRs are required for this behavior (Zamudio et al., 2019). However, the contributions of aromatic residues from the individual IDRs were not examined. Given that these regions have distinct roles in β-catenin function, i.e., N-IDR contains phosphorylation sites controlling β-catenin stability and C-IDR is required for co-regulator activity, we were motivated to examine the requirements for the aromatic residues in more detail.

To address the role of aromatics in each IDR of β-catenin, we recombinantly expressed four eGFP-β-catenin fusion proteins: one containing the full set of aromatic residues plus a S33Y point mutation (β-catenin*). This mutation was incorporated for direct comparison with the β-catenin mutants used for subsequent functional studies. Additional proteins have the N-IDR aromatic residues mutated to alanine (aroN; 9 substitutions), the C-IDR aromatics mutated to alanine (aroC; 10 substitutions), and aromatics in both IDRs mutated to alanine (aroNC; 19 substitutions) (Fig 2.1A and Fig S2.2 for sequence information). These proteins were tested for condensate formation using a buffer containing 10% polyethylene glycol 8000 (PEG-8000) as a crowding agent, following standard experimental guidelines (Alberti et al., 2018). At relatively low concentrations where β-catenin* efficiently formed droplets, the aromatic mutants are deficient in condensate formation (Fig 2.1B). aroN and aroC displayed a similar defect in droplet formation, while aroNC was more severe. At high concentrations, the aromatic mutants formed condensates at similar levels as β-catenin*. Our results with aroNC are inconsistent with those reported by Zamudio and colleagues (see Discussion for further comment). However, consistent with that report, eGFP alone or eGFP-β-catenin with both IDRs deleted (ΔNC; Fig 2.1A) is incapable of condensate formation (Fig 2.1B). Our results demonstrate that both the N-IDR and C-IDR contribute to β-catenin condensation, and these IDRs contain additional sequence information beyond aromatic residues that facilitate droplet formation.

To further examine the properties of the β-catenin* condensates we generated, we made use of the alcohol 1,6-hexanediol (1,6-HD), which is commonly used to inhibit biomolecular condensation (Alberti et al., 2019; Kroschwald et al., 2017). 2,5-hexanediol (2,5-HD), which is chemically similar but doesn't disrupt condensation was used as a control. Droplet formation of β-catenin* was sensitive to 1,6-HD, especially when the alcohol was added prior to the PEG-8000 crowding agent (Fig 2.1C). When 1,6-HD was added after PEG-8000, some condensation was still observed. The sensitivity to 1,6-HD is consistent with the idea that these assemblies are driven by hydrophobic interactions (Kroschwald et al., 2017; Patel et al., 2007; Ribbeck, 2002), but once the droplets form,

some may transition from a phase separated droplet to more static hydrogel, which can resist the effects of 1,6-HD (Nair et al., 2019).

In living cells, β-catenin regulates gene expression through interactions with many proteins, the most prominent of which are members of the TCF/LEF family of transcription factors (Mosimann et al., 2009). The central Arm repeats of β-catenin bind to the N-terminus of TCFs, as shown by traditional protein interaction assays and X-ray diffraction of co-crystals (Graham et al., 2000). To determine if β-catenin could form heterotypic *in vitro* condensates with a TCF/LEF member, we expressed human mCherry fused to LEF1 (Fig 2.2A and Fig S2.3A for sequence information). IUPred2A and AlphaFold analysis of LEF1 predicts that most of the protein is disordered, except for the DNA-binding HMG domain (Fig S2.1 C and D). Purified mCherry-LEF1 can form concentration-dependent droplets (Fig 2.2B). Next, we performed a dose with equal molar amounts of β-catenin* and LEF1 (Fig 2.2C). There is a high degree of co-localized fluorescent signal from both eGFP and mCherry, indicating a high degree of miscibility of β-catenin* and LEF1 droplets. Relative to β-catenin*, aroNC exhibits reduced co-localization with LEF1 (Fig 2.2D), as does ΔNC (Fig 2.2E). The degree of co-localization in individual BMCs was quantified with line traces, and as expected, the strongest colocalization was with β-catenin* and LEF1, followed by aroNC and ΔNC (Fig 2.2F-H and Fig S2.4). Control heterotypic *in vitro* droplet formation assays show that eGFP does not co-localize with mCherry-LEF1 (Fig S2.5A) and mCherry does not co-localize with eGFP-β-catenin* (Fig S2.5B). The results indicate that β-catenin is localized to LEF1 condensates by two primary interactions. The traditional Arm repeat-LEF1 interaction makes a detectable contribution, based on the ability of LEF1 to recruit ΔNC into a mixed condensate (Fig 2.2E). However, the presence of the terminal IDRs greatly enhanced the ability of β-catenin and LEF1 to form mixed condensates (Fig 2.2C) and the aromatic residues in these IDRs are required (Fig 2.2D).

Aromatic amino acid residues within β-catenin's IDRs are critical for nuclear function in cultured human cells

To test whether the ability of β-catenin to form homotypic and heterotypic condensates *in vitro* is relevant to its ability to activate Wnt targets in cultured cells, we expressed β-catenin*, aroN, aroC, and aroNC in HEK293T cells in the presence of several Wnt reporters. Using either the synthetic reporter TopFlash (containing six copies of high affinity TCF binding sites) (Caca et al., 1999) or a reporter with an endogenous WRE from the *Axin2* locus, known as CREAX (Ramakrishnan et al., 2021), we found that all three β-catenin aromatic mutants had greatly reduced transcriptional activation activity (Fig 2.3A) even though they were expressed to similar levels as β-catenin* (Fig 2.3B). Similar results were also obtained with the Defa5-luc reporter that is synergistically activated by Wnt/β-catenin signaling and SOX9 (Fig S2.6) (Ramakrishnan et al., 2023). In all three cases, aroN had some residual activity, aroC exhibited small but reproducible activity and aroNC had no detectable activity. To address whether the aromatic mutants were able to translocate into the nucleus, immunofluorescence (IF) was performed. We observed no detectable difference in the ability to these proteins to accumulate in the nucleus to similar levels as β-catenin* (Fig 2.3C and D). These results demonstrate the importance of the IDR aromatic residues for the ability of nuclear β-catenin to activate Wnt target gene expression. In addition, the defect in aroN reveals a previously unappreciated role for the N-terminus of β-catenin in transcriptional activation, which we suggest is due to the defect in the ability of the aromatic mutants to efficiently form BMCs.

Our studies clearly indicate that aromatic residues in both IDRs are necessary for signaling activity, but further mutagenesis is needed to determine whether all aromatic residues equally contribute to β-catenin activity. One popular model of condensation driven by aromatic residues posits that aromatic residues flanked by polar amino acids (i.e., stickers) are the drivers of IDR-IDR interactions, while other aromatics serve as "spacers" (Martin et al., 2020). To test this sticker/spacer model in the context of β-catenin transcriptional activity, we constructed four additional mutants (Fig S2.6D for sequence information). Per the model, we mutated five potential stickers and four

potential spacers in N-IDR, and five potential stickers and spacers each in the C-IDR. These mutants were tested for activity in the TopFlash reporter assay. All four mutants displayed reduced activity but were more active than their aroN or aroC counterparts (Fig S2.6). While N-sticker had a two-fold greater reduction in activity than N-spacer, the putative spacer aromatics in the C-IDR were more critical for activity than the putative stickers. Overall, our results do not support a strict sticker/spacer model for β-catenin's IDRs; the results are more consistent with a model where many/most of the aromatic residues in the IDRs contribute to biological activity.

To extend our analysis beyond reporter genes, we examined the role of the IDR aromatic residues in β-catenin's ability to regulate endogenous Wnt targets. We generated stable HeLa cell lines which expressed β-catenin* and the aromatic mutants from a DOX-inducible expression cassette via lentiviral transduction. We chose to assay the Wnt target genes *Axin2* and *Sp5* as they are strongly activated by Wnt signaling in HeLa cells (Han et al., 2022; Huggins et al., 2017). qPCR analysis of HeLa cells expressing β-catenin* and the aromatic mutants indicates that the relationship between aromatic amino acid residues and gene regulation is slightly more complex than the reporter activity (Fig 2.4A). For *Sp5*, all aromatic mutants are deficient, but not defective in activating expression. For *Axin2*, aroNC is defective in activating expression, while aroC is deficient and aroN has no detectable defect. These mutants were expression matched for comparison (Fig 2.4B). The observation that the aromatic mutants have a different effect on genes within the same cell type indicates that there can be gene-specific requirements for BMCs in Wnt target gene regulation. IF analysis revealed that β-catenin* forms puncta in these cells, while aroN is slightly deficient in forming puncta. aroC and aroNC do not form puncta (Fig 2.4C). These observations fit with the *in vitro* droplet formation data and roughly correlate with β-catenin's ability to transcriptionally activate Wnt target genes.

β-catenin/Armadillo IDR aromatic residues are critical for function in *Drosophila* development

To test whether the importance of aromatic residues for β-catenin function is conserved across species, we examined their role in Arm. Wingless (Wg)/Arm signaling

is required throughout *Drosophila* development and has been intensively studied in *Drosophila* embryos and larval imaginal discs (Swarup and Verheyen, 2012; Van Amerongen and Nusse, 2009). Similar to human β-catenin, Arm contains 9 and 10 aromatic residues in its N-IDR and C-IDR, respectively. Seven of the N-terminal aromatics and 5 of the C-terminal aromatics are conserved across multiple species. We constructed 5 Arm transgenes, under the control of the Gal4-UAS expression system (Fig S2.7 for protein sequences). These transgenes were integrated into two locations in the fly genome using phiC31 landing sites (Bischof et al., 2007), ensuring similar levels of transcription. These UAS-transgenes were expressed in various tissues and their effect on Wg/Arm readouts were assayed.

It has been previously shown that expressing Wg agonists in the larval eye via the GMR-Gal4 driver results in smaller eyes due to increased apoptosis (Lin et al., 2004; Parker et al., 2002). Using GMR-Gal4 to overexpress UAS-Arm*, a constitutively active mutant, we observed a reduction in adult eye size, and the loss of pigmentation and cone cells (Fig 2.5A-C). All the aromatic Arm mutants (which contain the stabilizing mutants of Arm*) exhibit minimal signaling activity in this assay, though they are expressed at similar levels, as detected by IF (Fig 2.5D). These data indicate that the aromatic residues within both IDRs are essential for Arm signaling activity in the developing *Drosophila* eye.

Wg/Arm signaling is important for patterning the wing imaginal disc during larval development. In this tissue, Wg is expressed across the dorsal/ventral boundary in a stripe, regulating targets at short and long range from the source of Wg synthesis (Swarup and Verheyen, 2012). This gradient of signaling can be detected with a synthetic Wg reporter containing 4 Grainy head binding sites upstream of 4 HMG-Helper site pairs, arranged for high affinity binding by Pangolin (the fly TCF ortholog) (Archbold et al., 2014; M. V. Chang et al., 2008; Zhang and Cadigan, 2017). Decapentaplegic-Gal4 (DPP-Gal4) was used to overexpress Arm* and the aromatic mutants in a stripe pattern that is perpendicular to the endogenous Wg expression stripe (Fig 2.6A, white arrowhead). To prevent major disruption to the wing disc morphology, the $Gal80^{ts}$ system was used to inhibit Gal4 activity (and Arm protein expression) until 18 hours prior to fixation. Arm* overexpression resulted in the

strongest ectopic activation of the Wg reporter, the aroN and aroN-cons constructs exhibited a moderate activation of the reporter, and the aroC, aroC-cons, and aroNC mutants exhibited the weakest ectopic activation (Fig 2.6A, top). The observations and categorizing the constructs into strong/moderate/weak activators is supported by quantification of the fluorescent reporter activity and subsequent statistical analyses (Fig S2.8). All mutant constructs were expressed at similar levels, as detected by FLAG IF (Fig 2.6A, bottom). These reporter data show that all the aromatic mutants have some residual capacity to activate transcription. These data are distinct from the developing eye, in which the aromatic mutants had little/no activity. This difference in sensitivity to loss of aromatic residues could be due to difference in the degree for BMC-dependency for activation of Wnt targets in different tissues.

Wg/Arm signaling also plays a key role in patterning the *Drosophila* embryo. Segments of the ventral embryonic epidermis feature a characteristic, trapezoidal-shaped belt of denticles. These denticle belts are separated by regions of naked cuticle. The establishment of denticle belts and naked cuticle is regulated by Wnt signaling (Alexandre et al., 1999). Increasing Wnt signaling throughout the embryo expands regions of naked cuticle at the expense of denticle band formation, and conversely, loss of Wnt signaling leads to ectopic denticle formation and a failure to form naked cuticle (Bejsovec, 2013). To test the effect that our aromatic mutants have on regulating this phenotype, we overexpressed our constructs to similar levels using a stock containing two constitutive Gal4 drivers, Daughterless-Gal4 (Da-Gal4) and Arm-Gal4, both of which are active throughout the embryonic epidermis (Bhanot et al., 1999; Cadigan et al., 2002) (Fig S2.9). When crossed to this Gal4 driver stock, UAS-Arm* displays a classic naked cuticle phenotype, with a 100% phenotype penetrance (Fig 2.6B). In contrast, overexpression of the aromatic mutants all resulted in a similar phenotype: a partial loss of denticle formation along the ventral midline (Fig 2.6B). These phenotypes were highly penetrant and consistent with a moderate level of Arm signaling activity. Our data indicates that the loss of aromatic residues in N-IDR and as little as five aromatic residues within the C-IDR (i.e., aroCcon) compromise Arm's signaling activity to similar extents.

To test the ability of an Arm protein lacking IDR aromatic residues to rescue an *arm* loss-of-function phenotype, we expressed our transgenes at a reduced level (Da-Gal4 plus one copy of a UAS-Arm transgene). We reasoned that at this lower level of expression, the transgenic Arm* would be able to rescue the severe cuticular phenotype of embryos lacking zygotic *arm* gene activity. Indeed, expression of Arm* was able to rescue the *arm* mutant phenotype to a high-degree with 100% penetrance (Fig 2.7A-C). Expression of aroNC also resulted in significant rescue (Fig 2.7D): the overall size of these embryos is similar to wild-type embryos and the Arm* rescue, head structures are restored and there is significant recovery of posterior-most structures. However, the degree of rescue was significantly less for aroNC than Arm*, as evidenced by the presence of excess denticles in all the abdominal segments. The difference in rescue may be reflected in the ability of these overexpression backgrounds to drive a naked cuticle phenotype in a wild-type Arm genetic background. Single-copy overexpression of Arm* causes a moderate naked cuticle phenotype, as some denticles are still present (Fig 2.7E), and aroNC overexpression exhibits weaker activity, as it only disrupts denticle formation in some segments (Fig 2.7F). The extent to which aroNC can rescue an *arm* loss of function phenotype relative to Arm* suggests a surprising degree of residual activity. Whether this is related to the residual ability of aroNC to form BMCs or because many molecular targets in embryonic epidermis do not require β-catenin condensation will require additional experiments (see Discussion for further comment).

Heterologous IDRs can rescue β-catenin signaling activity of a N-IDR deletion mutant

To this point, our mutagenesis approach has correlated a loss of aromatic residues within β-catenin's IDRs with a loss of BMC formation and transcriptional regulation function, providing a link between the ability to form BMCs *in vitro* and function *in vivo*. This argument is problematic for the C-IDR, which has been implicated in binding to co-activators (Valenta et al., 2012). This caveat is mitigated by the fact that there are no known co-activator binding partners for N-IDR. As shown below, deletion of the N-IDR dramatically affected the ability of β-catenin to form droplets *in vitro* and activate some Wnt targets. This provided an opportunity to test whether these activities

could be rescued by adding heterologous IDRs to β-catenin lacking the N-IDR. A collection of IDRs (Piovesan et al., 2016) was screened with the following criteria: (1) the IDR must come from a protein with no known nuclear function, (2) must be of similar size as N-IDR (~140aa), and (3) must have a similar frequency of aromatic amino acids. Two IDRs, from human Septin 4 (Sept4) and Sorting nexin 18 (SNX18) met these criteria and were utilized (S10 Fig for protein sequences).

We generated eGFP-tagged β-catenin mutant constructs with the heterologous IDRs at the N-terminus (Fig 2.8A). We then performed a concentration series with the *in vitro* droplet formation assay (Fig 2.8B). Consistent with our previous observations, eGFP-β-catenin* will form spherical BMCs across the concentration range. In contrast, eGFP-ΔN forms fibril-like structures at relatively high concentrations. These fibril-like structures are morphologically distinct from the BMCs formed by the other mutants. eGFP-Sept4 and eGFP-SNX18 form BMCs that are similar in shape to β-catenin, rescuing the fibril-like structures of eGFP-ΔN. Furthermore, mutating the aromatic residues within the Sept4 IDR compromises the ability to form BMCs, reminiscent of the aroN mutant. These data suggest that an N-terminal IDR with sufficient aromatic content is required for BMC formation *in vitro*, and that the primary sequence of β-catenin's endogenous N-IDR is not the driver of BMC formation.

We wanted to test if these heterologous IDR β-catenin mutants could rescue transcriptional activity of β-catenin. We utilized the TopFlash-Luciferase transcriptional reporter in a HEK293T β-catenin KO cell line (Doumpas et al., 2019). We transiently transfected these cells with the reporter and expression constructs for the heterologous IDR β-catenin mutants (Fig 2.9A). The ΔN construct is deficient in activity relative to β-catenin*. The Sept4 and SNX18 heterologous IDRs rescue transcriptional activity and mutating the aromatic residues within the Sept4 IDR (aroSept4) ablates activity, again in a manner reminiscent of aroN. The differences in reporter activity are not due to differences in expression (Fig 2.9B). Additionally, we made the equivalent heterologous IDR mutants in Arm and tested the activity of Sept4-Arm in the fly eye (Fig 2.9C and Fig S2.11 for protein sequences). Sept4-Arm has an intermediate effect on eye development, leading to an eye that is approximately 20% smaller than a fly eye which

is overexpressing the ΔN-Arm mutant (Fig 2.9D). Mutating the aromatic residues within the Sept4 IDR returns the level of Arm activity back to ΔN-Arm levels. Our data shows that heterologous IDRs, which rescue β-catenin BMC formation *in vitro,* can also rescue transcriptional activity *in vivo*. Additionally, aromatic residues within the heterologous IDRs that are responsible for facilitating this activity, providing strong evidence for a model where the aromatic residues within β-catenin's IDRs are important for transcriptional activity through a biomolecular condensation mechanism.

Discussion

This study provides evidence that β-catenin's ability to form BMCs is essential for its function as a transcriptional co-regulator. Mutations in β-catenin that affect the ability to form BMCs *in vitro* correlate with reduced activity as a transcriptional co-regulator cultured human cells (Fig 2.1-3). This correlation was also observed *Drosophila*, using several functional readouts, such as transcriptional reporters and developmental phenotypes (Fig 2.3 and 2.7). The finding that substitution of specific residues in the N-IDR (or deletion of the N-IDR) severely compromised BMC formation and signaling activity is crucial to our argument, as the N-IDR hasn't been thought to play a role in transcriptional activation (Cadigan, 2012; Valenta et al., 2012). Building on this result, the most compelling evidence linking BMCs to β-catenin's function involved replacing the N-IDR of β-catenin with two heterologous IDRs from proteins with no known role in transcription. These chimeric β-catenins rescue the deficiencies of the N-IDR deletion in BMC formation and provide significant rescue in transcriptional regulation (Fig 2.8 and 2.9). Taken together, our data provide strong support for a model where the ability of β-catenin to form BMCs is an important mechanism for its function as a transcriptional co-regulator.

The concept of BMCs playing an important role in transcriptional activation has generated a large level of support (Hnisz et al., 2017; Palacio and Taatjes, 2022; Sabari et al., 2020, 2018) but it is not without controversy. The Mediator subunit MED1 readily forms BMCs with Pol II subunits *in vitro*, and dynamic puncta containing both complexes can be visualized on regulatory chromatin in cultured cells (Cho et al., 2018). MED1 and

co-activators such as p300 and BRD4 also form mixed BMCs with various TFs *in vitro* and *in vivo* (Gibson et al., 2019; Han et al., 2020; Lyons et al., 2023; Ma et al., 2021; Sabari et al., 2018). Further studies link Pol II transcriptional bursting to a BMC model of regulatory control (Cho et al., 2018; Palacio and Taatjes, 2022; Quintero-Cadena et al., 2020). However, live imaging studies linking droplet formation with increased transcriptional output have produced conflicting results (Schneider et al., 2021; Trojanowski et al., 2022). Genetic evidence linking the ability of co-activators to undergo phase separation and perform its function in transcriptional activation are limited (Ma et al., 2021; Wang et al., 2019). There is a pressing need for further genetic studies in physiologically relevant contexts to Probe the role of condensates in gene regulation.

Our work builds upon the work of Zamudio and colleagues (Zamudio et al., 2019) by providing an extensive functional characterization of β-catenin mutants that are deficient in BMC formation. We find that the observed deficits in β-catenin's function cannot be attributed to a defect in nuclear import (Fig 2.3). Considering this, the ChIP-seq data in Zamudio and colleagues support a model in which β-catenin recruitment at WRE chromatin is driven by a combination of the Arm repeats (presumably due to direct binding to TCFs) and IDRs (presumably allowing β-catenin to be enriched in condensates on WRE chromatin). Our heterotypic *in vitro* droplet formation assay data with β-catenin and LEF1 corroborates this idea. β-catenin lacking both IDRs, which is unable to form homotypic condensates (Fig 2.1) can still be recruited to LEF1 BMCs, although at a reduced level compared to full length β-catenin (Fig 2.2). We suggest that IDR-driven condensation acts as an amplifier for protein-protein interactions between structured domains, allowing a sufficient concentration of co-activators to facilitate transcription.

Forces driving β-catenin condensate formation

One commonly proposed mechanism for BMC formation invokes pi-pi interactions between the side chain of aromatic amino acids (Choi et al., 2020). As previously reported (Zamudio et al., 2019) and extended in this report, aromatic residues in the terminal IDRs of β-catenin play a key role in the ability to form condensates *in vitro* and *in vivo*. Mutation of these residues also had a context-

dependent effect on β-catenin's ability to activate Wnt targets. To narrow down the number of mutations (aroN has 9; aroC 10) we mutated subsets of aromatic residues inspired by the sticker-spacer model (Martin et al., 2020) and tested for activation of a luciferase reporter. Our data indicated that both "sticker" and "spacer" aromatic residues were crucial for β-catenin activity (Fig S2.4). Comparison of pan-aromatic and conserved (between flies and humans) aromatic amino acids in *Drosophila* developmental assays (Fig 2.5 and 2.6) suggest that the conserved residues (7 in the N-IDR; 5 in the C-IDR) might be the most important. In *Drosophila* transgenic assays, we compared the effect of mutating all aromatics (as with human β-catenin, 9 in the N-IDR and 10 in the C-IDR) with only the residues conserved between flies and humans (7 in the N-IDR; 5 in the C-IDR). As the pan-aromatic and conserved mutants had similar defects in signaling (Fig 2.5 and 2.6), it is tempting to suggest that the conserved residues contribute most to Arm/β-catenin's activity. The N- and C-IDRs contain a mixture of tyrosines, phenylalanines and tryptophans (Fig S2.2 and S2.7). BMC formation of some proteins, for example, FUS, are predominately driven by tyrosine and arginine interactions. Mutating tyrosine residues to phenylalanine strongly reduces the ability of FUS to form BMCs (Wang et al., 2018). However, some of our mutants containing multiple phenylalanine substitutions, e.g., N-sticker (3 of 5) and aroN-con (5 of 7) have severe signaling defects (Fig 2.5 and 2.6, Fig S2.4), suggesting that these aromatic residues are important for condensation/activity. Our data is consistent with the idea that BMC formation is driven by multivalent interactions of all three types of aromatic residues and that many/most of the 19 residues in the IDRs contribute condensation and transcriptional activity. However, further mutagenesis is needed to test the relative contributions of each aromatic position.

Is β-catenin condensation universally required for Wnt target gene activation?

Our data support an important role for β-catenin condensation in transcriptional activation, but it is unclear if this is a universal requirement for the expression of all Wnt target genes. In nearly every case we examined (the one exception being aroN activating Axin2 in Hela cells; Fig. 2.4A), mutation of aromatic residues resulted in a

reduction of signaling activity. However, the degree of this defect depended on the assay employed. For the reporter gene assays in human cells (Fig 2.2, Fig S2.4) and the developing *Drosophil*a eye there was a strict requirement for aromatic residues, e.g., the five substitutions in aroC-con abolished Arm's signaling activity in the eye (Fig 2.5). For endogenous targets in Hela cells (Fig 2.4) and a Wg/Wnt reporter in wing imaginal discs (Fig 2.6), there was an intermediate defect in signaling. In the *Drosophila* embryo, a mutant (aroNC) with 19 substitutions still had the ability to rescue a strong *arm* loss-of-function phenotype (Fig 2.7). It is possible that some of this rescue is the result of aroNC de-repressing Wnt target gene expression through displacing co-repressors from TCF/Pangolin (Cavallo et al., 1998; Schweizer et al., 2003), but the modest level of expression of the aroNC transgene makes this unlikely. Clouding the interpretation is the fact that β-catenin lacking all 19 aromatic amino acids retains the ability to form BMCs *in vitro* at high concentrations (Fig 2.1). This is different from the results reported by Zamudio et al., but we note that in this study, the GFP-β-catenin fusions were purified under denaturing conditions and then renatured (Zamudio et al., 2019). This raises the possibility that aroNC did not properly refold. Given our results that aroNC can form BMCs (albeit only at higher concentrations), further studies are needed to identify additional residues in the N-and C-IDRs that contribute to condensate formation. This would allow the construction of a tighter condensate mutant, to address whether BMC formation is universally required for activation of Wnt targets with increased certainty.

Non-transcriptional BMCs containing β-catenin

In the absence of Wnt stimulation, β-catenin is targeted for proteasomal degradation by a "destruction" complex consisting of AXIN, APC, the kinases CKI and GSK3, and the E3-ubiquitin ligase Tr-BP (Schaefer and Peifer, 2019). The multivalency of the protein-protein interactions between destruction complex members led to the suggestion that it formed a BMC (Schaefer and Peifer, 2019). Indeed, the ability of AXIN to undergo phase separation has been genetically linked to efficient down-regulation of β-catenin (Nong et al., 2021) and evidence for a destruction complex BMC at endogenous levels of expression has been reported (Lach et al., 2022). The positive

Wnt effector Dvl2 has also been shown to form condensates, which has been suggested to play a role in inhibiting the destruction complex (Kang et al., 2022; Schubert et al., 2022; Vamadevan et al., 2022). The aromatic β-catenin/Arm mutants described in this report also contained point mutations blocking GSK3 phosphorylation, rendering them insensitive to degradation by the destruction complex. This allowed their role in transcriptional regulation to be unambiguously assayed. Further studies are needed to determine whether β-catenin mutants such as aroNC can be efficiently recruited to the destruction complex.

Conclusions

Our data suggests that there is a high degree of context-dependency regarding the relationship between aromatic/condensation and activation of specific Wnt targets. Understanding the molecular basis for this specificity will require a combination of transcriptomics and an in-depth examination of WREs that have a strong requirement for aromatic residues in N-IDR and C-IDR and those that do not. Nonetheless, this report provides strong evidence that a role for β-catenin condensation needs to be considered to fully understand how the Wnt pathway activates transcription.

Materials and Methods

Plasmids

FLAG-tagged β-catenin variants were expressed in transient transfection assays using the pCDNA3.1 vector (Thermo Fisher Scientific). A plasmid expressing human β-catenin containing a S33Y mutation (pCDNA3-S33Y) was the starting point for further mutagenesis (Sinha et al., 2021). β-catenin mutants were created using gBLOCKS (Integrated DNA Technologies) which were subcloned into pCDNA3-S33Y that was linearized with either *BamHI* & *PmlI* (N-IDR mutants) or *BbvCI* & *XbaI* (C-IDR mutants). To express the β-catenin proteins in *E. coli*, a pET28 expression vector expressing a His-tagged GFP-β-catenin (RY8686), which was a gift from R. Young (MIT) was used (Zamudio et al., 2019). Various β-catenin variants were subcloned into RY8686 using *BamHI* & *NotI*.

For the luciferase assays, the Topflash and CREAX reporter plasmids were constructed using pGL4.23 (Promega). Specific transcription factor binding sites or regulatory elements are upstream of a minimal TATA-box promoter driving the expression of the firefly luciferase gene. TopFlash has 6x TCF binding sites (plasmid was a gift from E. Fearon, University of Michigan). The CREAX luciferase reporters contain the endogenous WREs from the human *Axin2* locus (Ramakrishnan et al., 2021). For the *Defa5* reporter, the Defa5 promoter (WRE plus proximal promoter) was cloned into the promoter-less pGL4.10 plasmid (Ramakrishnan et al., 2023).

The pCW57.1 vector (gift from David Root, addgene plasmid #41393) was used to generate the lentiviral particles for cell transduction. In brief, the coding regions of various Flag-tagged β-catenin constructs were PCR amplified from the aforementioned pCDNA3 vectors, along with the SV40 polyadenylation site. Overlapping sequence was included to allow these amplicons to be combined with a 7.8kB *NdeI*/*SalI* fragment of the pCW57.1 lentiviral vector via Gibson assembly using the *NEBuilder HiFi DNA Assembly Master Mix (New England Biolabs). Products were confirmed with Sanger sequencing (Genewiz, South Plainfield, NJ).*

Vectors for transgenic *Drosophila* strains were constructed using the PhiC31 transgenesis system (Bischof et al., 2007). An *arm* cDNA encoding two activating mutations (T52A and S56A) was cloned into a pUAST-FLAG-attB vector (a gift from CY Lee, University of Michigan). This construct (pUAST-Arm*-FLAG-attB) expresses the stabilized Arm protein tagged with a C-terminal FLAG epitope. Additional Arm mutants were created using gBLOCKS (Integrate DNA Technologies) cloned into pUAST-Arm*-FLAG-attB using either *MluI* & *StuI* (for N-terminal IDR mutants) or SacI & ClaI for C-terminal IDR mutants.

Protein Purification

pET28 vectors encoding the various β-catenin mutants were transformed into C41 cells and plated on LB plates containing kanamycin (50μg/ml). Multiple fresh bacterial colonies were inoculated into 5ml LB broth with kanamycin and grown overnight at 37°C. The overnight cultures were diluted in 500ml of fresh LB broth with kanamycin and grown at 37°C until the cultures reached an OD_{600} of 0.6-0.8. IPTG was

added to a working concentration of 1mM, and the cells were grown for 18 hours at 16°C. Cells were collected by centrifugation.

Pellets from the 500ml cultures were resuspended in lysis buffer (50mM Tris-HCl pH: 7.5, 300mM NaCl, 4mM imidazole, 0.1% Triton-X 100, 1 tablet complete protease inhibitors (Roche, 11873580001)). Samples were then sonicated, 10 seconds on, 20 seconds off, for 3 minutes. Lysates were then cleared by centrifugation at 12,000xg for 12 minutes and added to 1ml of pre-equilibrated TALON metal affinity resin (Takara Bio, 635502). The slurry was rotated at 4°C for 1 hour. The slurry was then centrifuged at 700g for 5 minutes at 4°C. The bead pellets were then washed twice with 10ml of wash buffer (50mM Tris-HCl pH: 7.5, 300mM NaCl, 8mM imidazole). Protein was eluted in 1.5ml of elution buffer (50mM Tris-HCl pH: 7.5, 300mM NaCl, 50mM imidazole, 10% glycerol) and the samples were rotated for 10mins at 4°C. Protein samples were then concentrated using Amicon Ultra centrifugal filters (30k MWCO, Millipore). The protein concentration of eluates were estimated with a Bradford assay (BioRad) and analyzed on an 8.5% acrylamide gel stained with Coomassie.

In vitro droplet formation assay

Assays were carried out on chambered coverglass slides (Grace Bio-Labs, 112359) that were passivated with Pluronic F-127 (Sigma-Aldrich, P2243). A 5% (w/v) Pluronic F-127 solution was added to the slide's chambers and incubated for at least 1 hour. After the incubation, the chambers were washed with buffer (50mM Tris-HCl pH: 7.5, 300mM NaCl, 10% glycerol). Varying concentrations of eGFP- and mCherry-tagged proteins were added to the chambers with droplet formation buffer (50mM Tris-HCl pH: 7.5, 300mM NaCl, 10% glycerol, 10% PEG-8000). The mixture was incubated for 15 minutes before being imaged on a Leica DMI6000B with a 63x objective and a Hamamatsu ORCA-R2 camera. Images were processed and analyzed using Leica Application Suite X (LAS X). Line profile intensities were calculated using a single line through representative condensates.

For the hexanediol sensitivity assays, 10% (w/v) 1,6-hexanediol and 2,5-hexanediol (Sigma-Aldrich, 240117 and H11904, respectively) solutions were made. These solutions were added to protein diluted in buffer (50mM Tris-HCl pH: 7.5, 300mM

NaCl, 10% glycerol) before or after PEG-8000. All droplet assays shown were repeated at least three times on separate days (often with separate protein preps) and the results shown are representative.

Cell Culture, transfection, stable cell line generation, DOX treatment

HEK293T cells were obtained from the American Type Culture Collection. HeLa cells were a gift from Y. Wang (University of Michigan) and HEK293T β-catenin KO cells were a gift from K. Basler (University of Zurich) (Doumpas et al., 2019). All cells were grown at 37°C with 5% CO_2 and in Dulbecco's modified Eagle's medium (Gibco, 11995065) supplemented with 10% fetal bovine serum and penicillin-streptomycin-glutamine (Gibco, 10378016).

For transfection in HEK293T cells, 50,000 cells per well were plated in a 48 well plate and grown overnight. Cells were transfected using polyethylenimine-MAX (PEI-MAX, PolySciences, 24765-1) following the manufacturer's protocol. All luciferase assays were performed at least three times on separate days, with similar results obtained in each experiment.

For this study, stable HeLa cell lines containing DOX-inducible β-catenin mutant (β-catenin*, aroN, aroC, and aroNC) expression cassettes were generated by lentiviral transduction. Lentiviral supernatants were made by the University of Michigan Vector core lab. To generate the mutants, HeLa cells were incubated with viral supernatants for 24 hours, then the cell culture medium was replaced with fresh medium and cells were grown for an additional 24 hours. Transduced cells were then selected for and maintained in cell culture medium containing 1μg/ml puromycin. For DOX-induced expression of the mutant proteins, the individual HeLa cell lines were treated with varying doses of DOX to normalize expression across the tested mutants.

Western Blotting

Cell samples were lysed and denatured in hot 1x SDS loading buffer. Protein samples were separated by SDS-PAGE and transferred to a polyvinylidene fluoride membrane (PVDF, Bio-Rad, 1620177) and blocked in 5% bovine serum albumin (BSA). Protein blots were incubated in primary antibody (diluted in 5% BSA) overnight at 4°C.

After the incubation, protein blots were washed three times with tris-buffered saline containing 1% Tween-20 (TBS-T), then incubated with a secondary antibody (diluted in 5% BSA) for 1 hour at room temperature. Blots were then washed three times with TBS-T, developed with a chemiluminescent substrate (Pierce, 34577), and imaged using a LI-COR Odyssey CLx. Images were processed in Adobe Photoshop.

Antibodies used: anti-FLAG-horseradish peroxidase (HRP, Sigma-Aldrich, A8592, 1:5000), anti-β-tubulin (Proteintech, 66240-1, 1:20,000), anti-mouse HRP (Jackson ImmunoResearch, 115-035-003, 1:2000).

Immunofluorescence

HEK293T and HeLa cells were seeded on 12mm round glass coverslips (Warner Instruments, 64-0712) in 24 well plates and grown overnight. The following day, cells were either transfected or treated with DOX to express FLAG-tagged β-catenin mutant proteins. 24 hours after transfection or DOX treatment, cells were fixed with 4% paraformaldehyde (Electron Microscopy Sciences, 15710). The IF protocol was previously published (Leica, Quick guide to STED sample preparation). Briefly: following fixation, the cells were washed with PBS and permeabilized with 0.1% Triton-X 100 (MP Biomedicals, 807426). Cells were blocked with 4% bovine serum albumin for 1hr, then incubated in primary antibody solution overnight at 4°C. The following morning, cells were washed and incubated in secondary antibody solution for 1 hour at room temperature. Cells were then washed and counterstained with DAPI. Coverslips were mounted on slides with Vectashield Mounting Media (Vector Labs, H-1000). Images were acquired with a Leica Sp8 laser confocal microscope and processed using LAS X.

Antibodies used: anti-FLAG (Sigma-Aldrich, F3165, 1:1000), anti-mouse-Alexa568 (Molecular Probes, A11031, 1:1000), anti-Cut (Developmental Studies Hybridoma Bank, 2B10, 1:20)

qRT-PCR

Total RNA was extracted using the RNeasy Plus Mini Kit (QIAGEN, 74134). cDNA synthesis was done using SuperScript III reverse transcriptase (Invitrogen, 18080-044) with oligo-dT primers. For the qRT-PCR, *Power*SYBR Green PCR Master

Mix (Applied Biosystems, 4367659) was used and the reaction was carried out in a StepOnePlus Real-Time PCR System (Applied Biosystems). The β-actin and 18s genes were used as internal controls, and the relative expression of target genes was calculated using a modified Pfaffl equation which accounts for multiple reference genes (Pfaffl, 2001; Vandesompele et al., 2002). Primer sequences listed in table S1. Experiments were repeated three times with qualitatively similar results obtained.

Transgenic *Drosophila* strains

pUAST-Arm*-FLAG-attB and other UAS-arm derivatives were injected into M{3xP3-RFP.attP'}ZH-51C and M{3xP3-RFP.attP}ZH-86Fb embryos by BestGene Inc (Chino Hills, CA) or Rainbow Transgenic Flies (Camarillo, CA). Transformants were identified by the presence of the mini white gene. Transgenic chromosomes were balanced over the SM5a-TM6B compound balancer, either as single inserts or in combination (51C & 86Fb). Insertions at 51C were meiotically recombined with the P[GMR-Gal4] transgene. Other Gal4 lines were obtained from the Bloomington Stock Center. Da-Gal4 and Arm-Gal4 were meiotically recombined onto a single third chromosome and balanced over TM6c. All *Drosophila* stocks were raised on yeast/glucose food and experiments were performed at 25˚C unless otherwise indicated.

Imaging of Drosophila eye and wing tissues

Adult flies containing P[GMR-Gal4] and four copies of P[UAS-arm*] or its variants were frozen at -20°C overnight and photographed with a Leica Stereo Dissecting Scope (Leica DMI6000B) attached to a digital camera. Eye size was quantified using ImageJ. Crosses were repeated multiple times with similar results. For Cut immunostaining, white prepupa were selected and aged 40-44 hrs at 25˚C before dissection and fixation with 4% paraformaldehyde. Pupal eyes were stained with mouse anti-Cut (Developmental Studies Hybridoma Bank; 1:100). At least ten eyes were examined for each condition, with similar results.

Wg/Wnt signaling in the wing imaginal discs was measuring using a Wnt GFP synthetic reporter previously described (Zhang and Cadigan, 2017). This reporter

contains three copies of a grainy head binding site and four copies of a TCF-Helper upstream of a minimal promoter driving GFP. Larva containing this reporter and one copy each of P[Dpp-Gal4] and P[Tub-Gal80ts] and a single copy of P[UAS-arm*] or its variants were reared at 18˚C and then shifted to 29˚C for 18 hours before selecting late third larval instar for dissection, fixation with 4% paraformaldehyde and mounting. Crosses were repeated multiple times and at least twelve discs were visualized for each condition.

Quantification of fluorescent reporter activity was performed in ImageJ. A region of interest (ROI) was defined in the location of ectopic reporter activity, integrated density of the fluorescent signal was quantified, and the same ROI and calculation was used at a site of endogenous reporter activity. Data is presented as a ratio of the integrated density of the reporter at the ectopic activation site to the endogenous activation site.

To monitor expression of Arm* proteins, wing discs treated as described above and eye/antennal discs were fixed and subjected to IF using a mouse anti-FLAG antibody (Sigma-Aldrich, F3165, 1:100) and anti-mouse-Alexa568 (Molecular Probes, A11031, 1:200) as previously described (Zhang et al., 2014). All GFP and IF images were acquired with a Leica SP8 laser confocal microscope and processed using LAS X.

Preparation of embryonic *Drosophila* cuticles

Embryonic *Drosophila* cuticles were prepped for imaging using a previously described method (Stern and Sucena, 2011). Briefly, grape agar plates were added to *Drosophila* cultures for egg collection. Eggs were incubated at 25°C and allowed to develop to the point of death, which occurs in late embryogenesis.

The embryos were dechorionated by placing them in a 50% bleach solution for 2 minutes, then rinsing them with distilled water, and then dried. The embryos were then devitellinized by transferring them to a 1:1 heptane to methanol solution, and vigorously vortexing for 30 seconds. The heptane and methanol solution was decanted and the embryos were washed 3 times with methanol and a final time with a 0.1% Triton-X 100 in methanol solution. The embryos were then transferred to a glass slide, residual methanol was evaporated, and the embryos were mounted in a 1:1 solution of Hoyer’s

mounting medium (Hempstead Halide) and lactic acid. The embryos were imaged using a Nikon E800 Upright microscope equipped with a Nikon DS-Fi3 camera and a Nikon Dark Field Condenser (Dry 0.95-0.80). Images were processed using NIS-Elements software.

Various P[UAS-arm*] strains were crossed with P[Da-Gal4],P[Arm-Gal4] which are both active throughout the embryonic epidermis [45,46]. Embryos contained one copy of each P[Gal4] and two copies of P[UAS-arm] transgenes for the experiments described in Fig. 6. To test for rescuing activity of the different *arm* transgenes, males homozygous for P[UAS-arm] transgenes were crossed to arm^4/FM7; P[Da-Gal4] females. Arm^4 is an amorphic allele of arm that produces a protein truncated in the sixth Arm repeat that produces no detectable protein (Peifer and Wieschaus, 1990). Approximately 3/4s of the progeny displayed a consistent phenotype indistinguishable from those of embryos with P[Da-Gal4] and the respective P[UAS-arm] construct. Approximately one quarter had a highly penetrant but distinct phenotype consistent with an arm^4/Y embryos with significant phenotypic rescue. All crosses were repeated multiple times; the phenotypes obtained were highly penetrant (n>20 for each condition).

Acknowledgements

The authors would like to thank Richard Young and his co-workers for inspiring this study, and for providing their GFP-β-catenin plasmid. Thanks to Claudio Cantù and Konrad Basler for providing the HEK293T β-catenin knockout cell line. Special thanks to Sarah Bui for assistance with lentivirus infections and line analysis of heterotypic BMCs, and to Yanzhuang Wang for use of his BL2 biological safety cabinet. Thanks to Anthony Vecchiarelli for discussions on biomolecular condensates. Thanks to Hwajeong Yi, Jon Millar, Jonathan Calderon Juarez and Carla Peralta for assistance with the construction of plasmids and to Aravind Ramakrishnan and Jon Millar for critical reading of the manuscript.

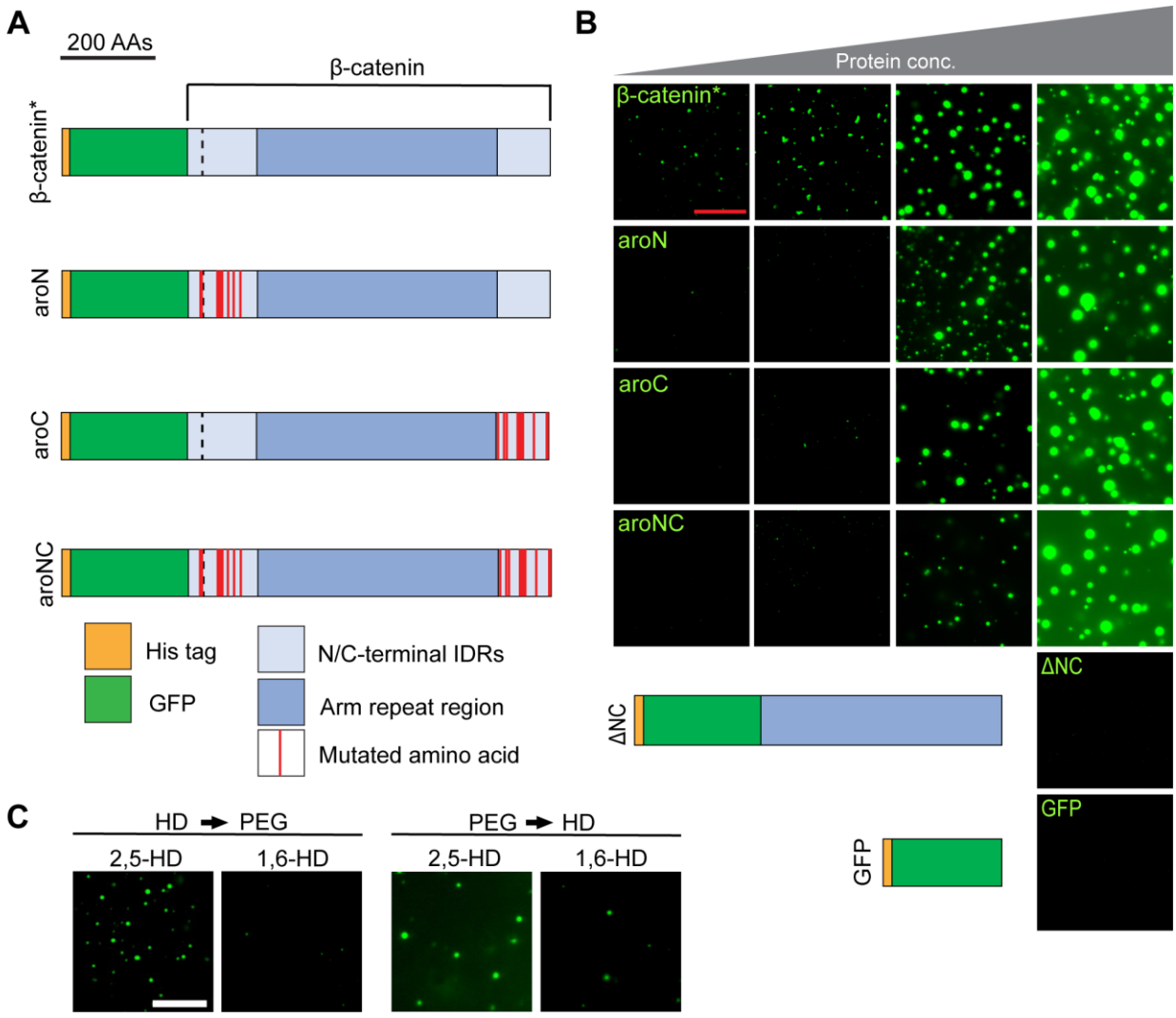

Figure 2.1. Aromatic amino acid residues in the terminal IDRs of β-catenin promote biomolecular condensate formation *in vitro*. (**A**) Cartoon representation of the eGFP-β-catenin* protein, the aromatic mutant derivatives, and control constructs. β-catenin* contains one S33Y mutation (dashed black line) in the N-IDR. aroN has all 9 endogenous aromatic amino acids within the N-IDR mutated to alanines. aroC has all 10 endogenous aromatic amino acids within the C-IDR mutated to alanines. aroNC contains all 19 aromatic amino acid mutations. The aromatic mutant constructs contain the same S33Y mutation as β-catenin*. (**B**) Representative images from an *in vitro* droplet formation assay with the indicated mutants. A protein concentration series of 2μM, 3μM, 4μM, and 8μM is depicted. Droplet assays were performed in 300mM NaCl and 10% PEG-8000. Scale bar = 20μm. (**C**) Representative images from an *in vitro* droplet formation assay testing eGFP-β-catenin* sensitivity to 1,6-hexanediol and 2,5-hexanediol (used as a control). 8μM eGFP-β-catenin* protein was exposed to the hexanediols prior to PEG-8000 (HD -> PEG) or PEG-8000 prior to the hexanediols (PEG -> HD). 10% hexanediol and 10% PEG-8000 was used. Scale bar = 20μm.

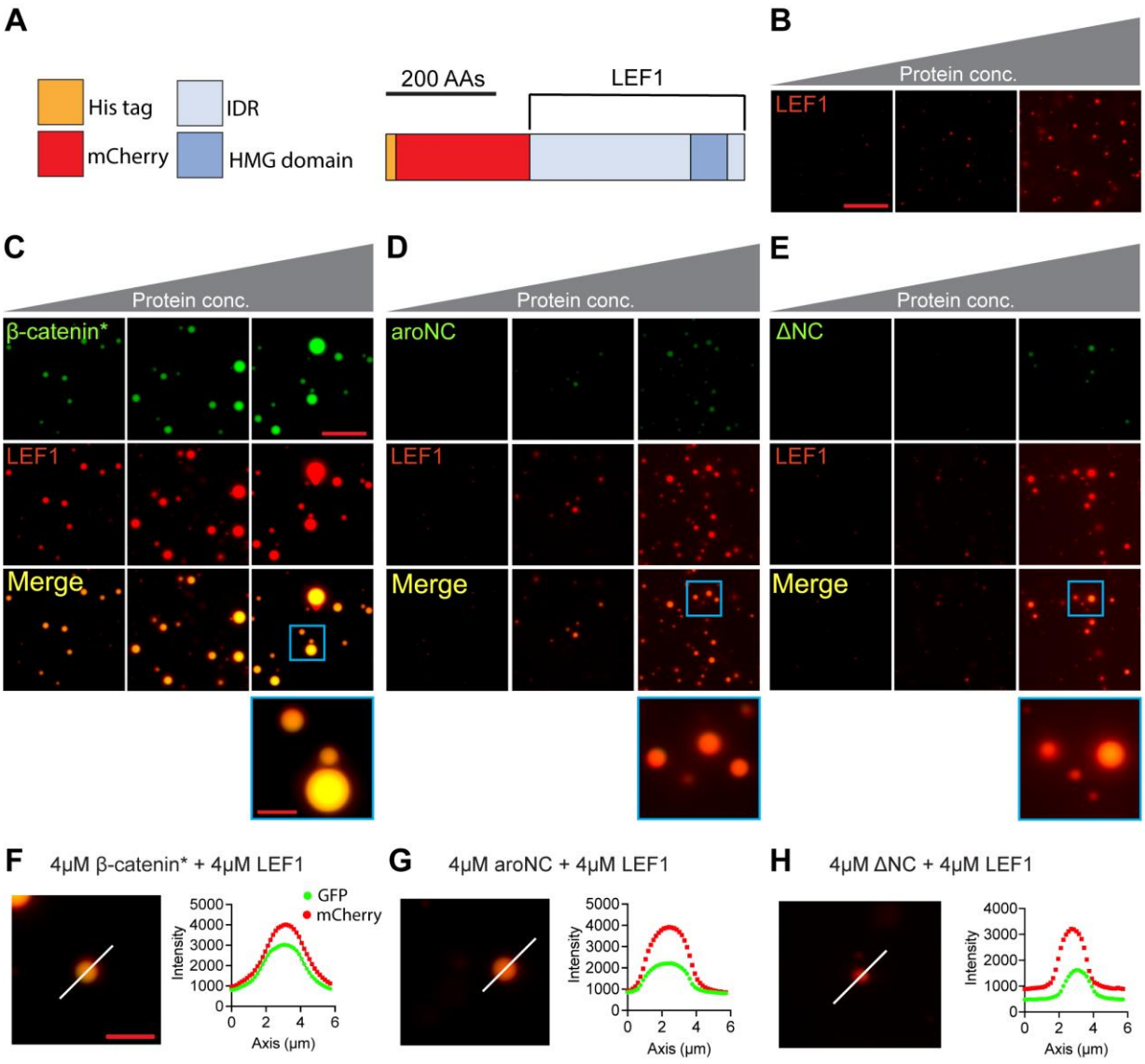

Fig 2.2. The β-catenin terminal IDRs promote β-catenin incorporation into Lef1 condensates *in vitro*. (**A**) Cartoon representation of the mCherry-LEF1 construct. (**B**) Representative images from an mCherry-LEF1 *in vitro* droplet formation assay. A concentration series of 4μM, 8μM, and 16μM total protein is depicted. Equal amounts of mCherry-LEF1 and eGFP (used as a control) were present in each reaction. No eGFP fluorescence was detected in the reaction and eGFP did not detectably affect the degree of mCherry-LEF1 droplet formation. Assays were performed in 300mM NaCl and 10% PEG-8000.Scale bar = 20μm. (**C-E**) Representative images from heterotypic *in vitro* droplet formation assays. (**C**) Equal amounts of eGFP-β-catenin* and mCherry-LEF1, (**D**) eGFP-aroNC and mCherry-LEF1, and (**E**) eGFP- ΔNC and mCherry-LEF1 were mixed, resulting in total protein concentrations of 4μM, 8μM, and 16μM. Reaction conditions are the same as panel B. Scale bar = 20μm, inset scale bar = 5μm. (F-H) Line plots showing eGFP-β-catenin* + mCherry-LEF1 (**F**), eGFP-aroNC and mCherry-LEF1 (**G**), and eGFP-ΔNC and mCherry-LEF1 (**H**) fluorescent intensity across a droplet.

Increased fluorescent signal for both proteins across a line indicates co-localization and the white lines represent the plotted trace. Scale bar = 5μm.

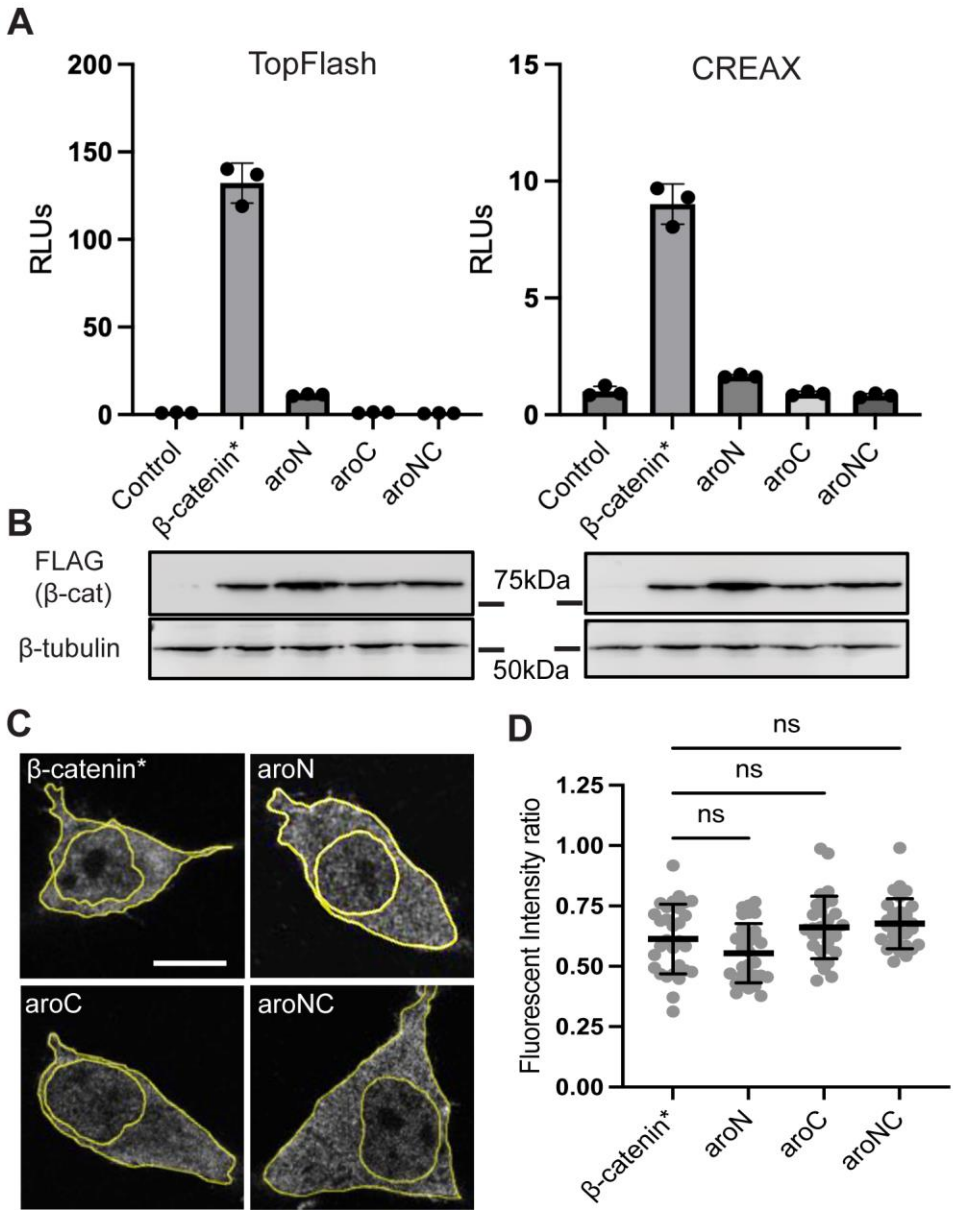

Figure 2.3. Aromatic residues within β-catenin's terminal IDRs are required for reporter gene activation and not nuclear accumulation. (**A**) TopFlash (left) or CREAX (right) luciferase reporter activity induced by β-catenin* or the aromatic mutant constructs in HEK293T cells. Cells were transfected with separate plasmids encoding the reporter genes and the FLAG-β-catenin mutant constructs or pcDNA3.1 as a negative control (NC). Luciferase activity was assayed 24hr post-transfection. Data are plotted as mean ± SD (n = 3). (**B**) Western blots of the HEK293T lysates that were transfected with the luciferase reporter gene and the FLAG-β-catenin mutant constructs. The lysate samples correspond to the luciferase reporter assay. α-FLAG blot shows β-catenin expression, α-tubulin was used as a loading control. (**C**) Representative IF images of HEK293T cells for the indicated FLAG-β-catenin mutants. Cells were transfected with plasmids encoding the FLAG-β-catenin mutant constructs. IF was

performed 24hr after transfection and the cells were stained with DAPI. The borders of the cell and nucleus are highlighted. Scale bar = 10μm. (**D**) Quantification of IF showing no significant difference in nuclear localization between β-catenin* and aromatic mutants. Data is presented as a ratio of the fluorescent intensity within the nucleus to the fluorescent intensity outside the nucleus. Data are presented as mean ± SD (n = 30). p-values were calculated by one-way ANOVA followed by Dunnett's test. ns = p > 0.05.

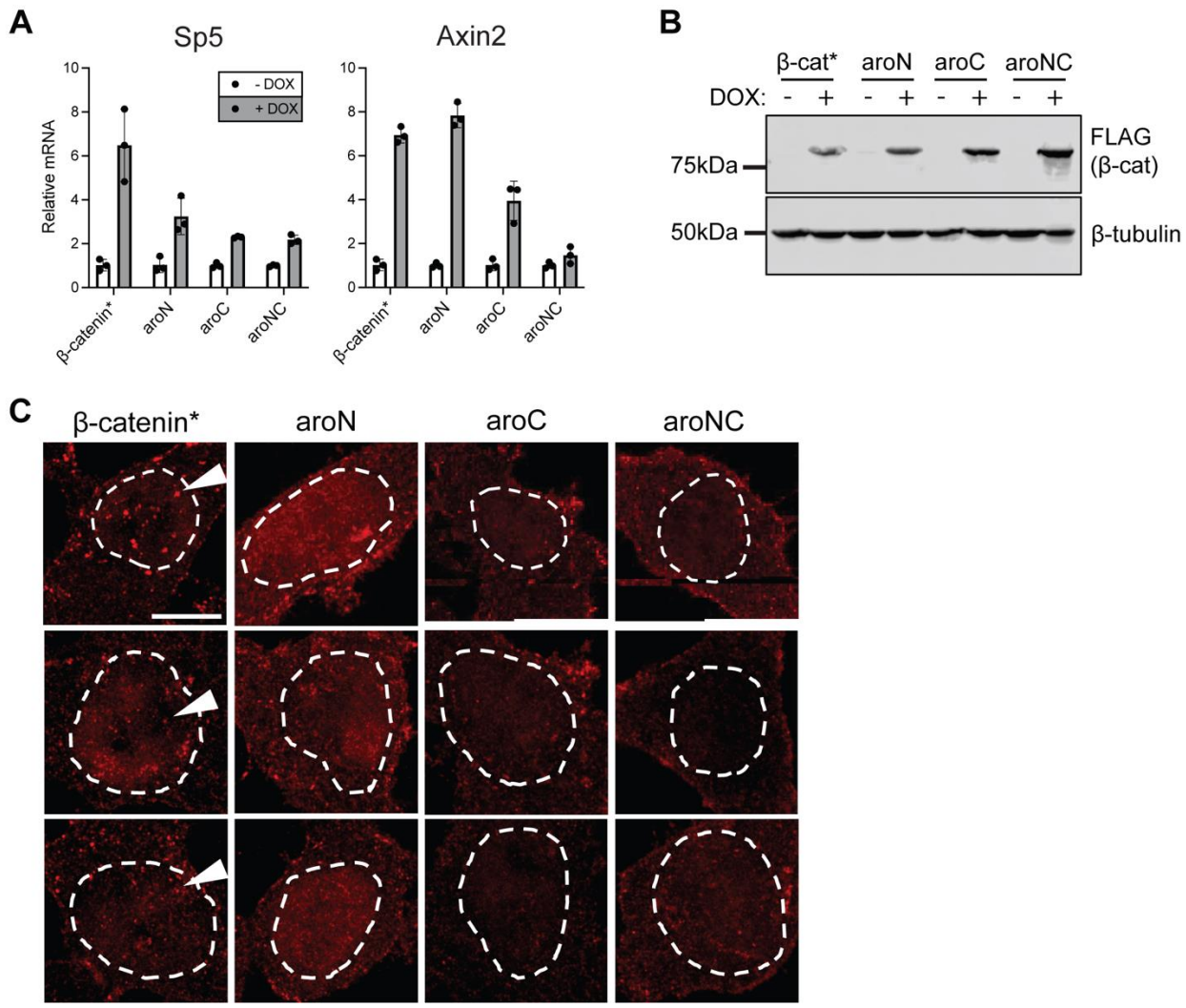

Fig 2.4. Select Wnt target genes exhibit different sensitivities to β-catenin aromatic mutant constructs. (**A**) qRT-PCR analysis of two Wnt target genes (*Sp5* and *Axin2*) in HeLa cells stably transformed with DOX-inducible, β-catenin mutant expression vectors. Cells were treated with DOX for 24hr. Data presented as mean ± SD (n=3). (**B**) Western blot analysis of DOX-treated HeLa cell lysate. Lysate samples correspond to the qPCR data. α-FLAG blot shows β-catenin expression. α-tubulin was used as a loading control. (**C**) Representative confocal IF images of HeLa cells expressing β-catenin mutants. 3 images per mutant are shown. Cells were treated with DOX for 24hr prior to IF. Cells were stained with DAPI, and dashed lines represent the nuclear border. Arrow indicates the presence of β-catenin* puncta, which are reduced in aroN expressing cells and not detectable in aroC and aroNC cells. Scale bar = 10μm.

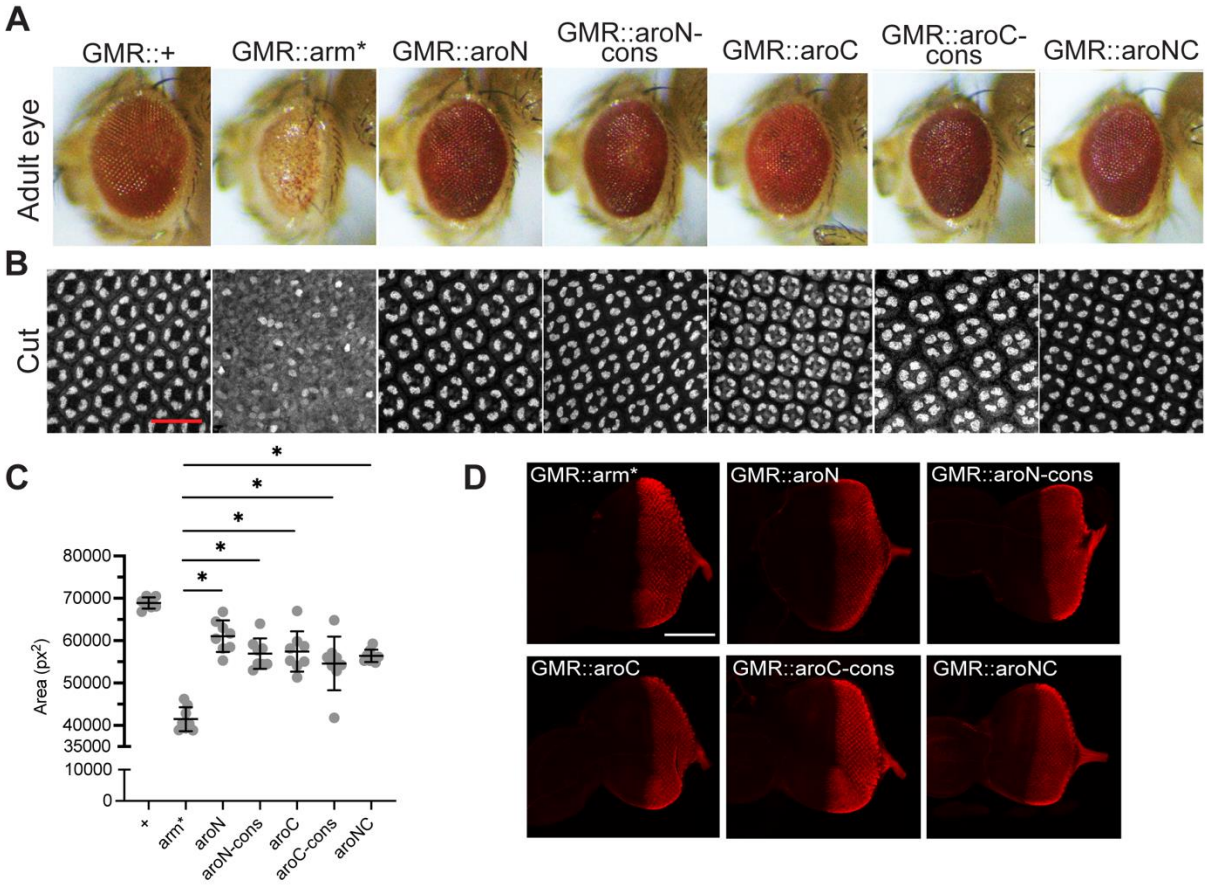

Fig 2.5. β-catenin/Arm activity in the adult Drosophila eye is attenuated by aromatic amino acid mutations within the terminal IDRs. (**A**) Micrographs of adult *Drosophila* eyes containing P[GMR-Gal4] and various P[UAS-Arm] transgenes. (**B**) Representative images of pupal *Drosophila* eye tissue immunostained for the cone cell marker Cut. Stabilized Arm (Arm*) disrupts cone cell specification while aromatic mutants do not. Scale bar = 20μm. (**C**) Quantification of adult *Drosophila* eye area. Data are presented as mean ± SD (n = 8). p-values were calculated by one-way ANOVA followed by Dunnett's test. * = $p < 0.05$. (**D**) Expression of the various Arm constructs is constant during late larval eye development. Representative images of larval *Drosophila* eye antennal discs immunostained for FLAG, representing β-catenin mutant expression. Scale bar = 100μm.

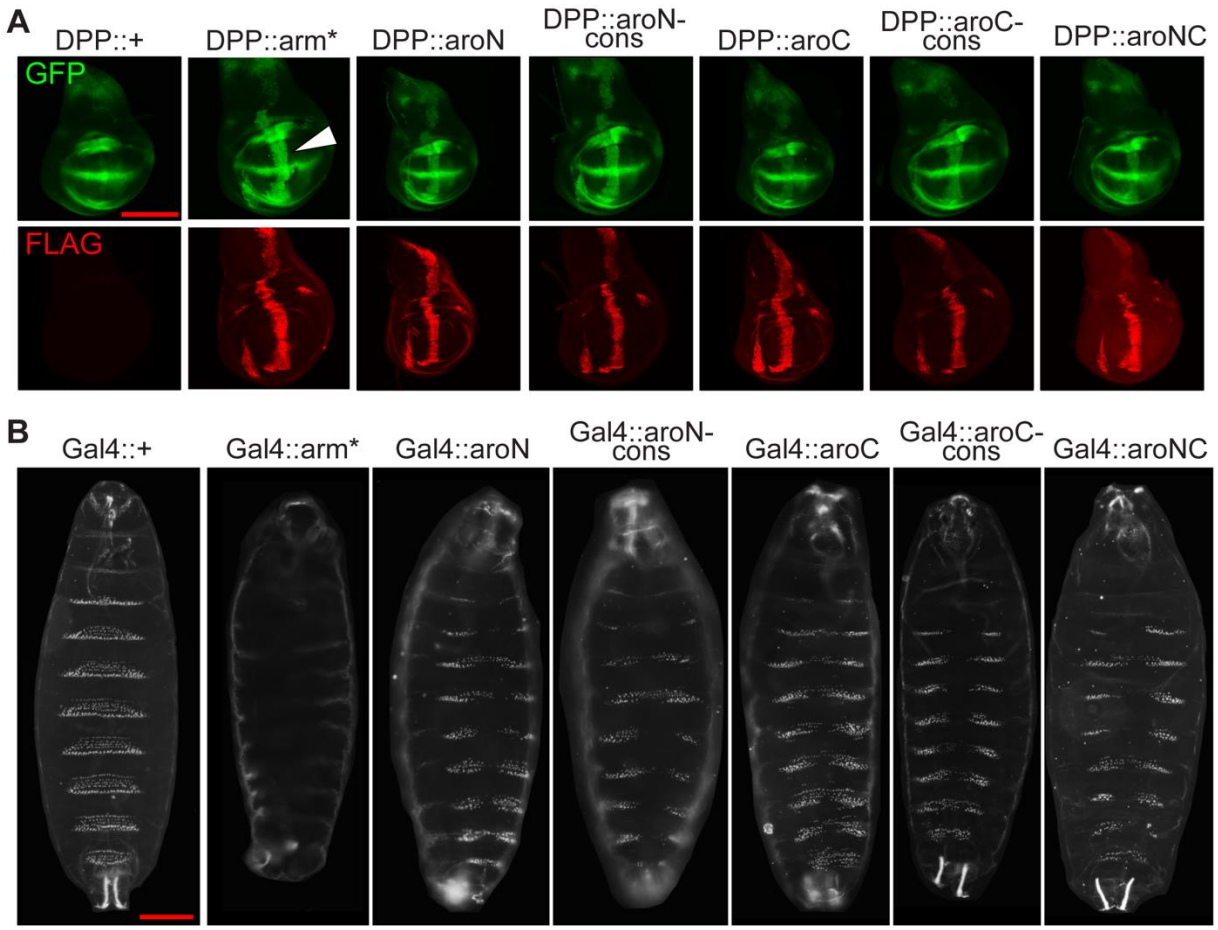

Fig 2.6. Aromatic β-catenin/Arm mutants exhibit different levels of activity in wing imaginal discs and embryonic epidermis. (**A**) Representative images of late third instar wing imaginal discs showing expression of a synthetic Wnt GFP reporter combined with a P[Dpp-Gal4] driving expression of various P[UAS-Arm] transgenes. Discs were also immunostained with α-FLAG to detect expression of the various Arm mutants. Gal4 activity was restricted to 18hr before fixation using a $Gal80^{ts}$ transgene. Scale bar = 100μm. (**B**) Representative darkfield images showing ventral side of late embryonic *Drosophila* cuticles containing P[Da-Gal4], P[Arm-Gal4] and two copies of the various P[UAS-Arm] transgenes. Scale bar = 100μm.

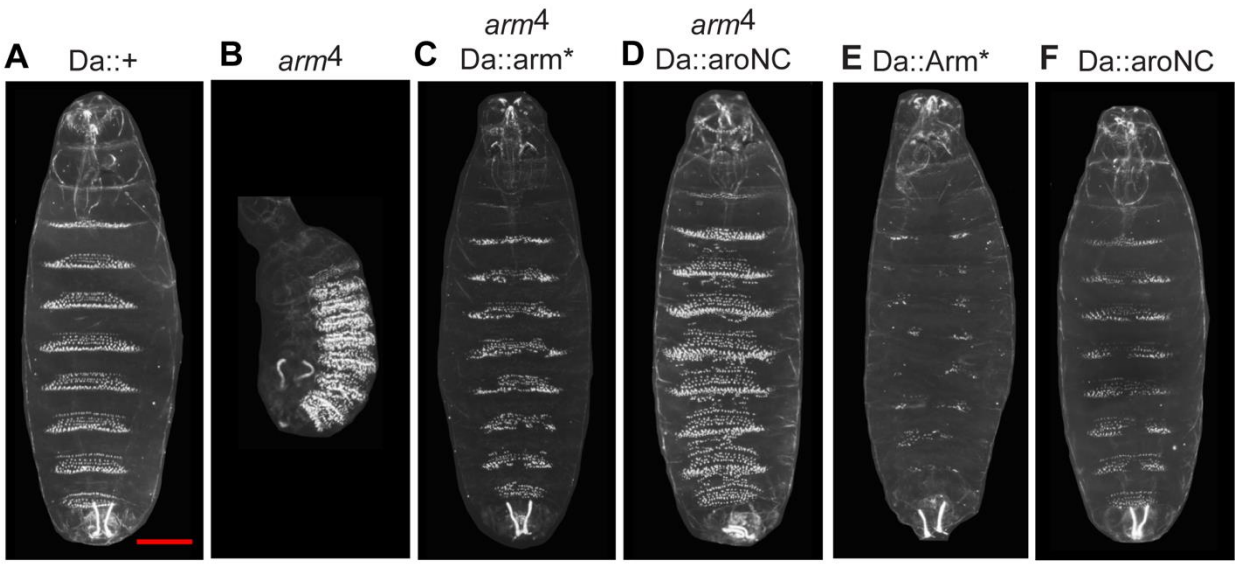

Fig 2.7. An aromatic β-catenin/Arm mutant (aroNC) partially rescues an *arm* loss-of-function allele. (**A**) Ventral side of a cuticle of an embryonic containing the P[Da-Gal4] transgene. Phenotype is indistinguishable from wild-type. (**B**) Cuticle of an amorphic *arm* mutant, displaying a classic Wg loss-of-function phenotype. The size of the embryo is greatly reduced, the head and posterior structures are missing or malformed, and the "naked" cuticle normally found on the posterior portion of each segment is absent, instead displaying ectopic denticles. (**C**) Cuticle of the *arm* mutant containing P[Da-Gal4] and P[UAS-Arm*]. This combination results in nearly complete rescue of the arm phenotype with 100% penetrance. (**D**) Cuticle of the *arm* mutant containing P[Da-Gal4] and P[UAS-aroNC]. The aromatic mutant rescues the size defect, most of the head structures, and some of the posterior. Segments still contain ectopic denticles indicating some reduction in Wg signaling. (**E**) Cuticle of an embryo containing P[Da-Gal4] and P[UAS-Arm*]. (**F**) Cuticle of an embryo containing P[Da-Gal4] and P[UAS-aroNC].

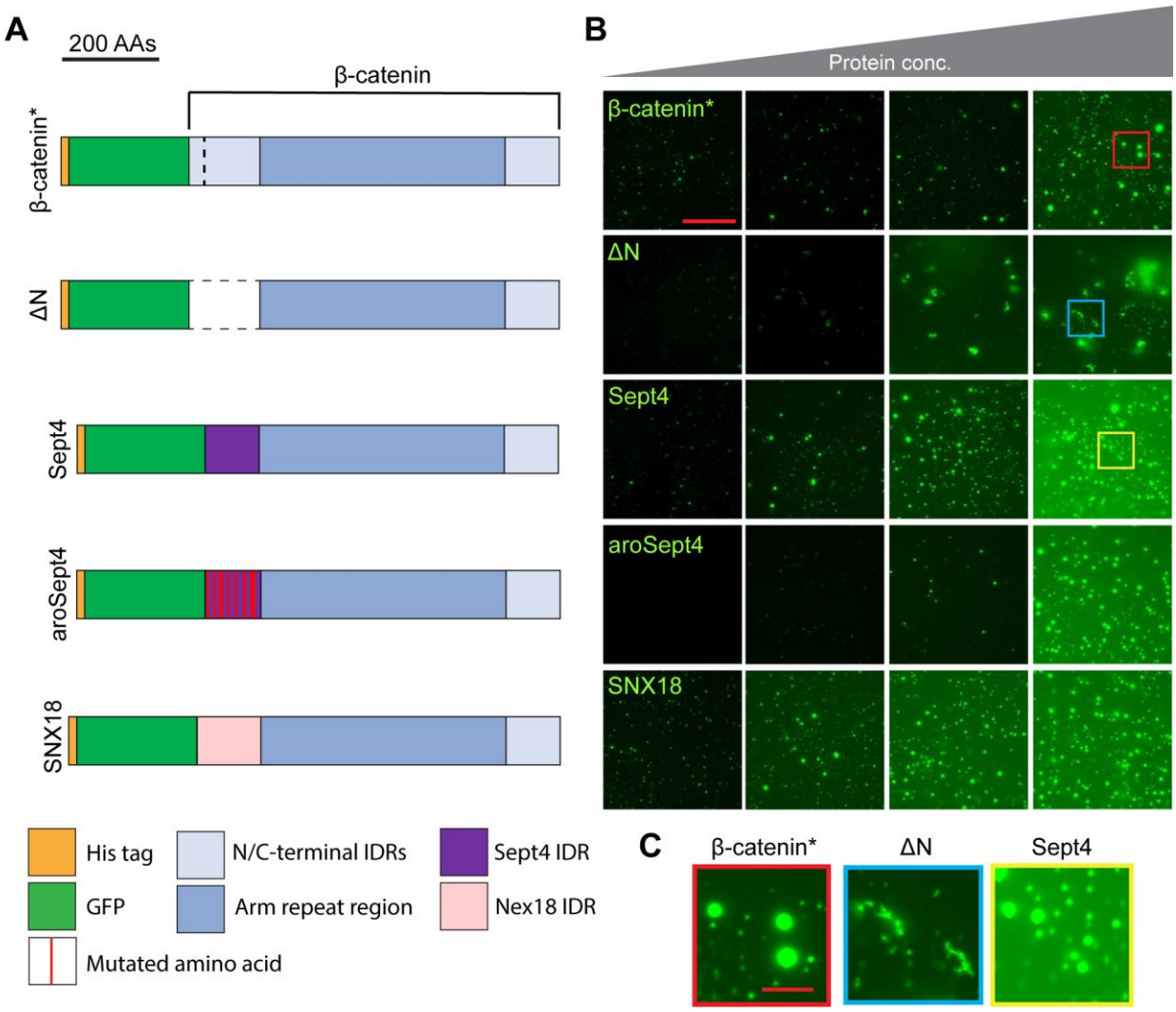

Fig 2.8. Heterologous IDRs rescue the *in vitro* droplet formation of an N-terminal β-catenin deletion mutant. (**A**) Cartoon representation of the eGFP-β-catenin* protein, ΔN (amino acids 1-151 deleted), Sept4 (119 amino acids from the Septin4 IDR), aroSept4 (Sept4 IDR with 11 aromatic amino acid mutations), and SNX18 (139 amino acids from the SNX18 IDR). (**B**) Representative images from an *in vitro* droplet formation assay with the indicated mutants. A protein concentration series of approximately 2μM, 3μM, 4μM, and 8μM is depicted. Droplet assays were performed in 300mM NaCl and 10% PEG-8000. At lower concentrations, ΔN is deficient in droplet formation; at higher concentrations ΔN forms non-spherical structures. The Sept4 and SNX18 droplets are qualitatively similar to those of β-catenin*, while aroSept4 is deficient in droplet formation compared to Sept4. Scale bar = 20μm. (**C**) Insets from the highlighted regions of panel B.

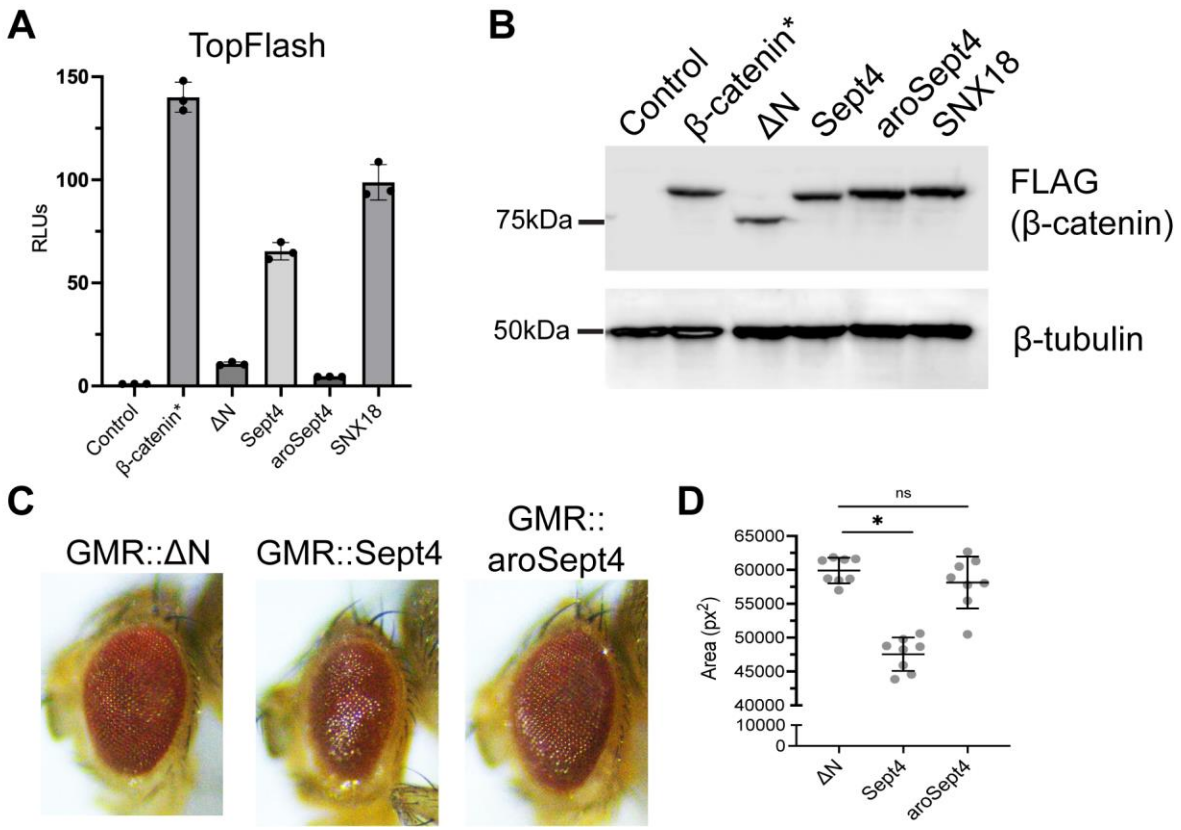

Fig 9. Heterologous IDRs can rescue the activity of a N-terminal β-catenin deletion mutant. (**A**) TopFlash luciferase reporter activity induced by β-catenin* or the derivative mutant constructs in HEK293T β-catenin KO cells. Cells were transfected with separate plasmids encoding the reporter gene and the FLAG-β-catenin mutant constructs. Luciferase activity was assayed 24hr post-transfection. Data are plotted as mean ± SD (n = 3). (**B**) Western blot analysis of transfected HEK293T β-catenin KO cell lysate. Lysate samples correspond to the luciferase reporter data. α-FLAG blot shows β-catenin expression. α-β-tubulin was used as a loading control. (**C**) Micrographs of adult Drosophila eyes containing P[GMR-Gal4] and UAS lines expressing ΔN, Sept or aroSept4. (**D**) Quantification of adult Drosophila eye area. Data are presented as mean ± SD (n = 8). p-values were calculated by one-way ANOVA followed by Dunnett's test. * = $p < 0.05$ and ns = $p > 0.05$.

Supplementary Figures

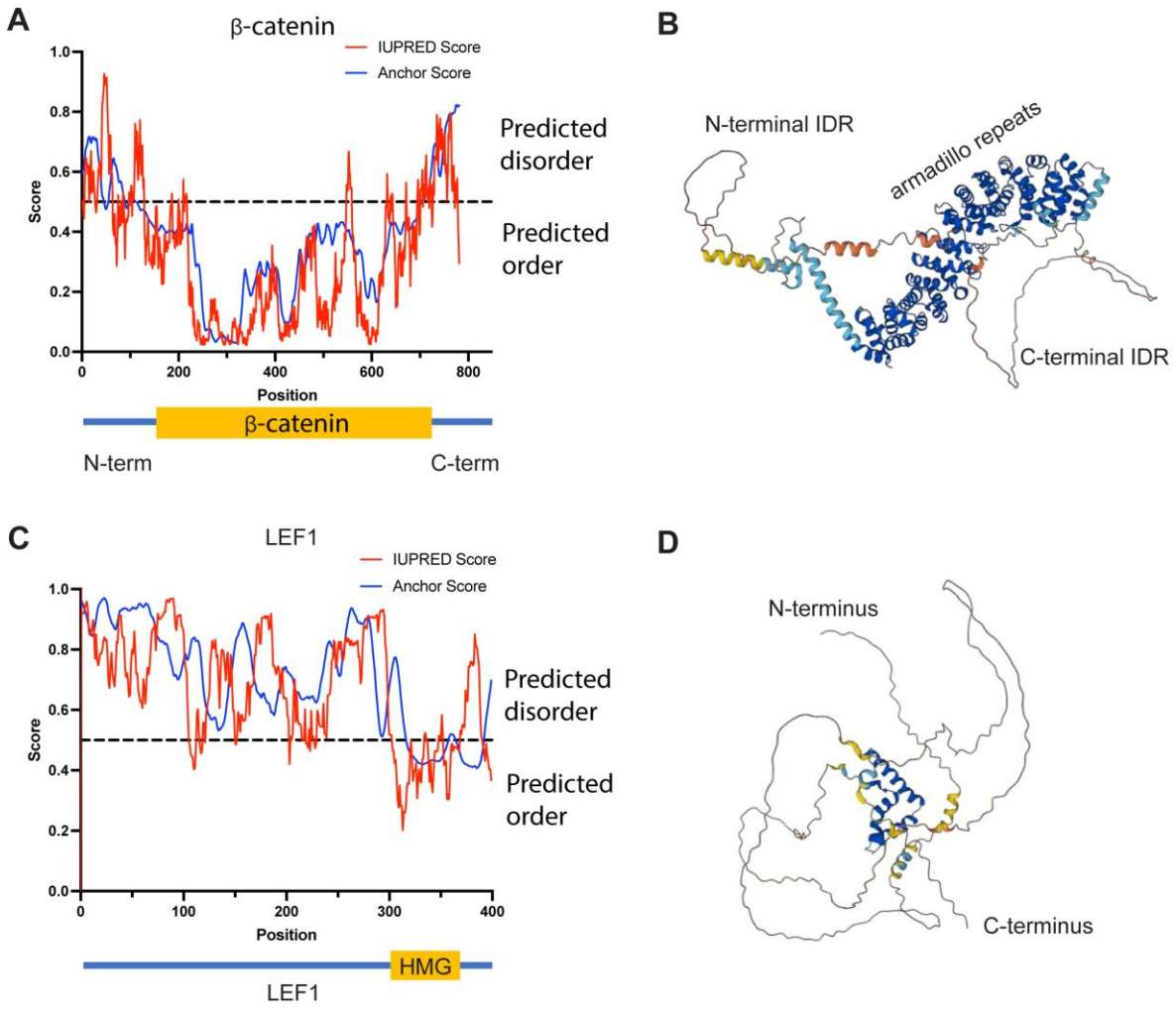

Figure S2.1. The N- and C-terminal β-catenin IDRs are predicted to be disordered. (**A**) IUPRED and Anchor analysis of human β-catenin. Regions with scores above 0.5 are predicted to be disordered, scores below 0.5 are predicted to be ordered. (**B**) AlphaFold prediction of β-catenin structure. The N- and C-termini lack a predicted structure, while the armadillo repeat region is α-helix rich and highly structured. (**C**) IUPRED and Anchor analysis of human LEF1. (**D**) AlphaFold prediction of LEF1 structure, indicating a mostly disordered structure.

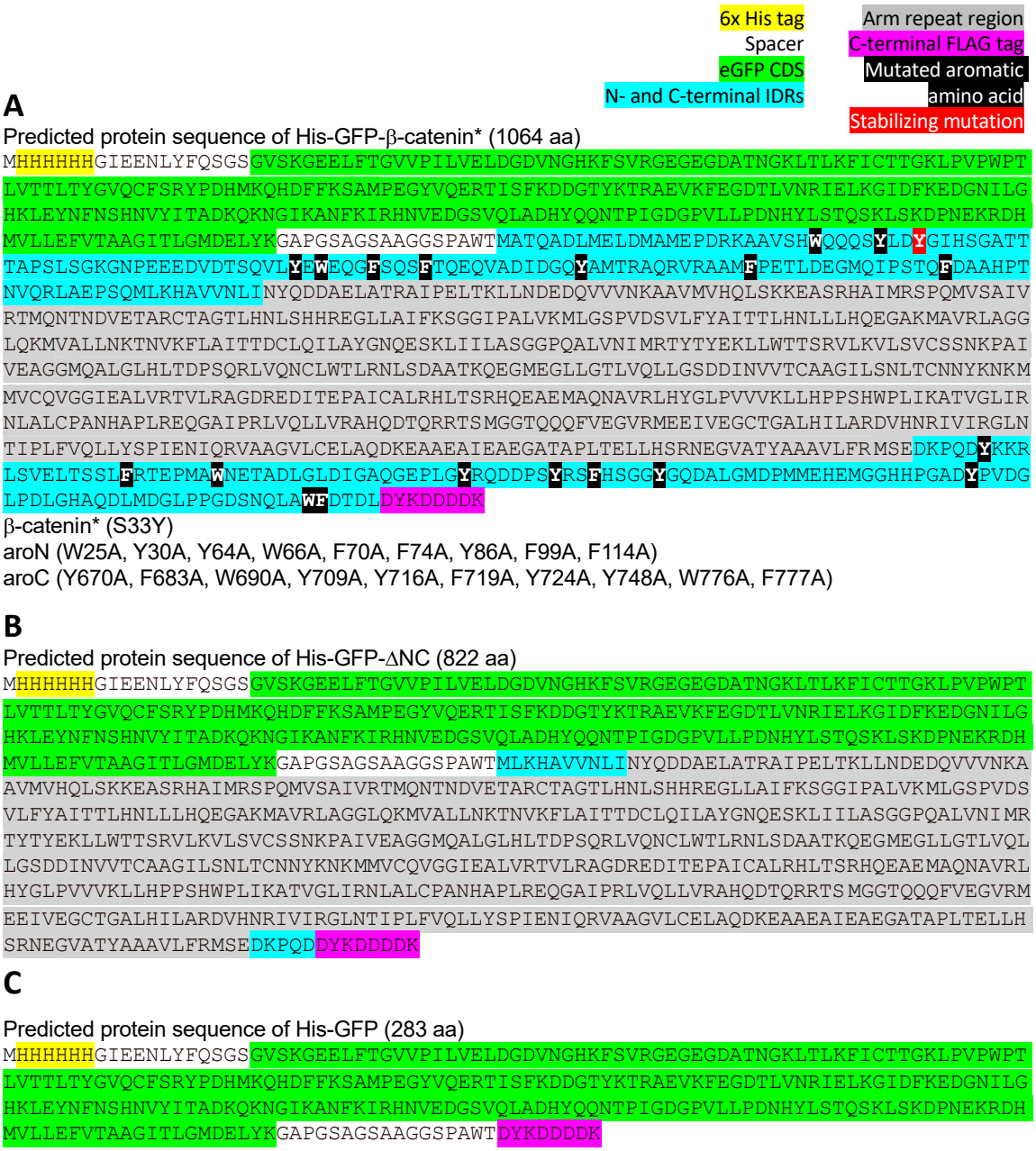

Figure S2.2. Sequences of the β-catenin mutants used for *in vitro* droplet formation assays. (**A**) Annotated amino acid sequences of recombinantly expressed His-eGFP-β-catenin* protein and its mutant derivatives. The specific amino acid residues that were mutated to create β-catenin*, aroN, and aroC are listed below the annotated sequence. AroNC contains all aroN and aroC mutations. (**B**) Annotated amino acid sequence of the His-eGFP-ΔNC mutant. (**C**) Annotated amino acid sequence of the His-eGFP mutant.

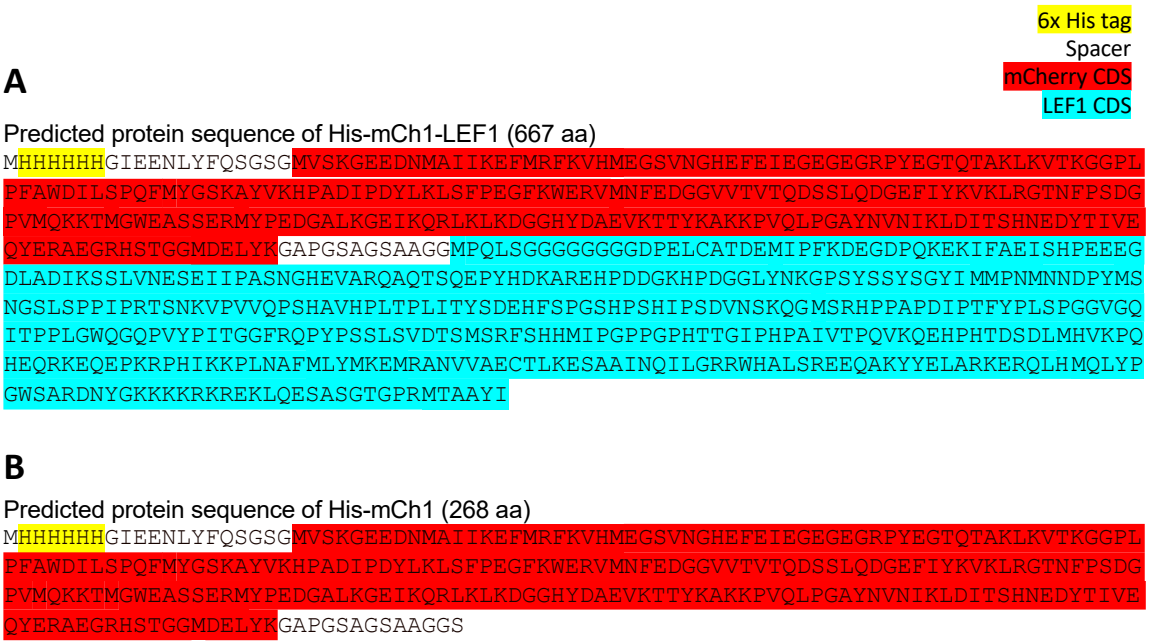

Figure S2.3. Sequence of the LEF1 mutant used for *in vitro* droplet formation assays. (**A**) Annotated amino acid sequence of recombinantly expressed His-mCherry-LEF1 protein. (**B**) Annotated amino acid sequence of His-mCherry.

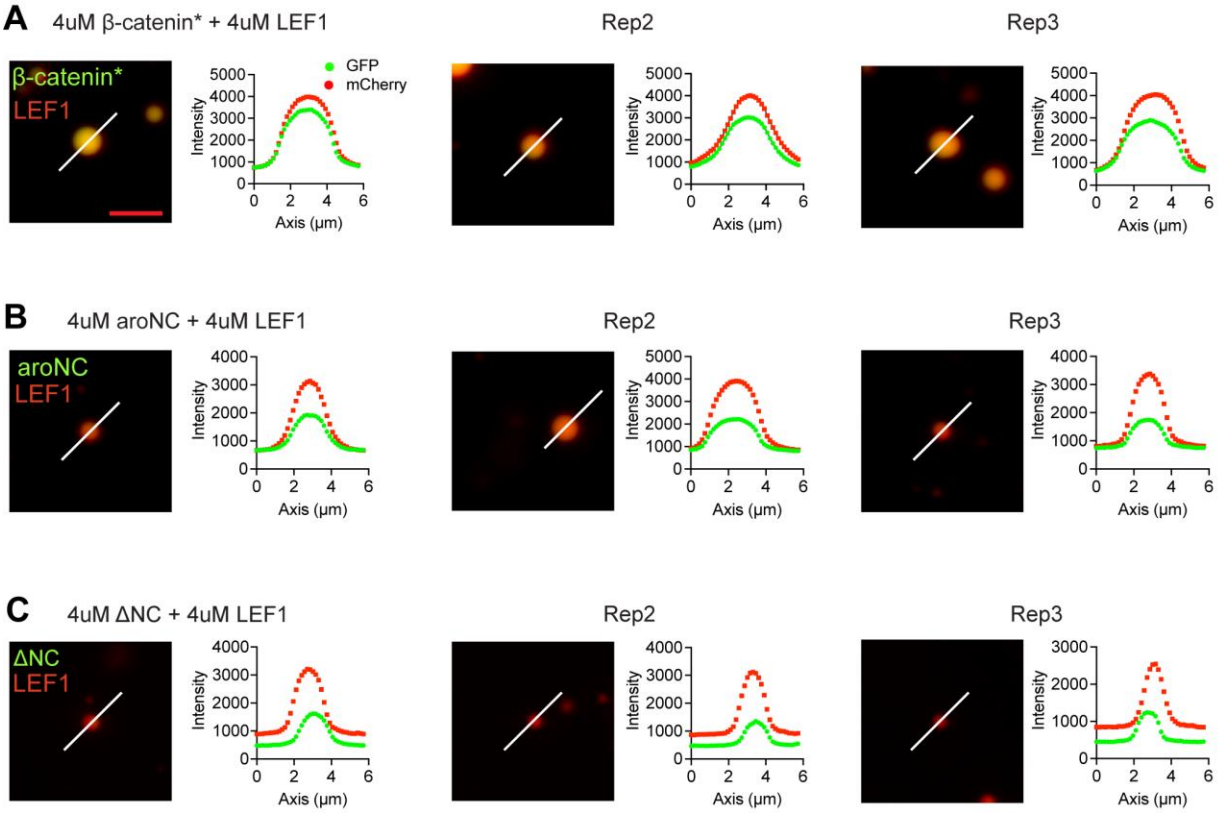

Figure S2.4. Additional line plots for β-catenin mutant and LEF1 heterotypic condensates. (**A**) Triplicate line plots showing eGFP-β-catenin* + mCherry-LEF1. (**B**) Triplicate line plots showing eGFP-aroNC and mCherry-LEF1. (**C**) Triplicate line plots showing eGFP-ΔNC and mCherry-LEF1. White lines represent the plotted trace. Scale bar = 5μm.

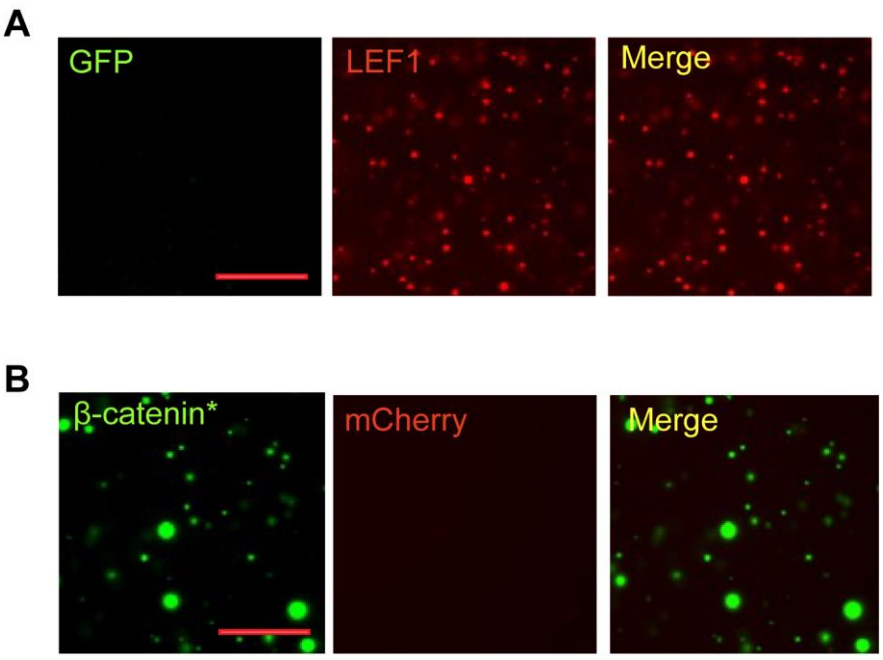

Figure S2.5. Fluorescent tag controls for heterotypic *in vitro* droplet formation assays. (**A**) Representative images from a heterotypic *in vitro* droplet formation assay with eGFP and mCherry-Lef1. The concentration of both eGFP and LEF1 protein is 8μM. Droplet assays were performed in 300mM NaCl and 10% PEG-8000. Scale bar = 20μm. (**B**) Representative images from a heterotypic *in vitro* droplet formation assay with eGFP-β-catenin*and mCherry. The concentration of both eGFP-β-catenin* and mCherry protein is 8μM. Droplet assays were performed in 300mM NaCl and 10% PEG-8000. Scale bar = 20μm.

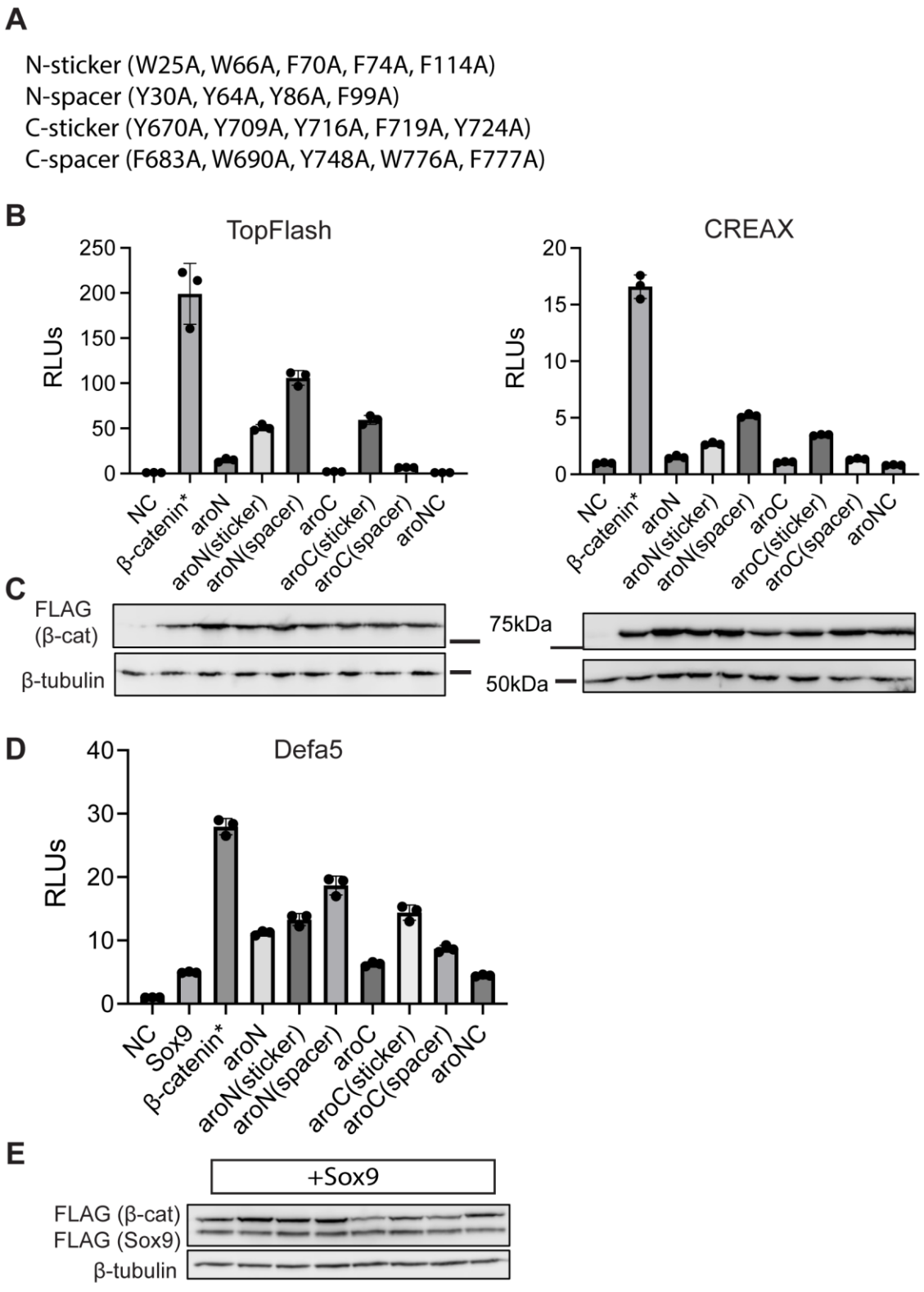

Figure S2.6. A broad array of aromatics in both IDRs contribute to β-catenin activity. (**A**) TopFlash (left) or CREAX (right) luciferase reporter activity induced by various sticker/spacer β-catenin mutants. (**B**) Western blots showing the expression of

each mutant construct. The protein samples used for the Western blot correspond to the samples used for the luciferase assay in (A). β-tubulin is used as a loading control. (**C**) HD5 luciferase reporter activity (Top) and corresponding Western blots (bottom). (**D**) The specific amino acids that were mutated to create the sticker and spacer mutants.

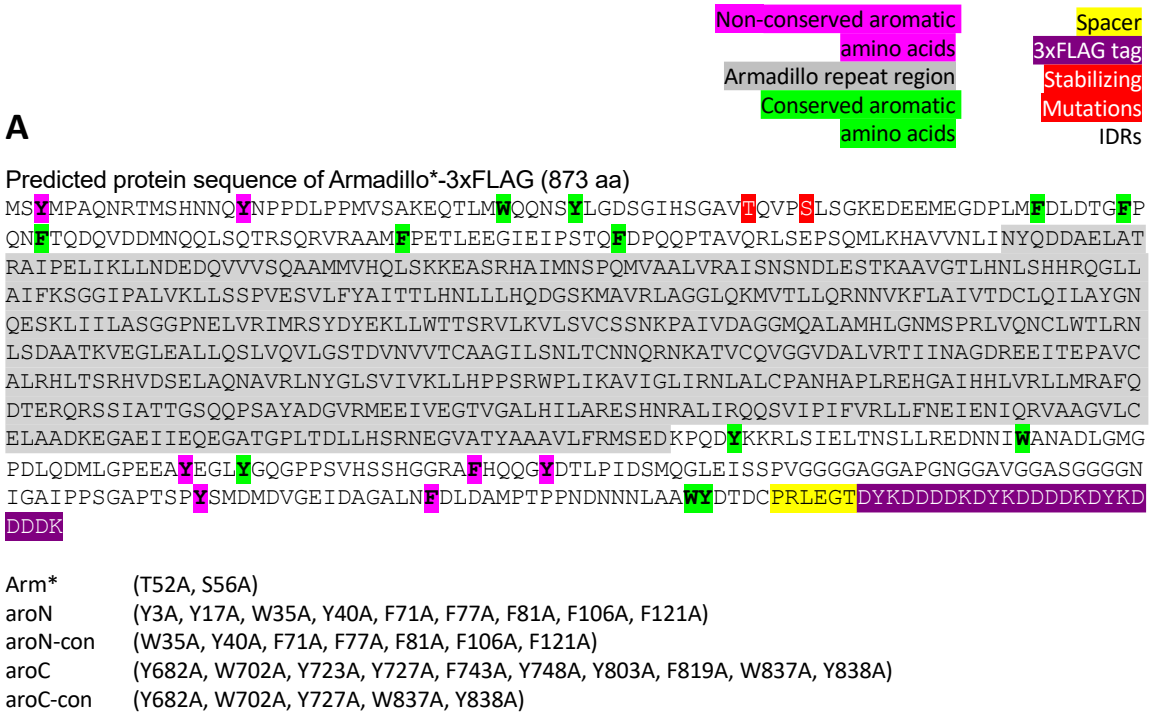

Figure S2.7. Sequences of the Arm* aromatic amino acid mutants. (**A**) Annotated amino acid sequence of the Arm protein. All of the aromatic mutants are built upon the Arm* mutation, i.e. they all have T52A and S56A.

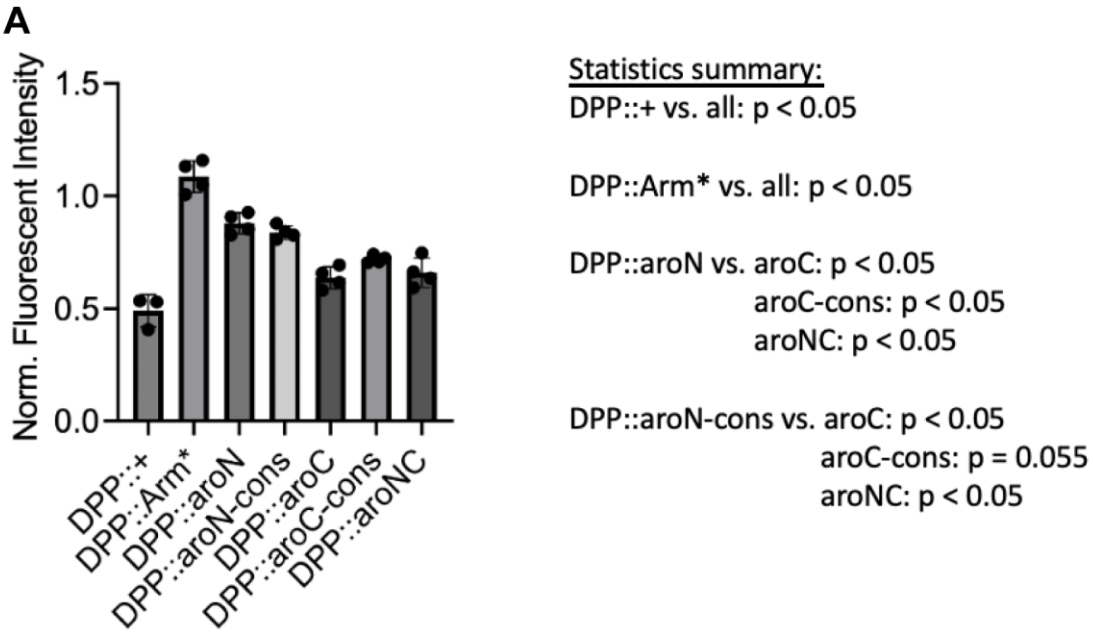

Figure S2.8. Quantification of fluorescent reporter activity in *Drosophila* larval wing discs. (**A**) Quantification of fluorescent intensity of a region of interest within the ectopic DPP-Gal4-driven reporter activity normalized to reporter activity driven by endogenous Wg signaling. Data are presented as mean ± SD. (**B**) Summary of statistics. P values were calculated with a one-way ANOVA followed by Tukey's HSD test. See table S2 for exact statistical test results.

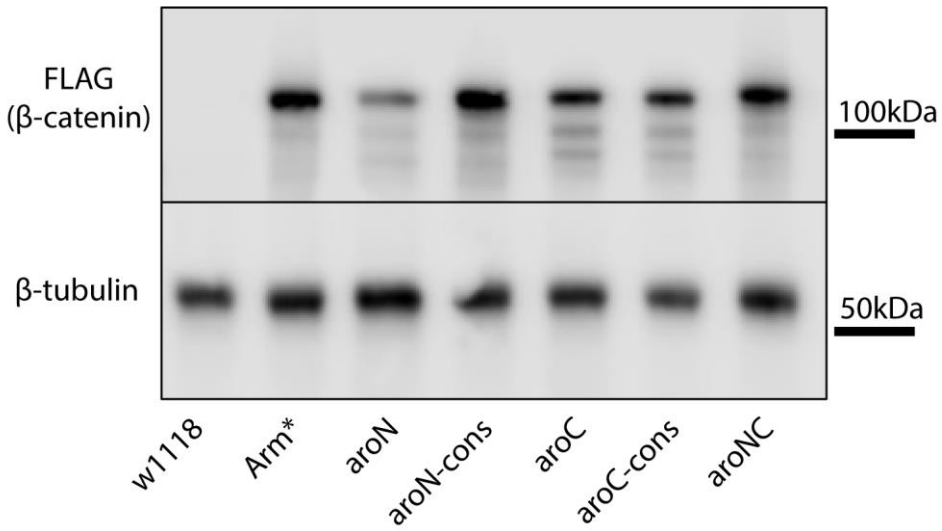

Figure S2.9. Expression of Arm* and Arm mutant proteins expression in *Drosophila* embryos. (**A**) Western blot analysis of *Drosophila* embryo lysates that were collected 4-8hr after laying. α-FLAG blot shows Arm protein expression and β-tubulin was used as a loading control.

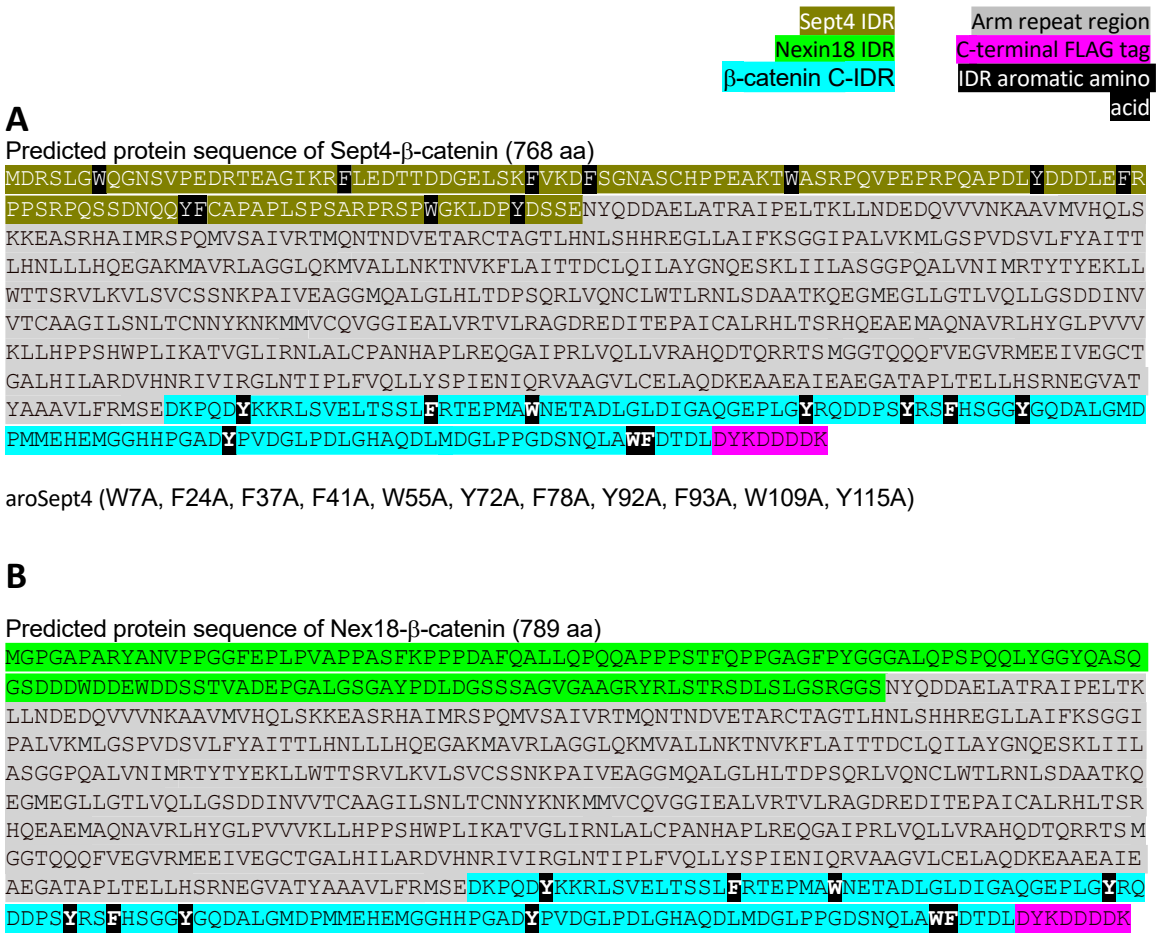

Figure S2.10. Sequences of the N-terminal heterologous IDR β-catenin mutants. (**A**) Annotated sequence of Sept4-β-catenin with indicated mutations for aroSept4-β-catenin. (**B**) Annotated sequence of Nex18-β-catenin.

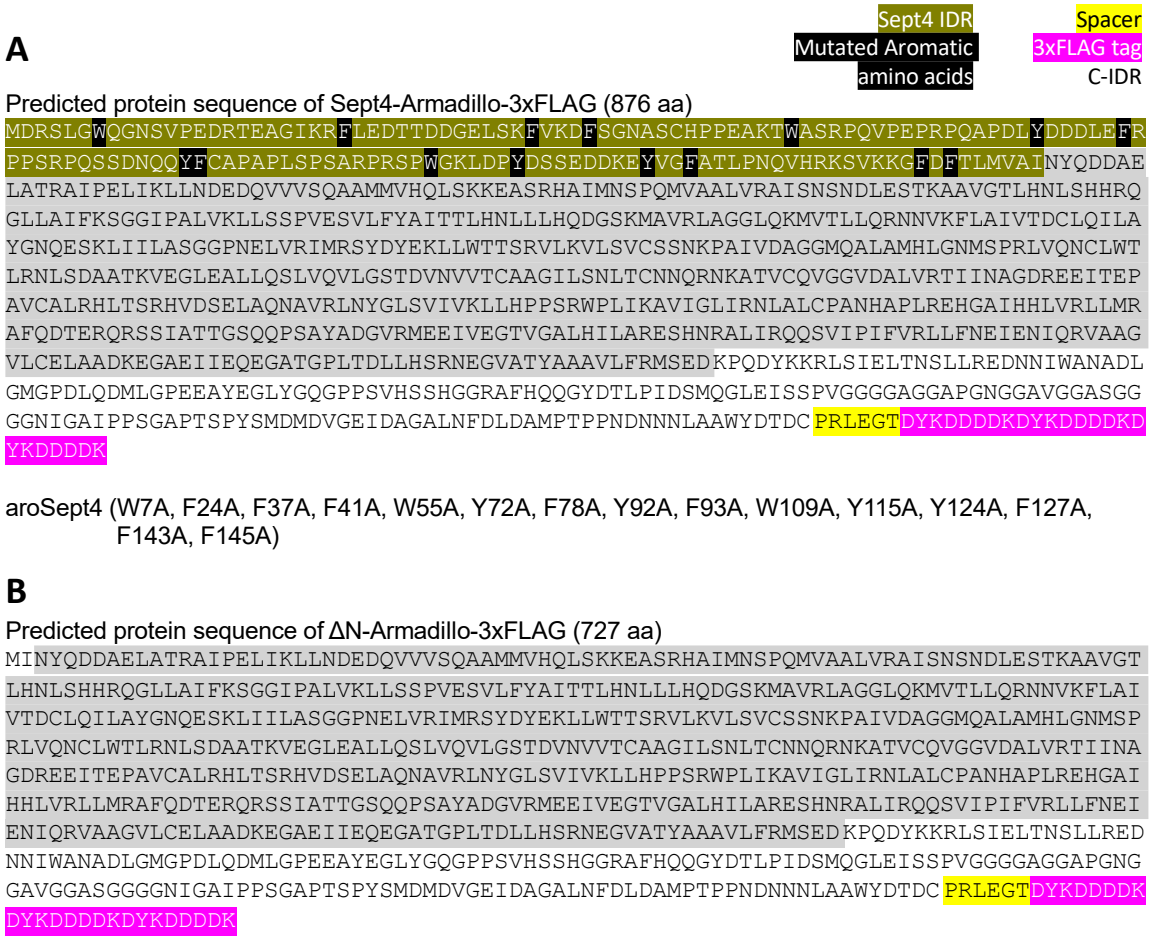

Figure S2.11. Sequences of the N-terminal heterologous IDR Armadillo mutants. (**A**) Annotated sequence of Sept4-Armadillo with indicated mutations for aroSept4-Armadillo. (**B**) Annotated sequence of ΔN-Armadillo.

Endogenous qRT-PCR Primers	
Primer Name	**Sequence (5' - 3')**
Axin2 Forward	CTGGCTTTGGTGAACTGTTG
Axin2 Reverse	AGTTGCTCACAGCCAAGACA
Sp5 Forward	GAAACAGTGCTCGGGTTTTC
Sp5 Reverse	TAGCTCTGCATGGAGCTGAA
β-actin Forward	CATGTACGTTGCTATCCAGGC
β-actin Reverse	CTCCTTAATGTCACGCACGAT
18S Forward	GTAACCCGTTGAACCCCATT
18S Reverse	CCATCCAATCGGTAGTAGCG

Table 2.1. Sequences of qPCR primers.

Number of families	1							
Number of comparisons per family	21							
Alpha	0.05							
Tukey's multiple comparisons test	**Mean Diff.**	**95.00% CI of diff.**	**Below threshold?**	**Summary**	**Adjusted P Value**			
DPP::+ vs. DPP::Arm*	-0.5963	-0.7270 to -0.4656	Yes	*	<0.000001			
DPP::+ vs. DPP::aroN	-0.3885	-0.5192 to -0.2578	Yes	*	<0.000001			
DPP::+ vs. DPP::aroN-cons	-0.3482	-0.4789 to -0.2175	Yes	*	<0.000001			
DPP::+ vs. DPP::aroC	-0.1462	-0.2768 to -0.01546	Yes	*	0.022259			
DPP::+ vs. DPP::aroC-cons	-0.2289	-0.3596 to -0.09824	Yes	*	0.000231			
DPP::+ vs. DPP::aroNC	-0.169	-0.2997 to -0.03829	Yes	*	0.006404			
DPP::Arm* vs. DPP::aroN	0.2078	0.08679 to 0.3288	Yes	*	0.000296			
DPP::Arm* vs. DPP::aroN-cons	0.2481	0.1271 to 0.3691	Yes	*	0.000029			
DPP::Arm* vs. DPP::aroC	0.4501	0.3291 to 0.5711	Yes	*	<0.000001			
DPP::Arm* vs. DPP::aroC-cons	0.3673	0.2463 to 0.4883	Yes	*	<0.000001			
DPP::Arm* vs. DPP::aroNC	0.4273	0.3063 to 0.5483	Yes	*	<0.000001			
DPP::aroN vs. DPP::aroN-cons	0.04027	-0.08073 to 0.1613	No	ns	0.92468			
DPP::aroN vs. DPP::aroC	0.2423	0.1213 to 0.3633	Yes	*	0.00004			
DPP::aroN vs. DPP::aroC-cons	0.1595	0.03852 to 0.2805	Yes	*	0.005327			
DPP::aroN vs. DPP::aroNC	0.2195	0.09848 to 0.3405	Yes	*	0.000149			
DPP::aroN-cons vs. DPP::aroC	0.202	0.08103 to 0.3230	Yes	*	0.000416			
DPP::aroN-cons vs. DPP::aroC-cons	0.1193	-0.001750 to 0.2403	No	ns	0.055043			
DPP::aroN-cons vs. DPP::aroNC	0.1792	0.05821 to 0.3002	Yes	*	0.001631			
DPP::aroC vs. DPP::aroC-cons	-0.08279	-0.2038 to 0.03822	No	ns	0.321307			
DPP::aroC vs. DPP::aroNC	-0.02283	-0.1438 to 0.09817	No	ns	0.995463			
DPP::aroC-cons vs. DPP::aroNC	0.05996	-0.06104 to 0.1810	No	ns	0.67275			
Test details	**Mean 1**	**Mean 2**	**Mean Diff.**	**SE of diff.**	**n1**	**n2**	**q**	**DF**
DPP::+ vs. DPP::Arm*	0.4902	1.086	-0.5963	0.04001	3	4	21.08	20
DPP::+ vs. DPP::aroN	0.4902	0.8787	-0.3885	0.04001	3	4	13.73	20
DPP::+ vs. DPP::aroN-cons	0.4902	0.8384	-0.3482	0.04001	3	4	12.31	20
DPP::+ vs. DPP::aroC	0.4902	0.6364	-0.1462	0.04001	3	4	5.166	20
DPP::+ vs. DPP::aroC-cons	0.4902	0.7191	-0.2289	0.04001	3	4	8.093	20
DPP::+ vs. DPP::aroNC	0.4902	0.6592	-0.169	0.04001	3	4	5.973	20
DPP::Arm* vs. DPP::aroN	1.086	0.8787	0.2078	0.03704	4	4	7.934	20
DPP::Arm* vs. DPP::aroN-cons	1.086	0.8384	0.2481	0.03704	4	4	9.472	20
DPP::Arm* vs. DPP::aroC	1.086	0.6364	0.4501	0.03704	4	4	17.19	20
DPP::Arm* vs. DPP::aroC-cons	1.086	0.7191	0.3673	0.03704	4	4	14.02	20
DPP::Arm* vs. DPP::aroNC	1.086	0.6592	0.4273	0.03704	4	4	16.31	20
DPP::aroN vs. DPP::aroN-cons	0.8787	0.8384	0.04027	0.03704	4	4	1.538	20
DPP::aroN vs. DPP::aroC	0.8787	0.6364	0.2423	0.03704	4	4	9.252	20
DPP::aroN vs. DPP::aroC-cons	0.8787	0.7191	0.1595	0.03704	4	4	6.091	20
DPP::aroN vs. DPP::aroNC	0.8787	0.6592	0.2195	0.03704	4	4	8.38	20
DPP::aroN-cons vs. DPP::aroC	0.8384	0.6364	0.202	0.03704	4	4	7.714	20
DPP::aroN-cons vs. DPP::aroC-cons	0.8384	0.7191	0.1193	0.03704	4	4	4.553	20
DPP::aroN-cons vs. DPP::aroNC	0.8384	0.6592	0.1792	0.03704	4	4	6.842	20
DPP::aroC vs. DPP::aroC-cons	0.6364	0.7191	-0.08279	0.03704	4	4	3.161	20
DPP::aroC vs. DPP::aroNC	0.6364	0.6592	-0.02283	0.03704	4	4	0.8716	20
DPP::aroC-cons vs. DPP::aroNC	0.7191	0.6592	0.05996	0.03704	4	4	2.289	20

Table 2.2. Statistical test results for Figure S2.7

Chapter 3 Investigating Chromatin Modifications Induced by a Wingless Signaling-Regulated Enhancer

This chapter contains unpublished work.

Introduction

In the nucleus of eukaryotic cells, DNA is packaged by histones and structural proteins into an organized complex referred to as chromatin. An important component of eukaryotic gene regulation is covalent post-translational modification (PTM) of the histone N-terminal tail (Lee and Grant, 2019). One commonly studied histone PTM is the addition of an acetyl group to lysine residues within the tail, which is positively correlated with transcription (Forsberg and Bresnick, 2001; Lee and Grant, 2019). Acetylated histone proteins are typically found at cis-regulatory elements such as enhancers and core promoters. These regions that contain acetylated histones are typically confined, spanning approximately 1-4kb (Roh et al., 2005).

Histone acetylation is generally thought to affect gene regulation in two ways: first, the negatively charged acetyl group neutralizes the positively charged histone N-terminal tail, thereby weakening electrostatic interactions with DNA and nucleosome-nucleosome interactions within the chromatin fiber, making it more accessible to proteins, and second, acetylated histones serve as a binding motif for bromodomain-containing transcriptional co-regulators (Shogren-Knaak et al., 2006; Shvedunova and Akhtar, 2022). The hypothesis that acetylation neutralizes the positively charged histone tail which makes the chromatin structure permissive to transcription has many conflicting results in the literature. The strongest evidence in support of it are the observations that acetylation of histone H4 at lysine residue 16 (H4K16ac) promotes open conformations of chromatin arrays *in vitro* and that the removal of H4K16ac promotes chromatin fiber compaction in yeast (Garcia-Ramirez et al., 1995; Wilkins et

al., 2014). Additional reports indicate that acetylation by CBP has a destabilizing effect on nucleosome structure *in vitro* (Choi and Howe, 2009; Morales and Richard-Foy, 2000). However, other studies indicate that H4K16 has little to no effect on chromatin compaction *in vivo* and *in vitro* (Lutter et al., 1992; Taylor et al., 2013). More recent studies suggest that the electrostatic interaction of RNA with histone tails neutralizes the tail's positive charge and affects chromatin structure (Dueva et al., 2019). The second point, histone acetylation affects gene regulation by creating a binding motif for bromodomain-containing proteins, is supported by ChIP-seq-based evidence and *in vitro* interactions (Morinière et al., 2009). The transcriptional co-regulators BRD4 and TFIID subunit 1 both contain bromodomains and are required for productive transcription (Shvedunova and Akhtar, 2022). This aspect of histone acetylation's role in gene regulation is less controversial.

In actively transcribed *Drosophila* genes, for instance, *β-tubulin*, small chromatin domains contain acetylated histones and this mark is confined to the regulatory DNA elements present in this locus (Parker et al., 2008; Roh et al., 2005). A second example, the *Raf1* locus in mouse embryonic stem cells (mESCs), also exemplifies this general histone acetylation model. ChIP-seq data shows that at the *Raf1* locus, sharp, narrow regions of H3K27ac are present at an intronic enhancer and the transcription start site (Weintraub et al., 2017). Analysis of the genes *naked cuticle* (*nkd*) and *notum* (*not*), which are regulated by the Wingless (Wg; fly Wnt) signaling pathway, has revealed a different pattern of histone acetylation in which broad regions of chromatin are acetylated. These modifications extend well beyond Wg response elements (WREs), which are the enhancers that mediate the transcriptional response to Wg signal transduction, and cover most of the gene body, spanning domains up to 30kb at the *nkd* locus (Parker et al., 2008). The enrichment of acetylated histones across the *nkd* locus is not uniform and the strongest enrichment of histone acetylation is observed at an intronic WRE, potentially indicating that this site serves as a nucleation point.

The mechanism by which this widespread histone acetylation is established is currently unknown, as is its importance in Wg target gene regulation. It is known that Armadillo (Arm, fly β-catenin) and the histone acetyltransferase Nejire, the *Drosophila* ortholog of CBP (from this point referred to as dCBP), localize to WREs in a Wg-

dependent manner (Parker et al., 2008). Chemical inhibition of RNA pol II elongation prior to activation of the Wg signaling pathway results in similar widespread histone acetylation pattern, indicating that this phenomenon is not a result of transcription. This suggests that chromatin remodeling occurs prior to gene expression and is thus a potential transcriptional regulatory mechanism. Furthermore, RNAi knockdown of dCBP abrogates localization to the WRE in response to Wg signaling, widespread histone acetylation, and subsequent gene expression, indicating that dCBP is the major HAT involved in acetylating the nkd locus (Parker et al., 2008). Due to technological limitations at the time of Parker and colleagues' publication, the nkd intronic WRE's specific contribution to the histone acetylation profile could not be assayed.

In this chapter, I attempt to address the hypothesis that the widespread histone acetylation observed at the Wg target gene *not* emanates from a single WRE, and that histone acetylation is sufficient for the expression of Wg target genes, in particular *nkd*. CRISPR/Cas9 gene editing was used to delete a WRE that regulates *not*, and downstream readouts were tested. To determine if histone acetylation is involved in activating transcription of nkd, it is necessary to acetylate the nkd locus independent of input from the Wg signaling pathway. A dCas9-CBP^{core} construct was constructed and targeted to the nkd intronic WRE, will allow for the direct assessment of the sufficiency of chromatin remodeling to activate Wg target gene expression. This work intends to characterize the link between enhancer activity and chromatin environment, with the long-term goal of understanding why genes regulated by the Wg signaling pathway exhibit a distinct chromatin profile.

Results

The broad domains of histone acetylation observed at active Wg target genes is highly reproducible

Published work from the Cadigan lab has shown that in Drosophila, the active Wnt target genes *nkd* and *not* exhibit a broad pattern of histone acetylation that spans the entire gene body (Parker et al., 2008). At the *nkd* gene locus, ChIP data suggests that β-catenin localization is confined to a single known Wnt-regulated enhancer (WRE) that's approximately 5.5kb downstream of the TSS, and histone acetylation extends far

beyond this WRE (Fig 2.1A) (Parker et al., 2008). As there was a significant period of time (approximately 10 years) between the publication of the work from Parker and colleagues and this follow-up work, it was first necessary to determine if the ChIP data in the manuscript was reproducible with modern reagents and antibodies.

I first set out to reproduce the widespread histone acetylation observed in the Wg-stimulated Kc167 cell line. Two major differences exist between the follow-up work and the original: first, for cell culture models, the Wg signaling pathway is activated with the chemical CHIR-99021 (CHIR) rather than Wg-conditioned cell culture medium. Second, histone acetylation was detected using an antibody produced by a different manufacturer. An increase in H3 acetylation is observed across the *nkd* locus in response to CHIR treatment (Fig 2.1B). The follow-up ChIP-qPCR data faithfully reproduces the original, with select primer pairs being used to detect enrichment of ChIP signal across the locus.

In *Drosophila* embryos, the broad increase in acetylated histone H3 is also reproducibly observed at the *not* locus. The original work from Parker and colleagues used the Gal4-UAS expression system to globally express Wg in the *Drosophila* embryo. Levels of histone H3 acetylation at the active *not* locus were then assayed with ChIP-qPCR (Parker et al., 2008). A domain of acetylated H3 enrichment of approximately 10kb was observed at the locus (Fig 2.1C). I reproduced this data by globally expressing a stabilized Arm mutant with the Gal4-UAS system. I also observed a broad domain enriched for acetylated H3, consisting of approximately 17.5kb (Fig 2.1D). These results confirm that Wg signaling induces widespread histone acetylation at Wg target genes.

Multiple WREs regulate *notum* expression in *Drosophila*

Since the Wg-induced widespread histone acetylation is reproducible, I next sought to test the hypothesis that the information coded in a single WRE is necessary to cause the widespread histone acetylation observed at active Wg target genes. To test this hypothesis, CRISPR/Cas9 genome editing technology was used to delete a WRE and determine any changes in histone acetylation with ChIP-qPCR. The next step is to choose a candidate WRE.

A WRE that is approximately 2kb upstream of the *not* TSS (referred to as *not* UpE, for upstream enhancer) was selected as a candidate for deletion in *Drosophila*. The *not* locus has two known WREs: the upstream enhancer and an intronic enhancer approximately 5.5kb downstream of the TSS (Fig 2.2A) (Parker et al., 2008). In the *Drosophila* Kc167 cell line, both WREs show Pangolin (Pan, fly TCF/LEF) localization, suggesting that they both might have activity. In *Drosophila* embryos, Pan has detectable localization at only the *not* UpE, suggesting that *not* UpE might be the main WRE regulating *not* expression in this context (Parker et al., 2008). Additionally, LacZ immunostainings of a transcriptional reporter consisting of *not* UpE driving the expression of LacZ recapitulates the endogenous expression pattern of *not* in the embryo (M. V. Chang et al., 2008). This further suggests that *not* UpE is the main regulator of *not* expression in the embryo. This data provided the justification to delete *not* UpE to determine the necessity of a single WRE for the widespread histone acetylation observed at the active *not* locus.

The CRISPR/Cas9 gene editing strategy employed was to dissect out *not* UpE and replace it with a floxed DsRed selectable marker, which could be removed with CRE recombinase prior to downstream analysis (Fig 2.2A). Four independent CRISPR/Cas9 edited fly lines were identified by the presence of the selectable marker, and *not* UpE KO was confirmed by PCR genotyping (Fig 2.2B), which was followed up with sanger sequencing.

Initial downstream analysis of *not* UpE KO flies sought to determine if there was a *not* expression deficiency. Embryos from two independent CRISPR edited lines, CLG1 and CLG2 were collected and *not* expression was analyzed with qPCR. CLG1 and CLG2 revealed no deficiency compared to the control parental strain or a wild-type lab strain, w^{1118} (Fig 2.2 C). Given that active transcription is likely to confound the necessary ChIP-qPCR experiments, as transcribed loci are typically enriched with acetylated histones (Martin et al., 2021), it was decided to not experimentally pursue the *not* UpE KO flies further.

To further test the hypothesis that a single WRE is necessary for widespread histone acetylation, additional WREs that regulate *not* need to be deleted until there is no detectable *not* expression.

Targeting a WRE that regulates *nkd* for deletion

A previous study in the lab showed that broad histone acetylation is present at the active *nkd* locus in the *Drosophila* Kc167 cell line (Parker et al., 2008). Chromatin immunoprecipitation experiments in this work revealed that there is one detectable localization site for both Arm and CBP, the histone acetyltransferase that is required for histone acetylation at this locus, at a WRE that is approximately 5.5kb downstream of the transcription start site (WRE is referred to as *nkd* IntE). This work hypothesized that the widespread histone acetylation detected at the active *nkd* locus emanated from *nkd* IntE. I sought to test this hypothesis by generating a *nkd* IntE deletion cell line with CRISPR/Cas9 gene editing technology and determining the effects on histone acetylation patterns at the active *nkd* locus.

I used an analogous gene editing strategy as described in the previous section. I targeted Cas9 to *nkd* IntE with 1 gRNA that was directly 5' of the WRE and 1 gRNA that was directly 3' of the WRE (Fig 3.3A). The double-strand breaks generated by Cas9 would then be used to knock-in a Floxed GFP expression cassette, to mark positive gene editing events. A CRISPR/Cas9-induced deletion of approximately 1400bp, spanning *nkd* IntE was identified by PCR genotyping (Fig 3.3B).

A qPCR was performed on this *nkd* IntE KO cell line to determine whether there was an effect on *nkd* expression (Fig 3.3C). The data indicates that *nkd* IntE KO cells are deficient in *nkd* expression compared to wild-type. However, the expression of an additional Wnt target gene, *not*, was tested and determined to also be deficient in expression (Fig 3.3C). This data indicates that either both genes are co-regulated by *nkd* IntE or that the cell line is globally deficient in activating Wnt target genes. The Kc167 cells were clonally expanded during the CRISPR/Cas9 gene editing protocol, which can potentially explain the global deficiency in activating Wnt target genes.

Ectopic histone acetylation is sufficient for *nkd* expression

To determine if histone acetylation is involved in activating transcription of *nkd*, it is necessary to acetylate the *nkd* locus independent of input from the Wg signaling pathway. Reports in the literature have shown that histone acetylation caused by dCas9-p300^{core}, a fusion protein consisting of a catalytically dead Cas9, which is unable

to cause double-strand breaks, and the core catalytic domain of the mammalian HAT p300 (the CBP paralog) is sufficient to activate gene expression in eukaryotic cells (Chavez et al., 2015; Hilton et al., 2015; Lopes et al., 2016). Localization of the dCas9-$p300^{core}$ fusion protein to enhancers and promoters can activate gene expression through targeted chromatin remodeling (Hilton et al., 2015). A similar study was done in a *Drosophila* cell line showing that a dCas9-VPR (a chimeric trans-activation domain consisting of VP64, p65, and Rta activation domains) fusion protein could also activate gene expression when targeted to enhancers and promoters (Chavez et al., 2016). These reports serve as the premise to study the sufficiency for histone acetylation to cause expression of *nkd*.

A dCas9-$dCBP^{core}$ fusion protein was overexpressed in the Kc167 cell line and targeted to the *nkd* intronic WRE. qPCR analysis of *nkd* expression indicates that dCas9-$dCBP^{core}$ can cause robust activation of *nkd* when targeted to the intronic WRE compared to a non-targeting control (Fig 3.4A). dCas9 constructs do not activate *nkd* expression, regardless of whether they're targeted to the intronic WRE. As this activation of *nkd* is independent of any Wg signaling input, it shows that histone acetylation is sufficient to cause *nkd* expression.

Discussion

These experiments are the start to a project that sought to determine a mechanism for the establishment of the widespread histone acetylation observed at active Wg target genes and the role that histone acetylation plays in regulating Wg target gene expression. The observation that broad regions of chromatin are acetylated at the active *not* and *nkd* gene loci is robust and reproducible (Fig 2.1). However, it is unclear if this phenomenon occurs at every Wg target gene in *Drosophila*, or if it is restricted to those two genes. Additionally, it is unclear if widespread histone acetylation is conserved across species and a feature of active Wnt target genes in mammals. Future experiments to assay genome-wide, Wg-dependent changes in histone acetylation should be performed. Data gained from these experiments can indicate whether widespread histone acetylation is a general feature of Wg target genes, which

would warrant further mechanistic investigation into how these widespread domains are established and if they serve a regulatory purpose.

Determining if widespread histone acetylation is a general feature of active Wnt target genes is important because it can be used as a criterion to identify direct Wnt targets, which are historically difficult to find. Wnt signaling regulates genes in a highly tissue specific manner (Archbold et al., 2012). Efforts to identify Wnt target genes have focused on identifying changes in the transcriptome of a cell type, which does not differentiate between direct and indirect targets. Additionally, establishing the presence of TCF/LEF and/or β-catenin near TSSs have been used to infer direct Wnt target genes, although mere presence does not establish a functional role (Ramakrishnan and Cadigan, 2017). Including a chromatin signature may increase the precision of Wnt target gene calls.

Mechanistically understanding if widespread histone acetylation emanates from a single WRE or is an additive effect from multiple WREs would provide important insight into WRE function. It is understood that genes, particularly those that are important for development, can be regulated by multiple enhancer elements (Kvon et al., 2021; Panigrahi and O'Malley, 2021). This is thought to confer robustness to transcriptional regulation. Both *nkd* and *notum* have validated WREs upstream of their TSSs and within their first introns (Parker et al., 2008), but the activity of these WREs in various tissue contexts is unknown. In *Drosophila* embryos, the WRE upstream of *not* is the only known localization site of Pan and Arm (Parker et al., 2008). This information made it a prime candidate for deletion, as it seemed likely that it was the only WRE regulating *not* in the embryo.

Deleting a WRE and observing differences in the histone acetylation profile of *not* would experimentally establish the necessity of WREs in causing widespread histone acetylation. The CRISPR/Cas9 deletion of *not* UpE failed to inhibit the expression of *not*, suggesting that there are other WREs acting on *not* which would confound our analysis (Fig 2.2C). This was a predicted outcome. To further build on this experiment, additional WREs that regulate *not* would need to be deleted, starting with the *not* intronic WRE. As the total number of WREs that regulate *not* is unknown, this could be an iterative process with an unknown end, so experimental progress was halted. So

whether a single WRE is necessary for widespread histone acetylation is still an open question.

A similar experimental modality was attempted for the *nkd* IntE WRE in the *Drosophila* Kc167 cell line. Kc167 cells are not highly amenable to CRISPR-induced gene editing at the *nkd* locus, likely due to the aneuploidy of the cell line. Still, a putative positive CRISPR-induced *nkd* IntE KO was identified. However, the *nkd* IntE KO cell line that was identified had a global deficiency in expressing Wnt target genes, likely due to an artifact from clonal expansion. It is likely that there is also not a specific effect on *nkd* expression for a reason similar to what was observed in *Drosophila*, i.e. that multiple WREs likely regulate *nkd* expression and provide a robustness to the gene's expression.

Ectopic acetylation at the *nkd* intronic WRE by dCas9-dCBP^{core} was sufficient for the transcriptional activation of *nkd* (Fig 2.3). Further control experiments still need to be performed, however. The best control for this experiment is to mutate the dCBP^{core} part of the chimeric protein to be catalytically dead, which has been done in previous reports (Hilton et al., 2015). dCBP^{core} may be recruiting additional transcriptional co-regulators to the WRE, which can confound the results. The utility of the dCas9-dCBP^{core} construct is that it can be readily targeted to additional enhancers. Further experiments can be performed to determine if histone acetylation at additional WREs which regulate *nkd* have the same effect. Furthermore, this can be tested at other Wg targets to determine if WRE acetylation is sufficient for expression.

Materials and methods

Cell culture, CHIR treatment, and transfections

Kc167 cells were grown in Schneider's *Drosophila* Medium (Gibco) supplemented with 5% FBS (Atlanta Biologicals) and 1% Penicillin-Streptomycin-Glutamine (Invitrogen). Cells were grown at 25 degrees Celsius.

To activate the Wg signaling pathway, cells were treated with 10μM CHIR-99021 (APExBIO) in DMSO (Sigma-Aldrich) and incubated for 24hr. DMSO was used as a vehicle control.

For transfections, Kc167 cells were seeded into 12 well plates and allowed to grow overnight. Plasmids were transfected with the FugeneHD reagent (Promega). The ratio of FugeneHD to plasmid used was 3:1, and 1ug of plasmid was used.

Plasmids

dCas9 was expressed from transient transfection assays from the pl018 vector (Gift from Norbert Perrimon) (Housden et al., 2015). To generate this construct, the dCas9 ORF was PCR amplified from pWalium20-10XUAS-3XFLAG-dCas9-VPR (Addgene #78897, gift from Norbert Perrimon). The primers used to amplify dCas9 created an AgeI restriction site immediately upstream of the dCas9 ORF. Downstream of the ORF, a multi-cloning site consisting of AseI, NheI, AvrII, and FscII was created, and an XhoI site was also created. The PCR product was digested with AgeI and XhoI (New England Biolabs) for directional cloning into the pl018 vector, which was also digested with the same enzymes. The PCR product was ligated into the pl018 vector with T4 DNA ligase (New England Biolabs).

dCas9-dCBP^{core} was expressed from transient transfection assays from the pl018 vector. To generate this construct, the Nejire (dCBP) catalytic core sequence was identified based on homology to the mammalian CBP core catalytic sequence identified by Hilton and colleagues (Hilton et al., 2015). This sequence was amplified from a cDNA library generated from Kc167 cells. PCR primers added an AscI restriction site upstream of the dCBP^{core} coding sequence and an AvrII restriction site downstream of the dCBP^{core} coding sequence. The PCR product and the pl018-dCas9 vector were digested with AscI and AvrII, fragments were purified by gel electrophoresis, and ligated with T4 DNA ligase (New England Biolabs).

To target the dCas9 and pl018 constructs to chromatin, oligos coding for the gRNA sequence were ordered (Integrated DNA Technologies) and ligated into pl018-dCas9 and pl018-dCas9-dCBP^{core} vectors that were linearized by BbsI (Housden et al., 2015). The gRNA sequence 5'- GCGGGCCCTGTTGGCTATGG -3' was used to target these constructs to the *nkd* intronic WRE. Non-targeting control constructs used the gRNA sequence: 5'- GTTCGGGTCTTCGAGAAGACCT -3', which is the original sequence in the pl018 vector.

CRISPR/Cas9 Genome editing in Kc167 cells

CRISPR/Cas9 genome editing was used to delete the *nkd* IntE in Kc167 cells. gRNA sequences targeting Cas9 upstream and downstream of *nkd* IntE were cloned into the pl018 vector (Gift from Norbert Perrimon). A donor vector plasmid was created, which contains 1kb arms homologous to the regions directly upstream and downstream to *nkd* IntE, flanking a floxed coppia-GFP expression cassette.

The pl018 vectors and the donor plasmid were transfected into Kc167 cells with the Fugene HD reagent (Promega), using a ratio of FugeneHD to DNA of 3:1. Five days after transfection, the cells underwent FACS using a Discovery S8 Cell Sorter (BD). Single cells were seeded in 96 well plates, and cells were grown in 50% conditioned cell culture medium. Cell culture lines were created from the clonal expansion of GFP+ cells.

PCR genotyping was performed to determine the presence or absence of a CRISPR-induced gene edit event. gRNA was extracted from the Kc167 cells with the Qiagen Blood and Tissue DNA extraction kit.

Transgenic *Drosophila* strain development

CRISPR/Cas9 genome editing was used to delete the *not* UpE. gRNA sequences targeting Cas9 upstream and downstream of the *not* UpE were cloned into pCFD3-dU6:3gRNA, which was a gift from Simon Bullock (Addgene plasmid # 49410) (Port et al., 2014). For a list of gRNA sequences used, see Table 2.2. A homologous recombination donor vector, used to incorporate a DsRed selectable marker in place of the endogenous *not* UpE, was constructed by PCR amplifying 1kb homologous sequence arms that were directly upstream and downstream of the Cas9 double-strand break sites. w^{1118} *Drosophila* genomic DNA was used as a template. PCR amplification of a floxed DsRed expression cassette being driven by a 3xP3 CRM, and a plasmid backbone were amplified from pDsRed-attP, which was a gift from Melissa Harrison & Kate O'Connor-Giles & Jill Wildonger (Addgene plasmid # 51019) (Gratz et al., 2014). PCR fragments were ligated with the NEBuilder Hi-Fi DNA Assembly Kit (New England Biolabs).

Two gRNA coding constructs were used to target the 5' end of *not* UpE and three gRNA coding constructs were used to target the 3' end of the *not* UpE. Plasmid constructs were injected by BestGene Inc. (Chino, CA). The fly stocks injected were yw; Cas9(II-attP40) (Port et al., 2014). CRISPR/Cas9-edited mutants were identified by DsRed fluorescence in the adult eye. Transgenic chromosomes were balanced over the TM6c balancer. To remove the DsRed expression cassette, flies were crossed with a Cre-recombinase expressing fly, y[1] w[67c23] P{y[+mDint2]=Crey}1b; sna[Sco]/CyO (BDSC stock #766). To PCR genotyping was performed to confirm the deletion of *not* UpE. Genotyping PCRs produced at WT band size of 2655bp and a transgene band size of 2182. Genomic DNA was extracted from flies with the Qiagen DNeasy Blood and Tissue kit.

Drosophila stocks used in this study

For the ChIP experiments, the Wg signaling pathway was activated by crossing flies containing a Da-Gal4 transgene with a UAS-Arm8 (stabilized Armadillo) transgene. The Wg pathway was inhibited by crossing a Da-Gal4 flies with a UAS-Arm RNAi flies.

Chromatin Immunoprecipitation

ChIP was performed according to the Cross-linking Chromatin Immunoprecipitation (X-ChIP) protocol available from Abcam. Cells were seeded in 10cm tissue culture dishes and allowed to grow overnight. Cells were then treated with CHIR and after 24hr, paraformaldehyde was added directly to the cell culture to a final concentration of 0.75%. Plates were incubated on a rocker at room temperature for 10 mins. After the incubation with paraformaldehyde, glycine was added to a final concentration of 125mM, and the plates were incubated on a rocker for an additional 5 mins. Cells were rinsed twice with cold PBS, resuspended in 5ml cold PBS, and transferred to a 50ml conical tube. Cells were centrifuged at 1000x g for 5 mins at 4 degrees Celsius. The PBS was aspirated, the cells were resuspended in 1.5ml of cold ChIP lysis buffer, and incubated on ice for 10 mins. Cells were sonicated with a Covaris Focused Ultrasonicator until the average fragment size was between 200 and 1000bp. Cell debris was pelleted by centrifugation at 8000x g for 10 mins at 4 degrees Celsius.

Supernatants were transferred to a new tube. Immunoprecipitation was done with a ChIPAb+ Acetyl-Histone H3 (Lys 9/18) (Millipore) antibody and protein A beads (Millipore). Protein a beads were blocked with BSA prior to use. Samples were incubated at 4 degrees for 1 hour with rotation. After incubation, samples were washed once with a low salt buffer and once with a high salt buffer, and once with a LiCl buffer. DNA was eluted by slow shaking at 30 degrees Celsius for 15mins.

RNA extraction from *Drosophila* embryos and Kc167 cells

Drosophila embryos were collected 12-18hr after egg laying and homogenized with a plastic micropestle in a 1.5ml centrifuge tube in 500μl TRIzol (Invitrogen). The manufacturer's protocol was followed for RNA extraction. The RNA pellet was dissolved in 40μl of ultra-pure water.

For Kc167 cells, RNA was extracted with the Qiagen RNeasy Plus Mini Kit, according to the manufacturer's protocol. RNA was eluted in 40μl of RNAse free water.

cDNA library synthesis

cDNA was synthesized with SuperScript III (Invitrogen), following the manufacturer's protocol. 1μg of RNA was used for each cDNA library. cDNA samples were diluted 1:2 in ultra-pure water for qPCR analysis.

qPCR

For qPCRs, *Power*SYBR Green PCR Master Mix (Applied Biosystems) was used and the reaction was carried out in a StepOnePlus Real-Time PCR System (Applied Biosystems). Relative expression of target genes was calculated using the Pfaffl method (Pfaffl, 2001). Experiments were repeated three times with qualitatively similar results obtained. For qPCRs performed with cDNA templates, the β-tubulin gene was used as an internal control. For primers used, refer to table 2.1.

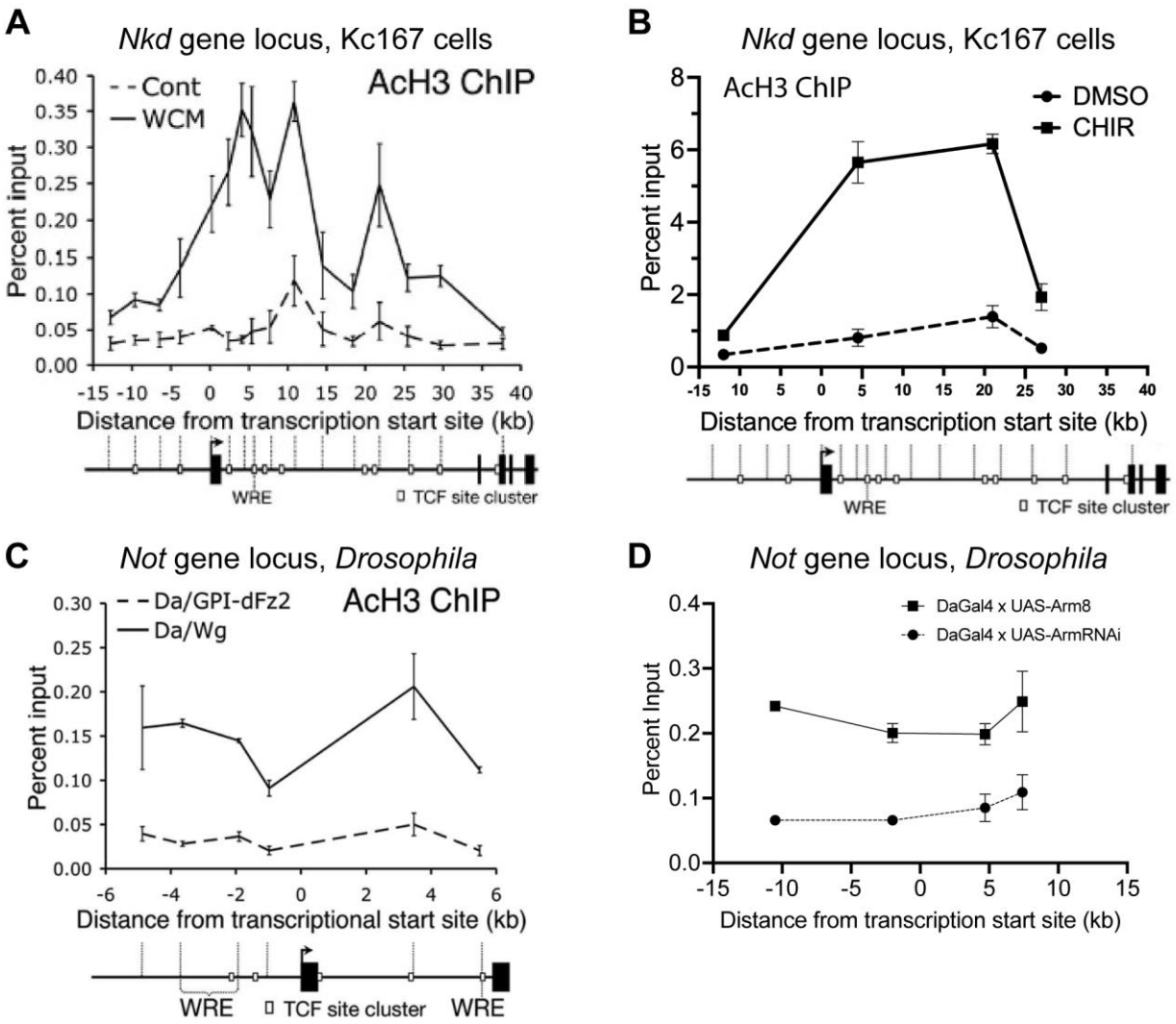

Fig 3.1. Widespread histone acetylation at *nkd* and *not* is reproducible. (**A**) Acetylated histone H3 levels are broadly enriched at the active *nkd* locus in Kc167 cells. Data dapted from Parker, et al. 2008. (**B**) Reproduction of Parker, et al. data showing elevated acetylated histone H3 levels at the active *nkd* locus in Kc167 cells. (**C**) Acetylated histone H3 levels are broadly enriched at the active *not* locus in *Drosophila* embryos. Data adapted from Parker et al. 2008. (**D**) Reproduction of Parker, et al. data showing elevated histone H3 levels at the active *not* locus in *Drosophila* embryos.

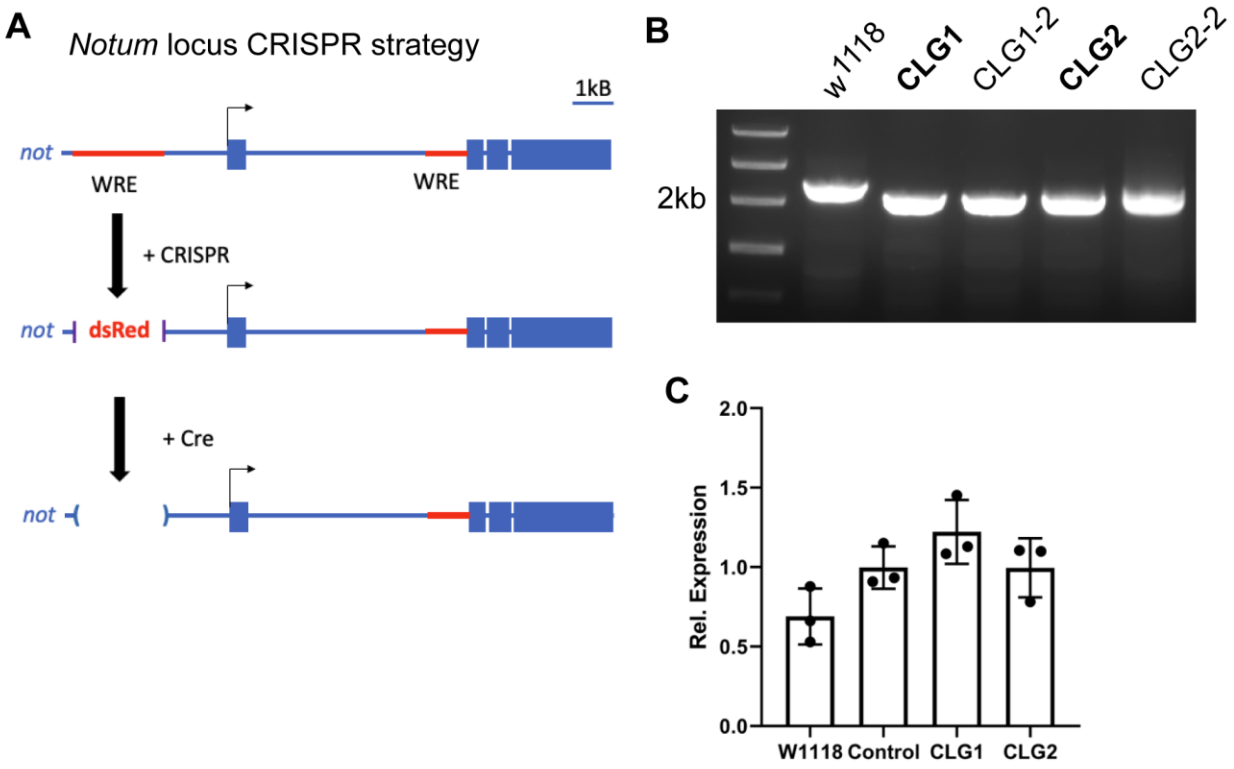

Fig 3.2. Deletion of the *not* Upstream WRE does not affect *not* expression. (**A**) CRISPR/Cas9 gene editing strategy to delete *not* UpE. Cas9 induced double strand breaks at the 5' and 3' ends of the WRE will be repaired with a template that will introduce a DsRed expression cassette in place of the endogenous WRE. The DsRed expression cassette will be floxed, so that it can be removed with Cre recombinase prior to downstream analysis. (**B**) Genotyping PCRs for CRISPR/Cas9 edited flies. W^{1118} flies are an unedited control and show the 2655bp WT band. Successfully edited flies have a slightly smaller band size of 2182. Four independent CRISPR/Cas9 edited lines were identified, and two were chosen for downstream analysis: CLG1 and CLG2. (**C**) qPCR for *not* expression. Deletion of the *not* UpE had no effect on *not* expression.

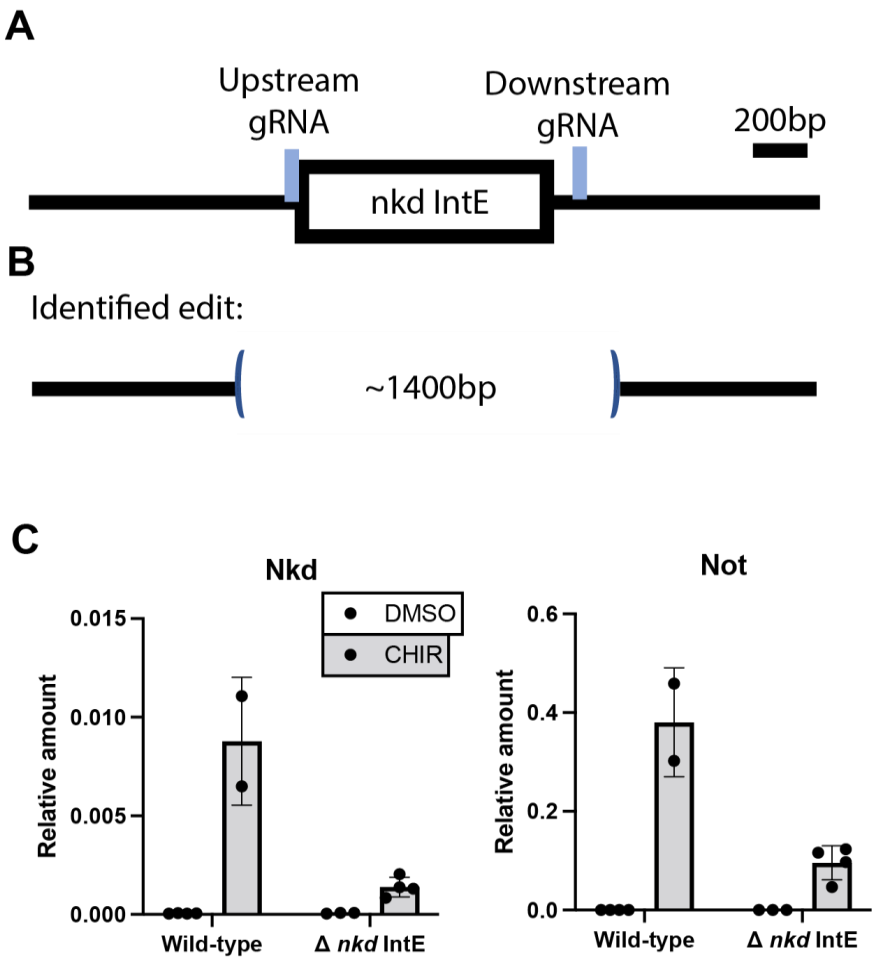

Fig 3.3. Deletion of the *nkd* IntE WRE in Kc167 cells. (**A**) Cartoon depicting the *nkd* IntE locus and sites targeted by gRNAs for CRISPR/Cas9 gene editing. (**B**) Cartoon depicting the identified deletion of the *nkd* IntE WRE in Kc167 cells. (**C**) qPCR for the Wnt target genes *nkd* and *not*, indicating the transcriptional response to CHIR treatment in control, wild-type Kc167 cells and the *nkd* IntE deletion cell line.

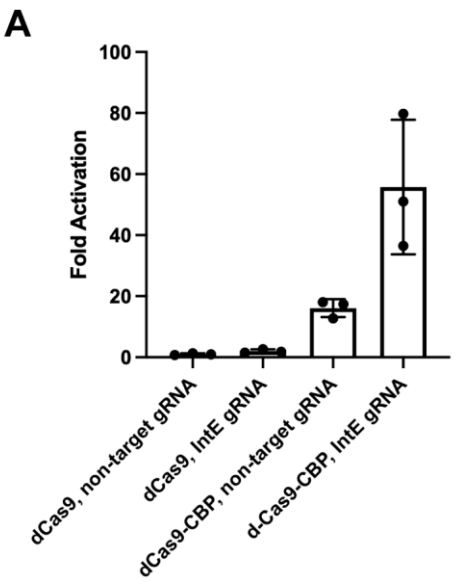

Figure 3.4. dCas9-dCBP^{core} is sufficient to express *nkd.* (**A**) Expression of dCas9-dCBP^{core} by transient transfection and gRNA targeting *nkd* IntE in Kc167 cells is sufficient to activate *nkd*. dCas9-dCBP^{core} that is not targeted to *nkd* IntE, and the dCas9 controls do not strongly activate *nkd* expression.

qPCR Primer Name	Sequence
not F	AGAGCAGCAGAAGCGTTAGC
not R	AAAGCCGGAGAAGCTACAAA
nkd F	GACCTGGACGGGCATCAC
nkd R	TTGCCAATGGACTCGTATATGG
beta-tubulin F	AGACCTACTGCATCGACAAC
beta-tubulin R	GACAAGATGGTTCAGGTCAC

Table 3.1. Sequences of qPCR primers

gRNA	Sequence
not UpE KO	
Upstream gRNA 1	TGTGCGACGCGCGTGTTAAG
Upstream gRNA 2	AAGTGGACTGTGAATATGAA
Downstream gRNA 1	CAGGAAAAACAGATCACGGG
Downstream gRNA 2	AAAAACAGATCACGGGCGGA
Downstream gRNA 3	AGATCACGGGCGGACGGACA
dCas9 targeting *nkd* intE	GCGGGCCCTGTTGGCTATGG
dCas9 non-targeting control	GTTCGGGTCTTCGAGAAGACCT

Table 3.2. gRNA sequences for *not* UpE KO and dCas9 *nkd* IntE targeting.

Chapter 4 Conclusions and Future Directions

The experiments described in this dissertation provide evidence that the biomolecular condensation of β-catenin is a newly appreciated aspect of its function as a transcriptional co-regulator. We performed extensive β-catenin mutagenesis to characterize the transcriptional activity of β-catenin mutants that were deficient in their ability to form biomolecular condensates, and chimeric β-catenin mutants that contained heterologous IDRs which could rescue the activity of condensate-deficient mutants. We tested our mutants using various assays in human cell culture and in various *Drosophila* developmental contexts. While there are contextual differences between the requirement of β-catenin to form biomolecular condensates and transcriptional activity, we have discovered a general rule that can describe our results: β-catenin mutants that are defective in forming biomolecular condensates *in vitro* and *in vivo* are always defective in transcriptional activity relative to wild-type β-catenin. The degree to which the mutants are defective is context dependent. While these experimental findings provide significant support for the role of biomolecular condensates in β-catenin function, there are many open questions that remain. This chapter discusses follow-up experiments and the rationale for performing them.

Determining if observed β-catenin condensates are functional

The observed *in vivo* puncta formed by β-catenin provides evidence for the ability to form BMCs, but whether these puncta are functional is an open question. In Chapter 2 and Appendix A, experimental evidence shows that stabilized β-catenin forms puncta *in vivo* while the aromatic IDR mutants do not. Separate experiments show that the aromatic IDR mutants fail to activate a Wnt reporter and are defective in regulating some Wnt target genes relative to stabilized β-catenin. The proposed model is that the puncta formed by β-catenin are functional and required for the productive transcription of Wnt target genes. Since these experiments were done separately, they're currently linked by correlation. Although, there is a substantial amount of correlative evidence.

A direct link between BMC formation and transcriptional activity is still needed for β-catenin. The MS2 and MS2-coat protein (MCP) system is commonly used to image RNA localization in live cells and *Drosophila* embryos (Garcia and Gregor, 2018; Tutucci et al., 2018). This experimental system can be used to determine if there is co-localization of active sites of Wnt target gene mRNA synthesis and β-catenin puncta. This would provide stronger evidence for a direct role in β-catenin BMCs with transcriptional function.

Setting this system up in the *Drosophila* embryo would be the place to start since the Cadigan lab already has *Drosophila* which express a GFP-Armadillo, which is tagged at the endogenous allele, and several strains with MCP-RFP on different chromosomes are available in the Bloomington *Drosophila* Stock Center. Published protocols describe CRISPR/Cas9 methods to MS2-tag endogenous genes, live cell imaging of the MS2-MCP system, and downstream analysis (Hoppe et al., 2020; Hoppe and Ashe, 2021a, 2021b). CRISPR/Cas9 MS2-tagging of Wg target genes *nkd* and *not* would be two genes to start with, as they are both expressed in the embryo and much is known about the regulation of these genes (J. L. Chang et al., 2008; M. V. Chang et al., 2008; Parker et al., 2008).

Embryos from flies containing all the necessary transgenes (GFP-Arm, MCP-RFP, MS2-tagged *nkd* or *not*) will need to be collected and prepared for live imaging (Garcia and Gregor, 2018). The expected outcome is that Wg signaling in the *Drosophila* embryo drives the nuclear accumulation of GFP-Armadillo, which forms

BMCs in the nucleus, and the MCP-RFP signal (indicating an actively transcribed *nkd* or *not*) co-localizes with GFP-Arm. A published immunofluorescence and RNA-FISH experiment shows that nuclear β-catenin puncta co-localize with *nanog* RNA in mESCs (Zamudio et al., 2019), which lends credence to prediction that GFP-Arm will co-localize with MCP-RFP. This result could be interpreted as the GFP-Arm BMCs are functional sites of transcription.

If GFP-Arm and MCP-RFP BMCs are sites of active transcription, they should also contain Pan (fly TCF). Pan can be fluorescently labeled at the endogenous locus with CRISPR/Cas9, and follow-up experiments can be performed to determine whether Pan, Arm, and the MCP reporter all co-localize to the same BMCs. Unpublished data from the Cadigan lab shows that β-catenin and LEF1 co-localize in BMCs in human cell culture models. Both Arm and Pan are required for the transcription of Wg target genes, so a BMC containing both proteins and the MCP transcriptional reporter is highly likely to be an active site (Franz et al., 2017).

If the GFP-Arm and MCP-RFP don't overlap, there are additional considerations. The large BMC puncta that are observed in the nucleus can potentially be artifactual, and BMCs that regulate Wg target genes are too small to be detected with fluorescent microscopy. Additionally, it is possible that BMCs are not required for *nkd* or *not* expression. We do not currently know the degree to which BMCs are required for Wg target gene expression, but it is possible that it is not a requirement for every gene.

Additionally, aroNC, an Arm mutant that is predicted to be deficient in forming BMCs (based on evidence from the aroNC β-catenin mutant and a deficiency in gene activation in *Drosophila*), can be expressed to determine whether MCP-RFP form in the absence of an Arm mutant that forms BMCs. The expected result is that aroNC does not form BMCs and has a diffuse signal throughout the nucleus. Our model predicts that a lack of BMC formation by Arm would fail to activate *nkd* or *not*, so there would not be an MCP-RFP signal in the nucleus. If *nkd* is expressed, and the MCP-RFP signal is present, it would be interesting to see whether it co-localizes with Pan BMCs. It is possible that transcriptionally active BMCs can still form with LEF1 and other transcriptional co-regulators, and sufficient aroNC can interact with LEF1 through

traditional interactions. Overall, this experiment would be an exciting test of whether the BMCs formed by β-catenin/Arm are functional.

A large part of the biomolecular condensate literature focuses on the correlation between a protein's ability to form biomolecular condensates and a functional output, such as transcription. It is common for scientific publications to utilize separate experiments for biomolecular condensate formation and functional activity (Lu et al., 2020; Zamudio et al., 2019; Zhao et al., 2023). The experiment proposed in this section will be able to provide a more direct link between BMC formation and transcription, utilizing a method that goes above the standards of the field.

Are Biomolecular condensates required for the expression of all Wnt target genes?

The most straightforward evidence that BMCs are involved in β-catenin activity and Wnt target gene regulation is the failure of condensate-deficient β-catenin mutants to activate a sensitive Wnt transcriptional reporter, while stabilized β-catenin can robustly activate the reporter. Endogenous Wnt target gene regulation is more complex. The expression of the Wnt target *sp5* in HeLa cells appears to be sensitive to BMC-deficient aromatic β-catenin mutants. aroN, aroC, and aroNC all modestly activate expression, while stabilized β-catenin robustly activates expression. Expression of *axin2* in HeLa cells appears to be less sensitive to these mutations. aroN activates *axin2* as well as stabilized β-catenin, and aroC activates *axin2* slightly more than aroNC, which negligibly activates *axin2*. The differences between these two genes suggests that different Wnt targets have different sensitivities to aromatic mutations within β-catenin's IDRs. This can be interpreted as different Wnt target genes have different requirement for β-catenin BMC formation.

Examples in the literature focus on BMCs forming at super-enhancers to regulate target genes (Sabari et al., 2018; Tang et al., 2022; Zamudio et al., 2019). Super-enhancers are clusters of enhancers, sometimes spanning a domain of more than 10kb, that are occupied by a high density of factors and control the expression of genes that define cell identify (Hnisz et al., 2013; Sabari et al., 2018; Tang et al., 2022). Super-

enhancers are also defined by strong ChIP-seq signal enrichment for master TFs, transcriptional co-regulators such as Med1, BRD4, p300, and strong enrichment of chromatin marks such as H3K27ac (Tang et al., 2022). The high concentrations of proteins at super-enhancers create a permissive environment for liquid-liquid phase separation that leads to BMC formation. The size and protein-dense nature of these elements makes them more amenable to study, and significantly less is known about how BMCs regulate the activity of typical enhancers.

To determine the global effect that BMC-deficient β-catenin mutants have on Wnt target gene regulation, a transcriptome analysis of HeLa cells expressing stabilized β-catenin compared to HeLa cells expressing BMC-deficient β-catenin mutants needs to be performed. The current literature would predict that Wnt target genes that are regulated by super-enhancers would be more sensitive to BMC perturbations compared to Wnt targets that are regulated by typical enhancers. However, it is currently unknown which Wnt target genes in HeLa cells are regulated by super-enhancers vs typical enhancers. For this experiment, RNA-seq can be used to identify these changes in Wnt target gene expression.

For genes that are activated by Wnt signaling, the expected outcome is that RNA-seq will identify a set of targets that fail to be expressed by BMC-deficient β-catenin mutants, a set of targets that are moderately affected, and a set of targets that are unaffected. Follow-up analysis would focus on differences in cis-regulatory elements that are potentially sensitive to BMC-deficient β-catenin. For instance, the Wnt target genes that are regulated by super-enhancers are highly sensitive to BMC-deficient β-catenin mutants, while targets regulated by typical enhancers are not. Additionally, the transcription factors that interact with Pan/β-catenin at WREs might play a role in determining sensitivity to loss of BMC formation. Alternatively, the majority of Wnt target genes may be sensitive to loss of BMC formation, indicating that BMCs might be fundamental to Wnt target gene regulation.

In the context of Wnt target gene regulation, β-catenin is typically framed as being an activator of target gene expression. However, β-catenin also mediates transcriptional repression (Valenta et al., 2012). It would be interesting to see if genes which are repressed by β-catenin fail to be repressed by BMC-deficient β-catenin

mutants. This aspect of BMC function is understudied relative to transcriptional activation, but there is evidence that BMCs are involved in transcriptional repression (Treen et al., 2021).

Do biomolecular condensate-deficient β-catenin mutants affect the broad histone acetylation patterns at active Wnt target genes?

Broad domains of histone acetylation are observed at the active Wnt targets *nkd* and *not* in *Drosophila* and the Kc167 cell line. These domains can reach sizes of up to 30kb. It is known that the histone acetyltransferase, CBP, is required for the establishment of these domains. Additionally, it is known that this histone acetylation pattern is established independently of transcription (Parker et al., 2008). Currently, a mechanistic understanding of how these domains can be established is unknown. It is possible that these broad domains of histone acetylation emanate from a single or multiple WREs. Most domains of histone acetylation are narrow, encompassing domains of 1-4kb. A key question is what makes active Wg targets different. BMCs provide a novel mechanism for explaining why the active *nkd* and *not* genes exhibit this pattern.

Reconstituted *in vitro* chromatin arrays have been shown to form liquid-liquid phase separated BMCs (Gibson et al., 2019). Interestingly, when the histone proteins that constitute these arrays were acetylated, they failed to form BMCs *in vitro*. However, when the acetylated chromatin arrays were bound by bromodomain-containing proteins, the ability to form BMCs was rescued. The histone acetyltransferases CBP and p300 can also form BMCs *in vivo* (Ma et al., 2021; Zhang et al., 2021). It is possible that this aspect of CBP activity is important for establishing broad domains of histone acetylation.

This can be experimentally tested by overexpressing a stabilized form of Arm and the aroNC mutant of Arm, and using ChIP to determine differences in histone acetylation enrichment at *nkd* and *not.* If BMC formation at the active loci is important for establishing these broad domains of histone acetylation, an expected outcome would be that aroNC produces a more restricted domain of histone acetylation. It would be interesting if this was coupled with a decrease in transcriptional output, as this can

additionally implicate broad histone acetylation in robust transcriptional output. If the establishment of broad domains of histone acetylation is not dependent on BMC formation, then additional mechanisms will need to be explored.

Can biomolecular condensates explain the flexible billboard model of enhancer activity?

The flexible billboard model of enhancer activity suggests that enhancer function is primarily dictated by their ability to recruit transcription factors to chromatin (Vockley et al., 2017). This is in opposition to the enhanceosome model of enhancer activity, which suggests that transcription binding site grammar (i.e. the order, orientation, and spacing between transcription factor binding sites) is important for functional activity (Panne et al., 2007). Analysis of WREs shows that there does not appear to be any conserved transcription factor binding site grammar. Given the importance of the spatial and temporal specificity that enhancers impart on gene expression, this is somewhat surprising. A key question that remains for Wnt target gene regulation is: why are WREs with differing transcription factor binding site grammar regulated in the same manner (i.e. by Wnt signaling)?

BMC models of transcription factor and co-activator function invoke a lack of site-specific binding interactions, instead relying on weak, multivalent interactions to form functional protein interactions (Sabari et al., 2020). In light of both the flexible billboard and enhanceosome models of enhancer function, an interesting hypothesis is that enhancer elements nucleate BMCs on chromatin by recruiting the necessary transcription factors through specific DNA binding, and these factors then go on to recruit additional proteins through weak, multivalent interactions until a BMC is formed. Since the interactions that are important for BMC formation are not site specific, there is no requirement for specific order of transcription factor binding to enhancers which would allow for specific transcription factor interactions.

A method to test this hypothesis would be to construct multiple synthetic WREs in which transcription factor binding sites are varied, and test whether various synthetic WREs can activate the transcription of a reporter gene. Published data from the Cadigan lab shows that a synthetic WRE consisting of TCF sites, CDX sites, and CAG

sites are highly active in HEK293T cells (Ramakrishnan et al., 2021). Additionally, a 48mer of TetO sites is sufficient for visualization of TetR-EGFP binding in HCT116 cells (Tasan et al., 2018). This data suggests that a minimum of a 48mer of TCF, CDX, and CAG sites should be sufficient for both visualization and testing for reporter activity.

The experiment is to integrate constructs consisting of different combinations of the mentioned binding sites and a reporter gene into the genome of HEK293T cells using CRISPR/Cas9 editing. Different strains of cells carrying synthetic WREs with different combinations of binding site arrays can then be imaged for the presence of BMCs. The expected outcome is that the order of the transcription factor binding sites does not matter for BMC formation or reporter activity. This experiment can provide evidence in support of the flexible billboard model.

Determining if there is a link between the flexible billboard model of condensate activity and the capacity for transcription factors and transcriptional co-regulators to form biomolecular condensates has important transcriptional implications beyond Wnt signaling. The flexible billboard model suggests that different classes of transcription factor binding sites within an enhancer serves to potentiate the enhancer's activity (Vockley et al., 2017), and ultimately this potentiation could occur through a biomolecular condensate mechanism.

Appendix

The appendices contain supplemental information. Both appendix A and B are supplements for Chapter 2.

Appendix A: Supplemental data for Chapter 2, Fig 2.4:

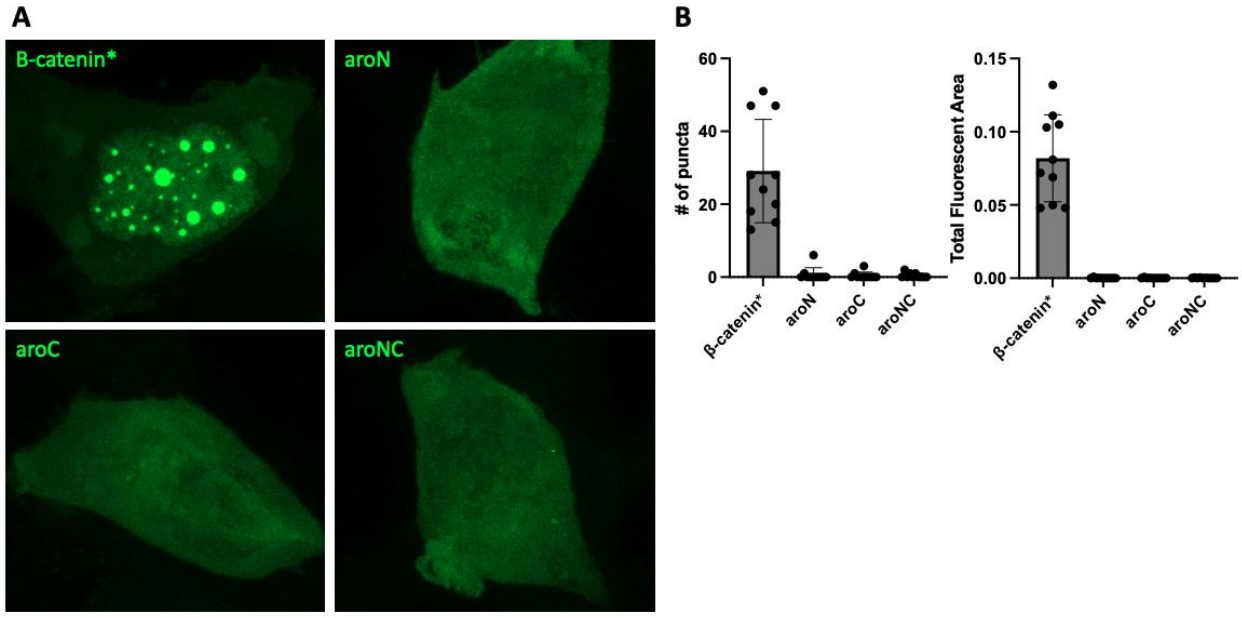

Fig A1. Aromatic amino acid residues are required for β-catenin BMC formation *in vivo*. (**A**) HEK293T β-catenin KO cells transiently transfected with a GFP-β-catenin or GFP-aromatic mutant expression construct. Aromatic amino acid mutations in β-catenin's terminal IDRs abolish the ability to form BMCs *in vivo*. (**B**) quantification of fluorescent images. n=10 for all mutants.

The purpose of this figure is to provide higher quality data showing that β-catenin BMC formation *in vivo* is negatively affected by aromatic amino acid mutations in the terminal IDRs.

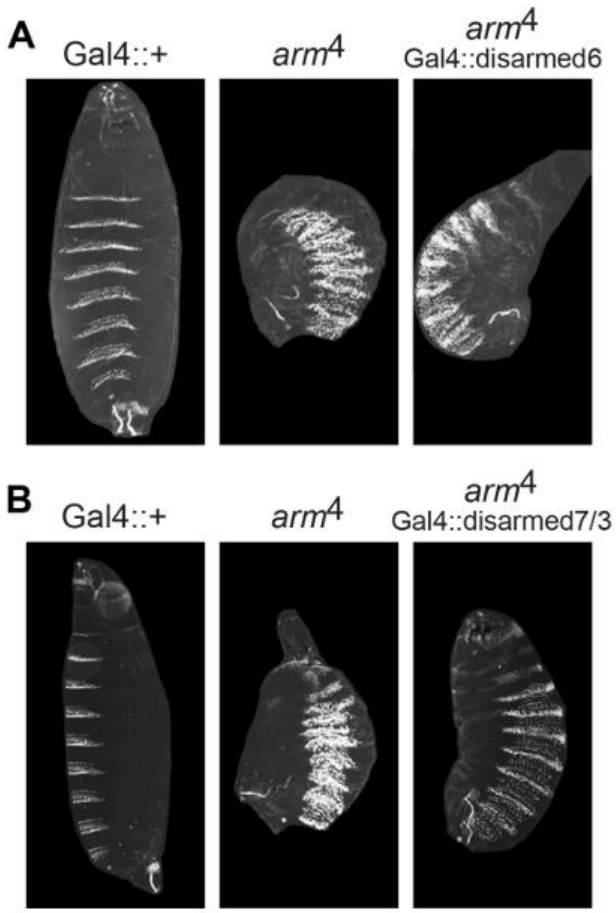

Fig A2. The DisArmed allele fails to rescue an Arm loss of function allele. (**A**) Embryonic cuticles depicting phenotypes that are wild-type, *arm*^{4} (*arm* loss of function), and an *arm*^{4} rescue by a disArmed6 allele. (**B**) Same series as A, except a stronger disArmed7/3 strain is used.

The purpose of this figure is to show that the rescue observed in Figure 2.7 by aroNC is not simply the result of de-repression caused by a non-functional β-catenin mutant. The DisArmed Arm mutant is lacking the C-terminal domain and evidenced to be deficient in transcriptional activation but not repression (Blauwkamp et al., 2008). The DisArmed7/3 mutant is able to provide a small degree of rescue. The aroNC mutant in Fig 2.7 is able to provide a greater degree of rescue, indicating that de-repression may be responsible for some of the observed phenotype in Fig 2.7, but not all of it. Importantly, the DisArmed mutants are not expression matched as well as the aromatic mutant series in Fig 2.7.

Bibliography

Alberti, S., Gladfelter, A., Mittag, T., 2019. Considerations and Challenges in Studying Liquid-Liquid Phase Separation and Biomolecular Condensates. Cell 176, 419–434. https://doi.org/10.1016/j.cell.2018.12.035

Alberti, S., Saha, S., Woodruff, J.B., Franzmann, T.M., Wang, J., Hyman, A.A., 2018. A User's Guide for Phase Separation Assays with Purified Proteins. J Mol Biol 430, 4806–4820. https://doi.org/10.1016/j.jmb.2018.06.038

Alexandre, C., Baena-Lopez, A., Vincent, J.-P., 2014. Patterning and growth control by membrane-tethered Wingless. Nature 505, 180–185. https://doi.org/10.1038/nature12879

Alexandre, C., Lecourtois, M., Vincent, J.-P., 1999. Wingless and Hedgehog pattern Drosophila denticle belts by regulating the production of short-range signals. Development 126, 5689–5698. https://doi.org/10.1242/dev.126.24.5689

Andersson, R., Sandelin, A., 2020. Determinants of enhancer and promoter activities of regulatory elements. Nat Rev Genet 21, 71–87. https://doi.org/10.1038/s41576-019-0173-8

Anthony, C.C., Robbins, D.J., Ahmed, Y., Lee, E., 2020. Nuclear Regulation of Wnt/β-Catenin Signaling: It's a Complex Situation. Genes 11, 886. https://doi.org/10.3390/genes11080886

Archbold, H.C., Broussard, C., Chang, M.V., Cadigan, K.M., 2014. Bipartite Recognition of DNA by TCF/Pangolin Is Remarkably Flexible and Contributes to Transcriptional Responsiveness and Tissue Specificity of Wingless Signaling. PLoS Genet 10, e1004591. https://doi.org/10.1371/journal.pgen.1004591

Archbold, H.C., Yang, Y.X., Chen, L., Cadigan, K.M., 2012. How do they do Wnt they do?: regulation of transcription by the Wnt/β-catenin pathway: Wnt/β-catenin transcriptional regulation. Acta Physiol 204, 74–109. https://doi.org/10.1111/j.1748-1716.2011.02293.x

Armingol, E., Officer, A., Harismendy, O., Lewis, N.E., 2021. Deciphering cell–cell interactions and communication from gene expression. Nat Rev Genet 22, 71–88. https://doi.org/10.1038/s41576-020-00292-x

Arnosti, D.N., Kulkarni, M.M., 2005. Transcriptional enhancers: Intelligent enhanceosomes or flexible billboards? J Cell Biochem 94, 890–898. https://doi.org/10.1002/jcb.20352

Banerji, J., Rusconi, S., Schaffner, W., 1981. Expression of a β-globin gene is enhanced by remote SV40 DNA sequences. Cell 27, 299–308. https://doi.org/10.1016/0092-8674(81)90413-X

Barker, N., 2001. The chromatin remodelling factor Brg-1 interacts with beta-catenin to promote target gene activation. EMBO J 20, 4935–4943. https://doi.org/10.1093/emboj/20.17.4935

Bejsovec, A., 2013. Wingless/Wnt signaling in Drosophila: The pattern and the pathway. Mol Reprod Dev 80, 882–894. https://doi.org/10.1002/mrd.22228
Berkes, C.A., Tapscott, S.J., 2005. MyoD and the transcriptional control of myogenesis. Semin Cell Dev Biol 16, 585–595. https://doi.org/10.1016/j.semcdb.2005.07.006
Bhambhani, C., Ravindranath, A.J., Mentink, R.A., Chang, M.V., Betist, M.C., Yang, Y.X., Koushika, S.P., Korswagen, H.C., Cadigan, K.M., 2014. Distinct DNA Binding Sites Contribute to the TCF Transcriptional Switch in C. elegans and Drosophila. PLoS Genet 10, e1004133. https://doi.org/10.1371/journal.pgen.1004133
Bhanot, P., Fish, M., Jemison, J.A., Nusse, R., Nathans, J., Cadigan, K.M., 1999. Frizzled and DFrizzled-2 function as redundant receptors for Wingless during *Drosophila* embryonic development. Development 126, 4175–4186. https://doi.org/10.1242/dev.126.18.4175
Bischof, J., Maeda, R.K., Hediger, M., Karch, F., Basler, K., 2007. An optimized transgenesis system for *Drosophila* using germ-line-specific ϕC31 integrases. Proc Natl Acad Sci USA 104, 3312–3317. https://doi.org/10.1073/pnas.0611511104
Blauwkamp, T.A., Chang, M.V., Cadigan, K.M., 2008. Novel TCF-binding sites specify transcriptional repression by Wnt signalling. EMBO J. https://doi.org/10.1038/emboj.2008.80
Boehning, M., Dugast-Darzacq, C., Rankovic, M., Hansen, A.S., Yu, T., Marie-Nelly, H., McSwiggen, D.T., Kokic, G., Dailey, G.M., Cramer, P., Darzacq, X., Zweckstetter, M., 2018. RNA polymerase II clustering through carboxy-terminal domain phase separation. Nat Struct Mol Biol 25, 833–840. https://doi.org/10.1038/s41594-018-0112-y
Bose, D.A., Donahue, G., Reinberg, D., Shiekhattar, R., Bonasio, R., Berger, S.L., 2017. RNA Binding to CBP Stimulates Histone Acetylation and Transcription. Cell 168, 135-149.e22. https://doi.org/10.1016/j.cell.2016.12.020
Buccitelli, C., Selbach, M., 2020. mRNAs, proteins and the emerging principles of gene expression control. Nat Rev Genet 21, 630–644. https://doi.org/10.1038/s41576-020-0258-4
Caca, K., Kolligs, F.T., Ji, X., Hayes, M., Qian, J., Yahanda, A., Rimm, D.L., Costa, J., Fearon, E.R., 1999. Beta- and gamma-catenin mutations, but not E-cadherin inactivation, underlie T-cell factor/lymphoid enhancer factor transcriptional deregulation in gastric and pancreatic cancer. Cell Growth Differ 10, 369–376.
Cadigan, K.M., 2012. TCFs and Wnt/β-catenin Signaling, in: Current Topics in Developmental Biology. Elsevier, pp. 1–34. https://doi.org/10.1016/B978-0-12-386499-4.00001-X
Cadigan, K.M., Fish, M.P., Rulifson, E.J., Nusse, R., 1998. Wingless repression of Drosophila frizzled 2 expression shapes the Wingless morphogen gradient in the wing. Cell 93, 767–777. https://doi.org/10.1016/s0092-8674(00)81438-5
Cadigan, K.M., Jou, A.D., Nusse, R., 2002. Wingless blocks bristle formation and morphogenetic furrow progression in the eye through repression of Daughterless. Development 129, 3393–3402. https://doi.org/10.1242/dev.129.14.3393
Cadigan, K.M., Waterman, M.L., 2012. TCF/LEFs and Wnt Signaling in the Nucleus. Cold Spring Harb Perspect Biol 4, a007906–a007906. https://doi.org/10.1101/cshperspect.a007906
Cai, Y., Zhang, Y., Loh, Y.P., Tng, J.Q., Lim, M.C., Cao, Z., Raju, A., Lieberman Aiden, E., Li, S., Manikandan, L., Tergaonkar, V., Tucker-Kellogg, G., Fullwood, M.J., 2021. H3K27me3-rich

genomic regions can function as silencers to repress gene expression via chromatin interactions. Nat Commun 12, 719. https://doi.org/10.1038/s41467-021-20940-y

Cavalheiro, G.R., Pollex, T., Furlong, E.E., 2021. To loop or not to loop: what is the role of TADs in enhancer function and gene regulation? Curr Opin in Genet Dev 67, 119–129. https://doi.org/10.1016/j.gde.2020.12.015

Cavallo, R.A., Cox, R.T., Moline, M.M., Roose, J., Polevoy, G.A., Clevers, H., Peifer, M., Bejsovec, A., 1998. Drosophila Tcf and Groucho interact to repress Wingless signalling activity. Nature 395, 604–608. https://doi.org/10.1038/26982

Chang, J.L., Chang, M.V., Barolo, S., Cadigan, K.M., 2008. Regulation of the feedback antagonist naked cuticle by Wingless signaling. Dev Biol 321, 446–454. https://doi.org/10.1016/j.ydbio.2008.05.551

Chang, M.V., Chang, J.L., Gangopadhyay, A., Shearer, A., Cadigan, K.M., 2008a. Activation of Wingless Targets Requires Bipartite Recognition of DNA by TCF. Curr Biol 18, 1877–1881. https://doi.org/10.1016/j.cub.2008.10.047

Chang, M.V., Chang, J.L., Gangopadhyay, A., Shearer, A., Cadigan, K.M., 2008b. Activation of Wingless Targets Requires Bipartite Recognition of DNA by TCF. Curr Biol 18, 1877–1881. https://doi.org/10.1016/j.cub.2008.10.047

Chavez, A., Scheiman, J., Vora, S., Pruitt, B.W., Tuttle, M., P R Iyer, E., Lin, S., Kiani, S., Guzman, C.D., Wiegand, D.J., Ter-Ovanesyan, D., Braff, J.L., Davidsohn, N., Housden, B.E., Perrimon, N., Weiss, R., Aach, J., Collins, J.J., Church, G.M., 2015. Highly efficient Cas9-mediated transcriptional programming. Nat Methods 12, 326–328. https://doi.org/10.1038/nmeth.3312

Chavez, A., Tuttle, M., Pruitt, B.W., Ewen-Campen, B., Chari, R., Ter-Ovanesyan, D., Haque, S.J., Cecchi, R.J., Kowal, E.J.K., Buchthal, J., Housden, B.E., Perrimon, N., Collins, J.J., Church, G., 2016. Comparison of Cas9 activators in multiple species. Nat Methods 13, 563–567. https://doi.org/10.1038/nmeth.3871

Cho, W.-K., Jayanth, N., English, B.P., Inoue, T., Andrews, J.O., Conway, W., Grimm, J.B., Spille, J.-H., Lavis, L.D., Lionnet, T., Cisse, I.I., 2016. RNA Polymerase II cluster dynamics predict mRNA output in living cells. eLife 5, e13617. https://doi.org/10.7554/eLife.13617

Cho, W.-K., Spille, J.-H., Hecht, M., Lee, C., Li, C., Grube, V., Cisse, I.I., 2018a. Mediator and RNA polymerase II clusters associate in transcription-dependent condensates. Science 361, 412–415. https://doi.org/10.1126/science.aar4199

Cho, W.-K., Spille, J.-H., Hecht, M., Lee, C., Li, C., Grube, V., Cisse, I.I., 2018b. Mediator and RNA polymerase II clusters associate in transcription-dependent condensates. Science 361, 412–415. https://doi.org/10.1126/science.aar4199

Choi, J.K., Howe, L.J., 2009. Histone acetylation: truth of consequences?This paper is one of a selection of papers published in this Special Issue, entitled CSBMCB's 51st Annual Meeting – Epigenetics and Chromatin Dynamics, and has undergone the Journal's usual peer review process. Biochem Cell Biol 87, 139–150. https://doi.org/10.1139/O08-112

Choi, J.-M., Holehouse, A.S., Pappu, R.V., 2020. Physical Principles Underlying the Complex Biology of Intracellular Phase Transitions. Annu. Rev. Biophys. 49, 107–133. https://doi.org/10.1146/annurev-biophys-121219-081629

Cisse, I.I., Izeddin, I., Causse, S.Z., Boudarene, L., Senecal, A., Muresan, L., Dugast-Darzacq, C., Hajj, B., Dahan, M., Darzacq, X., 2013. Real-Time Dynamics of RNA Polymerase II

Clustering in Live Human Cells. Science 341, 664–667. https://doi.org/10.1126/science.1239053
Cliffe, A., Hamada, F., Bienz, M., 2003. A Role of Dishevelled in Relocating Axin to the Plasma Membrane during Wingless Signaling. Curr Biol 13, 960–966. https://doi.org/10.1016/S0960-9822(03)00370-1
Cong, F., Schweizer, L., Chamorro, M., Varmus, H., 2003. Requirement for a Nuclear Function of β-Catenin in Wnt Signaling. Mol Cell Biol 23, 8462–8470. https://doi.org/10.1128/MCB.23.23.8462-8470.2003
Cramer, P., 2019. Organization and regulation of gene transcription. Nature 573, 45–54. https://doi.org/10.1038/s41586-019-1517-4
Dar, M.S., Singh, P., Mir, R.A., Dar, M.J., 2017. Beta-catenin N-terminal domain: An enigmatic region prone to cancer causing mutations. Mutat Res Rev Mutat Res 773, 122–133. https://doi.org/10.1016/j.mrrev.2017.06.001
De, A., 2011. Wnt/Ca^{2+} signaling pathway: a brief overview. ABBS 43, 745–756. https://doi.org/10.1093/abbs/gmr079
De La Roche, M., Worm, J., Bienz, M., 2008. The function of BCL9 in Wnt/β-catenin signaling and colorectal cancer cells. BMC Cancer 8, 199. https://doi.org/10.1186/1471-2407-8-199
Doumpas, N., Lampart, F., Robinson, M.D., Lentini, A., Nestor, C.E., Cantù, C., Basler, K., 2019. TCF / LEF dependent and independent transcriptional regulation of Wnt/β-catenin target genes. EMBO J 38, e98873. https://doi.org/10.15252/embj.201798873
Doumpas, N., Söderholm, S., Narula, S., Moreira, S., Doble, B.W., Cantù, C., Basler, K., 2021. TCF/LEF regulation of the topologically associated domain ADI promotes mESCs to exit the pluripotent ground state. Cell Rep 36, 109705. https://doi.org/10.1016/j.celrep.2021.109705
Dueva, R., Akopyan, K., Pederiva, C., Trevisan, D., Dhanjal, S., Lindqvist, A., Farnebo, M., 2019. Neutralization of the Positive Charges on Histone Tails by RNA Promotes an Open Chromatin Structure. Cell Chem Biol 26, 1436-1449.e5. https://doi.org/10.1016/j.chembiol.2019.08.002
Erdős, G., Dosztányi, Z., 2020. Analyzing Protein Disorder with IUPred2A. Curr Protoc Bioinform 70. https://doi.org/10.1002/cpbi.99
Fang, M., Li, J., Blauwkamp, T., Bhambhani, C., Campbell, N., Cadigan, K.M., 2006. C-terminal-binding protein directly activates and represses Wnt transcriptional targets in Drosophila. EMBO J 25, 2735–2745. https://doi.org/10.1038/sj.emboj.7601153
Fiedler, M., Mendoza-Topaz, C., Rutherford, T.J., Mieszczanek, J., Bienz, M., 2011. Dishevelled interacts with the DIX domain polymerization interface of Axin to interfere with its function in down-regulating β-catenin. Proc Natl Acad Sci USA 108, 1937–1942. https://doi.org/10.1073/pnas.1017063108
Flores-Solis, D., Lushpinskaia, I.P., Polyansky, A.A., Changiarath, A., Boehning, M., Mirkovic, M., Walshe, J., Pietrek, L.M., Cramer, P., Stelzl, L.S., Zagrovic, B., Zweckstetter, M., 2023. Driving forces behind phase separation of the carboxy-terminal domain of RNA polymerase II. Nat Commun 14, 5979. https://doi.org/10.1038/s41467-023-41633-8
Forsberg, E.C., Bresnick, E.H., 2001. Histone acetylation beyond promoters: long-range acetylation patterns in the chromatin world. BioEssays 23, 820–830. https://doi.org/10.1002/bies.1117

Franz, A., Shlyueva, D., Brunner, E., Stark, A., Basler, K., 2017. Probing the canonicity of the Wnt/Wingless signaling pathway. PLoS Genet 13, e1006700. https://doi.org/10.1371/journal.pgen.1006700

Fukaya, T., Lim, B., Levine, M., 2016. Enhancer Control of Transcriptional Bursting. Cell 166, 358–368. https://doi.org/10.1016/j.cell.2016.05.025

Garcia, H.G., Gregor, T., 2018. Live Imaging of mRNA Synthesis in Drosophila, in: Gaspar, I. (Ed.), RNA Detection, Methods in Molecular Biology. Springer New York, New York, NY, pp. 349–357. https://doi.org/10.1007/978-1-4939-7213-5_23

Garcia-Ramirez, M., Rocchini, C., Ausio, J., 1995. Modulation of Chromatin Folding by Histone Acetylation. J Biol Chem 270, 17923–17928. https://doi.org/10.1074/jbc.270.30.17923

Gates, A.J., Gysi, D.M., Kellis, M., Barabási, A.-L., 2021. A wealth of discovery built on the Human Genome Project — by the numbers. Nature 590, 212–215. https://doi.org/10.1038/d41586-021-00314-6

Gibson, B.A., Doolittle, L.K., Schneider, M.W.G., Jensen, L.E., Gamarra, N., Henry, L., Gerlich, D.W., Redding, S., Rosen, M.K., 2019. Organization of Chromatin by Intrinsic and Regulated Phase Separation. Cell 179, 470-484.e21. https://doi.org/10.1016/j.cell.2019.08.037

Godard, B.G., Heisenberg, C.-P., 2019. Cell division and tissue mechanics. Curr Opin Cell Biol 60, 114–120. https://doi.org/10.1016/j.ceb.2019.05.007

Goldman, N., Chandra, A., Johnson, I., Sullivan, M.A., Patil, A.R., Vanderbeck, A., Jay, A., Zhou, Y., Ferrari, E.K., Mayne, L., Aguilan, J., Xue, H.-H., Faryabi, R.B., John Wherry, E., Sidoli, S., Maillard, I., Vahedi, G., 2023. Intrinsically disordered domain of transcription factor TCF-1 is required for T cell developmental fidelity. Nat Immunol 24, 1698–1710. https://doi.org/10.1038/s41590-023-01599-7

Graham, T.A., Weaver, C., Mao, F., Kimelman, D., Xu, W., 2000. Crystal Structure of a β-Catenin/Tcf Complex. Cell 103, 885–896. https://doi.org/10.1016/S0092-8674(00)00192-6

Gratz, S.J., Ukken, F.P., Rubinstein, C.D., Thiede, G., Donohue, L.K., Cummings, A.M., O'Connor-Giles, K.M., 2014. Highly Specific and Efficient CRISPR/Cas9-Catalyzed Homology-Directed Repair in *Drosophila*. Genetics 196, 961–971. https://doi.org/10.1534/genetics.113.160713

Greer, E.L., Shi, Y., 2012. Histone methylation: a dynamic mark in health, disease and inheritance. Nat Rev Genet 13, 343–357. https://doi.org/10.1038/nrg3173

Grigoryan, T., Wend, P., Klaus, A., Birchmeier, W., 2008. Deciphering the function of canonical Wnt signals in development and disease: conditional loss- and gain-of-function mutations of β-catenin in mice. Genes Dev 22, 2308–2341. https://doi.org/10.1101/gad.1686208

Han, W., Koo, Y., Chaieb, L., Keum, B.-R., Han, J.-K., 2022. UCHL5 controls β-catenin destruction complex function through Axin1 regulation. Sci Rep 12, 3687. https://doi.org/10.1038/s41598-022-07642-1

Han, X., Yu, D., Gu, R., Jia, Y., Wang, Q., Jaganathan, A., Yang, X., Yu, M., Babault, N., Zhao, C., Yi, H., Zhang, Q., Zhou, M.-M., Zeng, L., 2020. Roles of the BRD4 short isoform in phase separation and active gene transcription. Nat Struct Mol Biol 27, 333–341. https://doi.org/10.1038/s41594-020-0394-8

Hecht, A., 2000. The p300/CBP acetyltransferases function as transcriptional coactivators of beta-catenin in vertebrates. EMBO J 19, 1839–1850. https://doi.org/10.1093/emboj/19.8.1839

Hecht, A., Litterst, C.M., Huber, O., Kemler, R., 1999. Functional Characterization of Multiple Transactivating Elements in β-Catenin, Some of Which Interact with the TATA-binding Proteinin Vitro. J Biol Chem 274, 18017–18025. https://doi.org/10.1074/jbc.274.25.18017

Heldin, C.-H., Lu, B., Evans, R., Gutkind, J.S., 2016. Signals and Receptors. Cold Spring Harb Perspect Biol 8, a005900. https://doi.org/10.1101/cshperspect.a005900

Hikasa, H., Ezan, J., Itoh, K., Li, X., Klymkowsky, M.W., Sokol, S.Y., 2010. Regulation of TCF3 by Wnt-Dependent Phosphorylation during Vertebrate Axis Specification. Dev Cell 19, 521–532. https://doi.org/10.1016/j.devcel.2010.09.005

Hikasa, H., Sokol, S.Y., 2011. Phosphorylation of TCF Proteins by Homeodomain-interacting Protein Kinase 2. J Biol Chem 286, 12093–12100. https://doi.org/10.1074/jbc.M110.185280

Hilton, I.B., D'Ippolito, A.M., Vockley, C.M., Thakore, P.I., Crawford, G.E., Reddy, T.E., Gersbach, C.A., 2015. Epigenome editing by a CRISPR-Cas9-based acetyltransferase activates genes from promoters and enhancers. Nat Biotechnol 33, 510–517. https://doi.org/10.1038/nbt.3199

Hnisz, D., Abraham, B.J., Lee, T.I., Lau, A., Saint-André, V., Sigova, A.A., Hoke, H.A., Young, R.A., 2013. Super-Enhancers in the Control of Cell Identity and Disease. Cell 155, 934–947. https://doi.org/10.1016/j.cell.2013.09.053

Hnisz, D., Shrinivas, K., Young, R.A., Chakraborty, A.K., Sharp, P.A., 2017. A Phase Separation Model for Transcriptional Control. Cell 169, 13–23. https://doi.org/10.1016/j.cell.2017.02.007

Hoppe, C., Ashe, H.L., 2021a. CRISPR-Cas9 strategies to insert MS2 stem-loops into endogenous loci in Drosophila embryos. STAR Protocols 2, 100380. https://doi.org/10.1016/j.xpro.2021.100380

Hoppe, C., Ashe, H.L., 2021b. Live imaging and quantitation of nascent transcription using the MS2/MCP system in the Drosophila embryo. STAR Protocols 2, 100379. https://doi.org/10.1016/j.xpro.2021.100379

Hoppe, C., Bowles, J.R., Minchington, T.G., Sutcliffe, C., Upadhyai, P., Rattray, M., Ashe, H.L., 2020. Modulation of the Promoter Activation Rate Dictates the Transcriptional Response to Graded BMP Signaling Levels in the Drosophila Embryo. Dev Cell 54, 727-741.e7. https://doi.org/10.1016/j.devcel.2020.07.007

Housden, B.E., Valvezan, A.J., Kelley, C., Sopko, R., Hu, Y., Roesel, C., Lin, S., Buckner, M., Tao, R., Yilmazel, B., Mohr, S.E., Manning, B.D., Perrimon, N., 2015. Identification of potential drug targets for tuberous sclerosis complex by synthetic screens combining CRISPR-based knockouts with RNAi. Sci Signal 8. https://doi.org/10.1126/scisignal.aab3729

Hrckulak, D., Kolar, M., Strnad, H., Korinek, V., 2016. TCF/LEF Transcription Factors: An Update from the Internet Resources. Cancers 8, 70. https://doi.org/10.3390/cancers8070070

Hsu, S.-C., Galceran, J., Grosschedl, R., 1998. Modulation of Transcriptional Regulation by LEF-1 in Response to Wnt-1 Signaling and Association with β-Catenin. Mol Cell Biol 18, 4807–4818. https://doi.org/10.1128/MCB.18.8.4807

Huber, A.H., Weis, W.I., 2001. The Structure of the β-Catenin/E-Cadherin Complex and the Molecular Basis of Diverse Ligand Recognition by β-Catenin. Cell 105, 391–402. https://doi.org/10.1016/S0092-8674(01)00330-0

Huggins, I.J., Bos, T., Gaylord, O., Jessen, C., Lonquich, B., Puranen, A., Richter, J., Rossdam, C., Brafman, D., Gaasterland, T., Willert, K., 2017. The WNT target SP5 negatively regulates WNT transcriptional programs in human pluripotent stem cells. Nat Commun 8, 1034. https://doi.org/10.1038/s41467-017-01203-1

Jindal, G.A., Farley, E.K., 2021. Enhancer grammar in development, evolution, and disease: dependencies and interplay. Dev Cell 56, 575–587. https://doi.org/10.1016/j.devcel.2021.02.016

Jumper, J., Evans, R., Pritzel, A., Green, T., Figurnov, M., Ronneberger, O., Tunyasuvunakool, K., Bates, R., Žídek, A., Potapenko, A., Bridgland, A., Meyer, C., Kohl, S.A.A., Ballard, A.J., Cowie, A., Romera-Paredes, B., Nikolov, S., Jain, R., Adler, J., Back, T., Petersen, S., Reiman, D., Clancy, E., Zielinski, M., Steinegger, M., Pacholska, M., Berghammer, T., Bodenstein, S., Silver, D., Vinyals, O., Senior, A.W., Kavukcuoglu, K., Kohli, P., Hassabis, D., 2021. Highly accurate protein structure prediction with AlphaFold. Nature 596, 583–589. https://doi.org/10.1038/s41586-021-03819-2

Jung, Y.-S., Park, J.-I., 2020. Wnt signaling in cancer: therapeutic targeting of Wnt signaling beyond β-catenin and the destruction complex. Exp Mol Med 52, 183–191. https://doi.org/10.1038/s12276-020-0380-6

Kang, K., Shi, Q., Wang, X., Chen, Y.-G., 2022a. Dishevelled phase separation promotes Wnt signalosome assembly and destruction complex disassembly. J Cell Biol 221, e202205069. https://doi.org/10.1083/jcb.202205069

Kang, K., Shi, Q., Wang, X., Chen, Y.-G., 2022b. Dishevelled phase separation promotes Wnt signalosome assembly and destruction complex disassembly. J Cell Biol 221, e202205069. https://doi.org/10.1083/jcb.202205069

Kim, S., Jeong, S., 2019. Mutation Hotspots in the β-Catenin Gene: Lessons from the Human Cancer Genome Databases. Mol Cells 42, 8–16. https://doi.org/10.14348/molcells.2018.0436

Kimelman, D., Xu, W., 2006. β-Catenin destruction complex: insights and questions from a structural perspective. Oncogene 25, 7482–7491. https://doi.org/10.1038/sj.onc.1210055

Kolligs, F.T., Hu, G., Dang, C.V., Fearon, E.R., 1999. Neoplastic Transformation of RK3E by Mutant β-Catenin Requires Deregulation of Tcf/Lef Transcription but Not Activation of c- *myc* Expression. Mol and Cell Biol 19, 5696–5706. https://doi.org/10.1128/MCB.19.8.5696

Kroschwald, S., Maharana, S., Simon, A., 2017. Hexanediol: a chemical probe to investigate the material properties of membrane-less compartments. Matters https://doi.org/10.19185/matters.201702000010

Kuroda, K., Tani, S., Tamura, K., Minoguchi, S., Kurooka, H., Honjo, T., 1999. Delta-induced Notch Signaling Mediated by RBP-J Inhibits MyoD Expression and Myogenesis. J Biol Chem 274, 7238–7244. https://doi.org/10.1074/jbc.274.11.7238

Kvon, E.Z., Waymack, R., Gad, M., Wunderlich, Z., 2021. Enhancer redundancy in development and disease. Nat Rev Genet 22, 324–336. https://doi.org/10.1038/s41576-020-00311-x

Lach, R.S., Qiu, C., Kajbaf, E.Z., Baxter, N., Han, D., Wang, A., Lock, H., Chirikian, O., Pruitt, B., Wilson, M.Z., 2022. Nucleation of the destruction complex on the centrosome accelerates degradation of β-catenin and regulates Wnt signal transmission. Proc Natl Acad Sci USA 119, e2204688119. https://doi.org/10.1073/pnas.2204688119

Lee, C.Y., Grant, P.A., 2019. Role of Histone Acetylation and Acetyltransferases in Gene Regulation, in: Toxicoepigenetics. Elsevier, pp. 3–30. https://doi.org/10.1016/B978-0-12-812433-8.00001-0

Lewis, B.A., Das, S.K., Jha, R.K., Levens, D., 2023. Self-assembly of promoter DNA and RNA Pol II machinery into transcriptionally active biomolecular condensates. Sci Adv 9, eadi4565. https://doi.org/10.1126/sciadv.adi4565

Lin, H.V., Rogulja, A., Cadigan, K.M., 2004. Wingless eliminates ommatidia from the edge of the developing eye through activation of apoptosis. Development 131, 2409–2418. https://doi.org/10.1242/dev.01104

Lopes, R., Korkmaz, G., Agami, R., 2016. Applying CRISPR–Cas9 tools to identify and characterize transcriptional enhancers. Nat Rev Mol Cell Biol 17, 597–604. https://doi.org/10.1038/nrm.2016.79

Lu, J., Wu, T., Zhang, B., Liu, S., Song, W., Qiao, J., Ruan, H., 2021. Types of nuclear localization signals and mechanisms of protein import into the nucleus. Cell Commun Signal 19, 60. https://doi.org/10.1186/s12964-021-00741-y

Lu, Y., Wu, T., Gutman, O., Lu, H., Zhou, Q., Henis, Y.I., Luo, K., 2020. Phase separation of TAZ compartmentalizes the transcription machinery to promote gene expression. Nat Cell Biol 22, 453–464. https://doi.org/10.1038/s41556-020-0485-0

Lutter, L.C., Judis, L., Paretti, R.F., 1992. Effects of Histone Acetylation on Chromatin Topology In Vivo. Mol Cell Biol 12, 5004–5014. https://doi.org/10.1128/mcb.12.11.5004-5014.1992

Lyons, H., Veettil, R.T., Pradhan, P., Fornero, C., De La Cruz, N., Ito, K., Eppert, M., Roeder, R.G., Sabari, B.R., 2023. Functional partitioning of transcriptional regulators by patterned charge blocks. Cell 186, 327-345.e28. https://doi.org/10.1016/j.cell.2022.12.013

Ma, L., Gao, Z., Wu, J., Zhong, B., Xie, Y., Huang, W., Lin, Y., 2021. Co-condensation between transcription factor and coactivator p300 modulates transcriptional bursting kinetics. Mol Cell 81, 1682-1697.e7. https://doi.org/10.1016/j.molcel.2021.01.031

Malik, S., Roeder, R.G., 2023. Regulation of the RNA polymerase II pre-initiation complex by its associated coactivators. Nat Rev Genet 24, 767–782. https://doi.org/10.1038/s41576-023-00630-9

Mao, C.D., Byers, S.W., 2011. Cell-Context Dependent TCF/LEF Expression and Function: Alternative Tales of Repression, De-Repression and Activation Potentials. Crit Rev Eukar Gene Expr 21, 207–236. https://doi.org/10.1615/CritRevEukarGeneExpr.v21.i3.10

Martin, B.J.E., Brind'Amour, J., Kuzmin, A., Jensen, K.N., Liu, Z.C., Lorincz, M., Howe, L.J., 2021. Transcription shapes genome-wide histone acetylation patterns. Nat Commun 12, 210. https://doi.org/10.1038/s41467-020-20543-z

Martin, E.W., Holehouse, A.S., Peran, I., Farag, M., Incicco, J.J., Bremer, A., Grace, C.R., Soranno, A., Pappu, R.V., Mittag, T., 2020. Valence and patterning of aromatic residues determine the phase behavior of prion-like domains. Science 367, 694–699. https://doi.org/10.1126/science.aaw8653

Mayeuf-Louchart, A., Lagha, M., Danckaert, A., Rocancourt, D., Relaix, F., Vincent, S.D., Buckingham, M., 2014. Notch regulation of myogenic versus endothelial fates of cells that migrate from the somite to the limb. Proc Natl Acad Sci USA 111, 8844–8849. https://doi.org/10.1073/pnas.1407606111

Mészáros, B., Erdős, G., Dosztányi, Z., 2018. IUPred2A: context-dependent prediction of protein disorder as a function of redox state and protein binding. Nucleic Acids Research 46, W329–W337. https://doi.org/10.1093/nar/gky384

Miller, J.R., Rowning, B.A., Larabell, C.A., Yang-Snyder, J.A., Bates, R.L., Moon, R.T., 1999. Establishment of the Dorsal–Ventral Axis in *Xenopus* Embryos Coincides with the Dorsal Enrichment of Dishevelled That Is Dependent on Cortical Rotation. J Cell Biol 146, 427–438. https://doi.org/10.1083/jcb.146.2.427

Morales, V., Richard-Foy, H., 2000. Role of Histone N-Terminal Tails and Their Acetylation in Nucleosome Dynamics. Mol Cell Biol 20, 7230–7237. https://doi.org/10.1128/MCB.20.19.7230-7237.2000

Morinière, J., Rousseaux, S., Steuerwald, U., Soler-López, M., Curtet, S., Vitte, A.-L., Govin, J., Gaucher, J., Sadoul, K., Hart, D.J., Krijgsveld, J., Khochbin, S., Müller, C.W., Petosa, C., 2009. Cooperative binding of two acetylation marks on a histone tail by a single bromodomain. Nature 461, 664–668. https://doi.org/10.1038/nature08397

Mosimann, C., Hausmann, G., Basler, K., 2009. β-Catenin hits chromatin: regulation of Wnt target gene activation. Nat Rev Mol Cell Biol 10, 276–286. https://doi.org/10.1038/nrm2654

Musacchio, A., 2022. On the role of phase separation in the biogenesis of membraneless compartments. EMBO J 41. https://doi.org/10.15252/embj.2021109952

Nair, S.J., Yang, L., Meluzzi, D., Oh, S., Yang, F., Friedman, M.J., Wang, S., Suter, T., Alshareedah, I., Gamliel, A., Ma, Q., Zhang, J., Hu, Y., Tan, Y., Ohgi, K.A., Jayani, R.S., Banerjee, P.R., Aggarwal, A.K., Rosenfeld, M.G., 2019. Phase separation of ligand-activated enhancers licenses cooperative chromosomal enhancer assembly. Nat Struct Mol Biol 26, 193–203. https://doi.org/10.1038/s41594-019-0190-5

Nong, J., Kang, K., Shi, Q., Zhu, X., Tao, Q., Chen, Y.-G., 2021a. Phase separation of Axin organizes the β-catenin destruction complex. J Cell Biol 220, e202012112. https://doi.org/10.1083/jcb.202012112

Nong, J., Kang, K., Shi, Q., Zhu, X., Tao, Q., Chen, Y.-G., 2021b. Phase separation of Axin organizes the β-catenin destruction complex. J Cell Biol 220, e202012112. https://doi.org/10.1083/jcb.202012112

Nusse, R., Clevers, H., 2017. Wnt/β-Catenin Signaling, Disease, and Emerging Therapeutic Modalities. Cell 169, 985–999. https://doi.org/10.1016/j.cell.2017.05.016

Ogryzko, V.V., Schiltz, R.L., Russanova, V., Howard, B.H., Nakatani, Y., 1996. The Transcriptional Coactivators p300 and CBP Are Histone Acetyltransferases. Cell 87, 953–959. https://doi.org/10.1016/S0092-8674(00)82001-2

Orphanides, G., Lagrange, T., Reinberg, D., 1996. The general transcription factors of RNA polymerase II. Genes Dev 10, 2657–2683. https://doi.org/10.1101/gad.10.21.2657

Pagella, P., Söderholm, S., Nordin, A., Zambanini, G., Ghezzi, V., Jauregi-Miguel, A., Cantù, C., 2023. The time-resolved genomic impact of Wnt/β-catenin signaling. Cell Systems 14, 563-581.e7. https://doi.org/10.1016/j.cels.2023.06.004

Palacio, M., Taatjes, D.J., 2022. Merging Established Mechanisms with New Insights: Condensates, Hubs, and the Regulation of RNA Polymerase II Transcription. J Mol Biol 434, 167216. https://doi.org/10.1016/j.jmb.2021.167216
Panigrahi, A., O'Malley, B.W., 2021. Mechanisms of enhancer action: the known and the unknown. Genome Biol 22, 108. https://doi.org/10.1186/s13059-021-02322-1
Panne, D., Maniatis, T., Harrison, S.C., 2007. An Atomic Model of the Interferon-β Enhanceosome. Cell 129, 1111–1123. https://doi.org/10.1016/j.cell.2007.05.019
Parker, D.S., Jemison, J., Cadigan, K.M., 2002. Pygopus, a nuclear PHD-finger protein required for Wingless signaling in *Drosophila*. Development 129, 2565–2576. https://doi.org/10.1242/dev.129.11.2565
Parker, D.S., Ni, Y.Y., Chang, J.L., Li, J., Cadigan, K.M., 2008. Wingless Signaling Induces Widespread Chromatin Remodeling of Target Loci. Mol Cell Biol 28, 1815–1828. https://doi.org/10.1128/MCB.01230-07
Patel, S.S., Belmont, B.J., Sante, J.M., Rexach, M.F., 2007. Natively Unfolded Nucleoporins Gate Protein Diffusion across the Nuclear Pore Complex. Cell 129, 83–96. https://doi.org/10.1016/j.cell.2007.01.044
Peifer, M., Wieschaus, E., 1990. Mutations in the Drosophila gene extradenticle affect the way specific homeo domain proteins regulate segmental identity. Genes Dev 4, 1209–1223. https://doi.org/10.1101/gad.4.7.1209
Perrimon, N., Pitsouli, C., Shilo, B.-Z., 2012. Signaling Mechanisms Controlling Cell Fate and Embryonic Patterning. Cold Spring Harb Perspect Biol 4, a005975–a005975. https://doi.org/10.1101/cshperspect.a005975
Petkovich, M., Chambon, P., 2022. Retinoic acid receptors at 35 years. J Mol Endocrinol 69, T13–T24. https://doi.org/10.1530/JME-22-0097
Pfaffl, M.W., 2001. A new mathematical model for relative quantification in real-time RT-PCR. Nucleic Acids Res 29, 45e–445. https://doi.org/10.1093/nar/29.9.e45
Piovesan, D., Tabaro, F., Mičetić, I., Necci, M., Quaglia, F., Oldfield, C.J., Aspromonte, M.C., Davey, N.E., Davidović, R., Dosztányi, Z., Elofsson, A., Gasparini, A., Hatos, A., Kajava, A.V., Kalmar, L., Leonardi, E., Lazar, T., Macedo-Ribeiro, S., Macossay-Castillo, M., Meszaros, A., Minervini, G., Murvai, N., Pujols, J., Roche, D.B., Salladini, E., Schad, E., Schramm, A., Szabo, B., Tantos, A., Tonello, F., Tsirigos, K.D., Veljković, N., Ventura, S., Vranken, W., Warholm, P., Uversky, V.N., Dunker, A.K., Longhi, S., Tompa, P., Tosatto, S.C.E., 2016. DisProt 7.0: a major update of the database of disordered proteins. Nucleic Acids Res gkw1279. https://doi.org/10.1093/nar/gkw1279
Plys, A.J., Kingston, R.E., 2018. Dynamic condensates activate transcription. Science 361, 329–330. https://doi.org/10.1126/science.aau4795
Port, F., Chen, H.-M., Lee, T., Bullock, S.L., 2014. Optimized CRISPR/Cas tools for efficient germline and somatic genome engineering in *Drosophila*. Proc Natl Acad Sci USA 111. https://doi.org/10.1073/pnas.1405500111
Portin, P., Wilkins, A., 2017. The Evolving Definition of the Term "Gene." Genetics 205, 1353–1364. https://doi.org/10.1534/genetics.116.196956
Poy, F., Lepourcelet, M., Shivdasani, R.A., Eck, M.J., 2001. Structure of a human TCF4-beta-catenin complex. Nat Struct Biol 8, 1053–1057. https://doi.org/10.1038/nsb720

Quintero-Cadena, P., Lenstra, T.L., Sternberg, P.W., 2020. RNA Pol II Length and Disorder Enable Cooperative Scaling of Transcriptional Bursting. Mol Cell 79, 207-220.e8. https://doi.org/10.1016/j.molcel.2020.05.030

Ramakrishnan, A.-B., Burby, P.E., Adiga, K., Cadigan, K.M., 2023. SOX9 and TCF transcription factors associate to mediate Wnt/β-catenin target gene activation in colorectal cancer. J Biol Chem 299, 102735. https://doi.org/10.1016/j.jbc.2022.102735

Ramakrishnan, A.-B., Cadigan, K.M., 2017. Wnt target genes and where to find them. F1000Res 6, 746. https://doi.org/10.12688/f1000research.11034.1

Ramakrishnan, A.-B., Chen, L., Burby, P.E., Cadigan, K.M., 2021. Wnt target enhancer regulation by a CDX/TCF transcription factor collective and a novel DNA motif. Nucleic Acids Res 49, 8625–8641. https://doi.org/10.1093/nar/gkab657

Ramakrishnan, A.-B., Sinha, A., Fan, V.B., Cadigan, K.M., 2018. The Wnt Transcriptional Switch: TLE Removal or Inactivation? BioEssays 40, 1700162. https://doi.org/10.1002/bies.201700162

Ravindranath, A., Cadigan, K.M., 2014. Structure-Function Analysis of the C-clamp of TCF/Pangolin in Wnt/ß-catenin Signaling. PLoS ONE 9, e86180. https://doi.org/10.1371/journal.pone.0086180

Ribbeck, K., 2002. The permeability barrier of nuclear pore complexes appears to operate via hydrophobic exclusion. EMBO J 21, 2664–2671. https://doi.org/10.1093/emboj/21.11.2664

Rim, E.Y., Clevers, H., Nusse, R., 2022. The Wnt Pathway: From Signaling Mechanisms to Synthetic Modulators. Annu Rev Biochem 91, 571–598. https://doi.org/10.1146/annurev-biochem-040320-103615

Roh, T.-Y., Cuddapah, S., Zhao, K., 2005. Active chromatin domains are defined by acetylation islands revealed by genome-wide mapping. Genes Dev 19, 542–552. https://doi.org/10.1101/gad.1272505

Sabari, B.R., 2020. Biomolecular Condensates and Gene Activation in Development and Disease. Dev Cell 55, 84–96. https://doi.org/10.1016/j.devcel.2020.09.005

Sabari, B.R., Dall'Agnese, A., Boija, A., Klein, I.A., Coffey, E.L., Shrinivas, K., Abraham, B.J., Hannett, N.M., Zamudio, A.V., Manteiga, J.C., Li, C.H., Guo, Y.E., Day, D.S., Schuijers, J., Vasile, E., Malik, S., Hnisz, D., Lee, T.I., Cisse, I.I., Roeder, R.G., Sharp, P.A., Chakraborty, A.K., Young, R.A., 2018. Coactivator condensation at super-enhancers links phase separation and gene control. Science 361, eaar3958. https://doi.org/10.1126/science.aar3958

Sabari, B.R., Dall'Agnese, A., Young, R.A., 2020. Biomolecular Condensates in the Nucleus. Trends Biochem Sci 45, 961–977. https://doi.org/10.1016/j.tibs.2020.06.007

Sampietro, J., Dahlberg, C.L., Cho, U.S., Hinds, T.R., Kimelman, D., Xu, W., 2006a. Crystal Structure of a β-Catenin/BCL9/Tcf4 Complex. Mol Cell 24, 293–300. https://doi.org/10.1016/j.molcel.2006.09.001

Sampietro, J., Dahlberg, C.L., Cho, U.S., Hinds, T.R., Kimelman, D., Xu, W., 2006b. Crystal Structure of a β-Catenin/BCL9/Tcf4 Complex. Mol Cell 24, 293–300. https://doi.org/10.1016/j.molcel.2006.09.001

Scarpa, E., Mayor, R., 2016. Collective cell migration in development. J Cell Biol 212, 143–155. https://doi.org/10.1083/jcb.201508047

Schaefer, K.N., Peifer, M., 2019. Wnt/Beta-Catenin Signaling Regulation and a Role for Biomolecular Condensates. Dev Cell 48, 429–444. https://doi.org/10.1016/j.devcel.2019.01.025

Schneider, N., Wieland, F.-G., Kong, D., Fischer, A.A.M., Hörner, M., Timmer, J., Ye, H., Weber, W., 2021. Liquid-liquid phase separation of light-inducible transcription factors increases transcription activation in mammalian cells and mice. Sci Adv 7, eabd3568. https://doi.org/10.1126/sciadv.abd3568

Schoenfelder, S., Fraser, P., 2019. Long-range enhancer–promoter contacts in gene expression control. Nat Rev Genet 20, 437–455. https://doi.org/10.1038/s41576-019-0128-0

Schubert, A., Voloshanenko, O., Ragaller, F., Gmach, P., Kranz, D., Scheeder, C., Miersch, T., Schulz, M., Trümper, L., Binder, C., Lampe, M., Engel, U., Boutros, M., 2022. Superresolution microscopy localizes endogenous Dvl2 to Wnt signaling-responsive biomolecular condensates. Proc Natl Acad Sci USA 119, e2122476119. https://doi.org/10.1073/pnas.2122476119

Schwarz-Romond, T., Fiedler, M., Shibata, N., Butler, P.J.G., Kikuchi, A., Higuchi, Y., Bienz, M., 2007. The DIX domain of Dishevelled confers Wnt signaling by dynamic polymerization. Nat Struct Mol Biol 14, 484–492. https://doi.org/10.1038/nsmb1247

Schweizer, L., Nellen, D., Basler, K., 2003. Requirement for Pangolin/dTCF in *Drosophila* Wingless signaling. Proc Natl Acad Sci USA 100, 5846–5851. https://doi.org/10.1073/pnas.1037533100

Shogren-Knaak, M., Ishii, H., Sun, J.-M., Pazin, M.J., Davie, J.R., Peterson, C.L., 2006. Histone H4-K16 Acetylation Controls Chromatin Structure and Protein Interactions. Science 311, 844–847. https://doi.org/10.1126/science.1124000

Shvedunova, M., Akhtar, A., 2022. Modulation of cellular processes by histone and non-histone protein acetylation. Nat Rev Mol Cell Biol 23, 329–349. https://doi.org/10.1038/s41580-021-00441-y

Siebel, C., Lendahl, U., 2017. Notch Signaling in Development, Tissue Homeostasis, and Disease. Physiol Rev 97, 1235–1294. https://doi.org/10.1152/physrev.00005.2017

Simon, J.A., Lange, C.A., 2008. Roles of the EZH2 histone methyltransferase in cancer epigenetics. Mutat Res-Fund Mol M 647, 21–29. https://doi.org/10.1016/j.mrfmmm.2008.07.010

Simsek, M.F., Özbudak, E.M., 2022. Patterning principles of morphogen gradients. Open Biol 12, 220224. https://doi.org/10.1098/rsob.220224

Sinha, A., Fan, V.B., Ramakrishnan, A.-B., Engelhardt, N., Kennell, J., Cadigan, K.M., 2021. Repression of Wnt/β-catenin signaling by SOX9 and Mastermind-like transcriptional coactivator 2. Sci Adv 7, eabe0849. https://doi.org/10.1126/sciadv.abe0849

Soutourina, J., 2018. Transcription regulation by the Mediator complex. Nat Rev Mol Cell Biol 19, 262–274. https://doi.org/10.1038/nrm.2017.115

Spitz, F., Furlong, E.E.M., 2012. Transcription factors: from enhancer binding to developmental control. Nat Rev Genet 13, 613–626. https://doi.org/10.1038/nrg3207

Städeli, R., Basler, K., 2005. Dissecting nuclear Wingless signalling: Recruitment of the transcriptional co-activator Pygopus by a chain of adaptor proteins. Mech Dev 122, 1171–1182. https://doi.org/10.1016/j.mod.2005.07.004

Stern, D.L., Sucena, E., 2011. Preparation of Cuticles from Unhatched First-Instar *Drosophila* Larvae. Cold Spring Harb Protoc 2011, pdb.prot065532. https://doi.org/10.1101/pdb.prot065532

Stewart, R.A., Ramakrishnan, A.-B., Cadigan, K.M., 2019. Diffusion and function of Wnt ligands. PLoS Genet 15, e1008154. https://doi.org/10.1371/journal.pgen.1008154

Strigini, M., Cohen, S.M., 2000. Wingless gradient formation in the Drosophila wing. Curr Biol 10, 293–300. https://doi.org/10.1016/s0960-9822(00)00378-x

Swanson, C.I., Evans, N.C., Barolo, S., 2010. Structural Rules and Complex Regulatory Circuitry Constrain Expression of a Notch- and EGFR-Regulated Eye Enhancer. Dev Cell 18, 359–370. https://doi.org/10.1016/j.devcel.2009.12.026

Swarup, S., Verheyen, E.M., 2012. Wnt/Wingless Signaling in Drosophila. Cold Spring Harbor Perspect Biol 4, a007930–a007930. https://doi.org/10.1101/cshperspect.a007930

Takemaru, K.-I., Moon, R.T., 2000. The Transcriptional Coactivator Cbp Interacts with β-Catenin to Activate Gene Expression. J Cell Biol 149, 249–254. https://doi.org/10.1083/jcb.149.2.249

Tang, S.C., Vijayakumar, U., Zhang, Y., Fullwood, M.J., 2022. Super-Enhancers, Phase-Separated Condensates, and 3D Genome Organization in Cancer. Cancers 14, 2866. https://doi.org/10.3390/cancers14122866

Tasan, I., Sustackova, G., Zhang, L., Kim, J., Sivaguru, M., HamediRad, M., Wang, Y., Genova, J., Ma, J., Belmont, A.S., Zhao, H., 2018. CRISPR/Cas9-mediated knock-in of an optimized TetO repeat for live cell imaging of endogenous loci. Nucleic Acids Res 46, e100–e100. https://doi.org/10.1093/nar/gky501

Taylor, G.C.A., Eskeland, R., Hekimoglu-Balkan, B., Pradeepa, M.M., Bickmore, W.A., 2013. H4K16 acetylation marks active genes and enhancers of embryonic stem cells, but does not alter chromatin compaction. Genome Res 23, 2053–2065. https://doi.org/10.1101/gr.155028.113

Tian, A., Duwadi, D., Benchabane, H., Ahmed, Y., 2019. Essential long-range action of Wingless/Wnt in adult intestinal compartmentalization. PLoS Genet 15, e1008111. https://doi.org/10.1371/journal.pgen.1008111

Treen, N., Shimobayashi, S.F., Eeftens, J., Brangwynne, C.P., Levine, M., 2021. Properties of repression condensates in living Ciona embryos. Nat Commun 12, 1561. https://doi.org/10.1038/s41467-021-21606-5

Trojanowski, J., Frank, L., Rademacher, A., Mücke, N., Grigaitis, P., Rippe, K., 2022. Transcription activation is enhanced by multivalent interactions independent of phase separation. Mol Cell 82, 1878-1893.e10. https://doi.org/10.1016/j.molcel.2022.04.017

Tutucci, E., Livingston, N.M., Singer, R.H., Wu, B., 2018. Imaging mRNA In Vivo, from Birth to Death. Annu Rev Biophys 47, 85–106. https://doi.org/10.1146/annurev-biophys-070317-033037

Valenta, T., Hausmann, G., Basler, K., 2012. The many faces and functions of β-catenin: β-Catenin: a life by, beyond, and against the Wnt canon. EMBO J 31, 2714–2736. https://doi.org/10.1038/emboj.2012.150

Vamadevan, V., Chaudhary, N., Maddika, S., 2022. Ubiquitin-assisted phase separation of dishevelled-2 promotes Wnt signalling. J Cell Sci 135, jcs260284. https://doi.org/10.1242/jcs.260284

Van Amerongen, R., Nusse, R., 2009. Towards an integrated view of Wnt signaling in development. Development 136, 3205–3214. https://doi.org/10.1242/dev.033910

van den Heuvel, M., Nusse, R., Johnston, P., Lawrence, P.A., 1989. Distribution of the wingless gene product in Drosophila embryos: a protein involved in cell-cell communication. Cell 59, 739–749. https://doi.org/10.1016/0092-8674(89)90020-2

Vandesompele, J., De Preter, K., Pattyn, F., Poppe, B., Van Roy, N., De Paepe, A., Speleman, F., 2002. Accurate normalization of real-time quantitative RT-PCR data by geometric averaging of multiple internal control genes. Genome Biol 3, research0034.1. https://doi.org/10.1186/gb-2002-3-7-research0034

Varadi, M., Anyango, S., Deshpande, M., Nair, S., Natassia, C., Yordanova, G., Yuan, D., Stroe, O., Wood, G., Laydon, A., Žídek, A., Green, T., Tunyasuvunakool, K., Petersen, S., Jumper, J., Clancy, E., Green, R., Vora, A., Lutfi, M., Figurnov, M., Cowie, A., Hobbs, N., Kohli, P., Kleywegt, G., Birney, E., Hassabis, D., Velankar, S., 2022. AlphaFold Protein Structure Database: massively expanding the structural coverage of protein-sequence space with high-accuracy models. Nucleic Acids Res 50, D439–D444. https://doi.org/10.1093/nar/gkab1061

Vockley, C.M., McDowell, I.C., D'Ippolito, A.M., Reddy, T.E., 2017. A long-range flexible billboard model of gene activation. Transcription 8, 261–267. https://doi.org/10.1080/21541264.2017.1317694

Wagh, K., Garcia, D.A., Upadhyaya, A., 2021. Phase separation in transcription factor dynamics and chromatin organization. Curr Opin Struct Biol 71, 148–155. https://doi.org/10.1016/j.sbi.2021.06.009

Wang, C., Zhang, E., Wu, F., Sun, Y., Wu, Y., Tao, B., Ming, Y., Xu, Y., Mao, R., Fan, Y., 2019. The C-terminal low-complexity domain involved in liquid–liquid phase separation is required for BRD4 function in vivo. J Mol Cell Biol 11, 807–809. https://doi.org/10.1093/jmcb/mjz037

Wang, H., Fan, Z., Shliaha, P.V., Miele, M., Hendrickson, R.C., Jiang, X., Helin, K., 2023. H3K4me3 regulates RNA polymerase II promoter-proximal pause-release. Nature 615, 339–348. https://doi.org/10.1038/s41586-023-05780-8

Wang, J., Choi, J.-M., Holehouse, A.S., Lee, H.O., Zhang, X., Jahnel, M., Maharana, S., Lemaitre, R., Pozniakovsky, A., Drechsel, D., Poser, I., Pappu, R.V., Alberti, S., Hyman, A.A., 2018. A Molecular Grammar Governing the Driving Forces for Phase Separation of Prion-like RNA Binding Proteins. Cell 174, 688-699.e16. https://doi.org/10.1016/j.cell.2018.06.006

Weintraub, A.S., Li, C.H., Zamudio, A.V., Sigova, A.A., Hannett, N.M., Day, D.S., Abraham, B.J., Cohen, M.A., Nabet, B., Buckley, D.L., Guo, Y.E., Hnisz, D., Jaenisch, R., Bradner, J.E., Gray, N.S., Young, R.A., 2017. YY1 Is a Structural Regulator of Enhancer-Promoter Loops. Cell 171, 1573-1588.e28. https://doi.org/10.1016/j.cell.2017.11.008

Wilkins, B.J., Rall, N.A., Ostwal, Y., Kruitwagen, T., Hiragami-Hamada, K., Winkler, M., Barral, Y., Fischle, W., Neumann, H., 2014. A Cascade of Histone Modifications Induces Chromatin Condensation in Mitosis. Science 343, 77–80. https://doi.org/10.1126/science.1244508

Wilson, B.G., Roberts, C.W.M., 2011. SWI/SNF nucleosome remodellers and cancer. Nat Rev Cancer 11, 481–492. https://doi.org/10.1038/nrc3068

Wittkopp, P.J., Kalay, G., 2012. Cis-regulatory elements: molecular mechanisms and evolutionary processes underlying divergence. Nat Rev Genet 13, 59–69. https://doi.org/10.1038/nrg3095

Woodruff, J.B., Hyman, A.A., Boke, E., 2018. Organization and Function of Non-dynamic Biomolecular Condensates. Trends Biochem Sci 43, 81–94. https://doi.org/10.1016/j.tibs.2017.11.005

Yang, Y., Mlodzik, M., 2015. Wnt-Frizzled/Planar Cell Polarity Signaling: Cellular Orientation by Facing the Wind (Wnt). Annu Rev Cell Dev Biol 31, 623–646. https://doi.org/10.1146/annurev-cellbio-100814-125315

Yi, F., Pereira, L., Hoffman, J.A., Shy, B.R., Yuen, C.M., Liu, D.R., Merrill, B.J., 2011. Opposing effects of Tcf3 and Tcf1 control Wnt stimulation of embryonic stem cell self-renewal. Nat Cell Biol 13, 762–770. https://doi.org/10.1038/ncb2283

Zamudio, A.V., Dall'Agnese, A., Henninger, J.E., Manteiga, J.C., Afeyan, L.K., Hannett, N.M., Coffey, E.L., Li, C.H., Oksuz, O., Sabari, B.R., Boija, A., Klein, I.A., Hawken, S.W., Spille, J.-H., Decker, T.-M., Cisse, I.I., Abraham, B.J., Lee, T.I., Taatjes, D.J., Schuijers, J., Young, R.A., 2019. Mediator Condensates Localize Signaling Factors to Key Cell Identity Genes. Mol Cell 76, 753-766.e6. https://doi.org/10.1016/j.molcel.2019.08.016

Zhan, T., Rindtorff, N., Boutros, M., 2017. Wnt signaling in cancer. Oncogene 36, 1461–1473. https://doi.org/10.1038/onc.2016.304

Zhang, C.U., Blauwkamp, T.A., Burby, P.E., Cadigan, K.M., 2014. Wnt-Mediated Repression via Bipartite DNA Recognition by TCF in the Drosophila Hematopoietic System. PLoS Genet 10, e1004509. https://doi.org/10.1371/journal.pgen.1004509

Zhang, C.U., Cadigan, K.M., 2017. The matrix protein Tiggrin regulates plasmatocyte maturation in *Drosophila* larva. Development dev.149641. https://doi.org/10.1242/dev.149641

Zhang, W., Garcia, N., Feng, Y., Zhao, H., Messing, J., 2015. Genome-wide histone acetylation correlates with active transcription in maize. Genomics 106, 214–220. https://doi.org/10.1016/j.ygeno.2015.05.005

Zhang, Y., Brown, K., Yu, Y., Ibrahim, Z., Zandian, M., Xuan, H., Ingersoll, S., Lee, T., Ebmeier, C.C., Liu, J., Panne, D., Shi, X., Ren, X., Kutateladze, T.G., 2021. Nuclear condensates of p300 formed though the structured catalytic core can act as a storage pool of p300 with reduced HAT activity. Nat Commun 12, 4618. https://doi.org/10.1038/s41467-021-24950-8

Zhang, Y., Wang, X., 2020. Targeting the Wnt/β-catenin signaling pathway in cancer. J Hematol Oncol 13, 165. https://doi.org/10.1186/s13045-020-00990-3

Zhao, B., Li, Z., Yu, S., Li, Tingting, Wang, W., Liu, R., Zhang, B., Fang, X., Shen, Y., Han, Q., Xu, X., Wang, K., Gong, W., Li, Tao, Li, A., Zhou, T., Li, W., Li, Teng, 2023. LEF1 enhances β-catenin transactivation through IDR-dependent liquid–liquid phase separation. Life Sci Alliance 6, e202302118. https://doi.org/10.26508/lsa.202302118